NANYANG TECHNOLOGICAL UNIVERSITY

PART I: TOWARDS A TOTAL SYNTHESIS OF PAPULACANDIN D
PART II: TOWARDS A TOTAL SYNTHESIS OF AMPHIDINOLIDE X

GOH HONG HENG

SCHOOL OF PHYSICAL AND MATHEMATICAL SCIENCES

2010

PART I: TOWARDS A TOTAL SYNTHESIS OF PAPULACANDIN D
PART II: TOWARDS A TOTAL SYNTHESIS OF AMPHIDINOLIDE X

Goh Hong Heng

BSc GDip (NUS) MMedSc (UNSW)

CBiol MSB MRSC

School of Physical and Mathematical Sciences

A thesis submitted to the Nanyang Technological University
in partial fulfilment of the requirements for the degree of
Doctor of Philosophy

2010

Declaration of Authorship

I, GOH HONG HENG, declare that this thesis titled, 'PART I : TOWARDS A TOTAL SYNTHESIS OF PAPULACANDIN D & PART II : TOWARDS A TOTAL SYNTHESIS OF AMPHIDINOLIDE X' and the work presented in it are my own. I confirm that:

- This work was done wholly or mainly while in candidature for a research degree at this University.
- Where any part of this thesis has previously been submitted for a degree or any other qualification at this University or any other institution, this has been clearly stated.
- Where I have consulted the published work of others, this is always clearly attributed.
- Where I have quoted from the work of others, the source is always given. With the exception of such quotations, this thesis is entirely my own work.
- I have acknowledged all main sources of help.
- Where the thesis is based on work done by myself jointly with others, I have made clear exactly what was done by others and what I have contributed myself.

Signed: Hong-Heng Goh

Date: 08-Feb-2010

"Education is a progressive discovery of our own ignorance."

Will Durant

Abstract

The facile β,γ- to α,β-isomerization upon hydrolysis of the three-carbon homologated Wittig olefination product using the homoenolate anion equivalent (3,3-dimethoxypropyl)triphenylphosphonium salt has always been viewed as a complicating side reaction in organic synthesis. Perhaps arising from such prejudiced views, its utility and practicality to organic syntheses has long been overlooked.

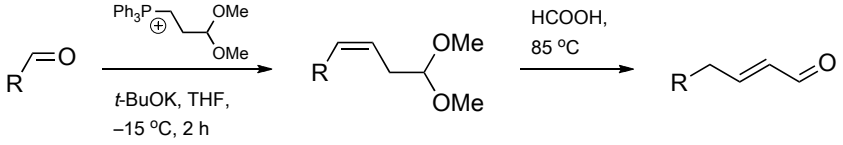

In this thesis, we first surveyed the ways similar phosphonium salt-based homoenolate anion equivalents had been used in organic synthesis and uncovered the dearth of information on the application of this facile isomerization to organic synthesis. Thence we embarked on a systematic screening to first establish the substrate scope of this facile isomerization, before commencing on the application of this methodology to the syntheses of two natural products — papulacandin D and amphidinolide X.

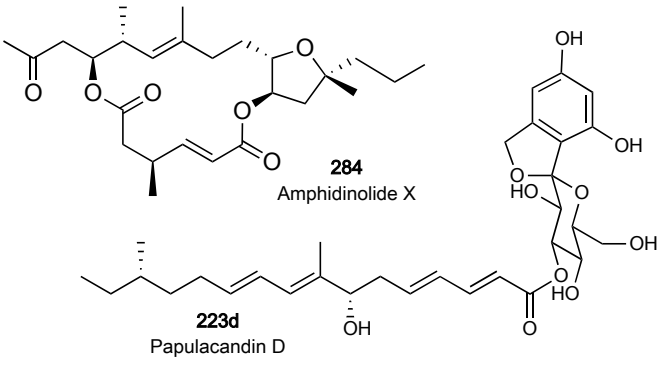

We report herein our findings on the feasibility of applying this method for the generation of α,β-unsaturated aldehydes via a three-carbon homologation/isomerization, that holds potential for shortened synthetic routes and offers the possibility of further synthetic manipulations typified by aldehydes belonging to such a class.

Acknowledgements

בָּרוּךְ אַתָּה יְיָ אֱלֹהֵינוּ מֶלֶךְ הָעוֹלָם שֶׁהֶחֱיָנוּ וְקִיְּמָנוּ וְהִגִּיעָנוּ לַזְּמַן הַזֶּה

As with all endeavours of man, no enterprise is ever accomplished through the sheer effort of one person. And though there are innumerable opportunities for others to leave indelible marks on us through our encounters in life, occasions for us to gratefully and formally acknowledge them are too few and far in between.

Seizing this opportune moment, I would first like to express my profound gratitude to the Lee Foundation, whose generous bursary at a time of need allowed me to finish my BSc at the National University of Singapore (NUS) in 1992–1995, thus enabling me to continue pursuing my research aspirations.

And NUS was where I first met my current thesis advisor Prof Loh Teck Peng — freshly graduated from Harvard University and ardent to implement needful changes to organic chemistry pedagogy and research. Taking a different didactic approach, his memorable first lectures on organic reaction mechanisms revealed a brilliant mind, adept at conveying and unifying abstract concepts for organic syntheses. His timely advice and comments at various points in my career have been pivotal in the research path that I took, culminating eventually in this current doctoral studies, where I had the privilege of experiencing his brilliance again.

I am also deeply indebted to my previous supervisor, Dr Bernard Leung, whose infectious passion for immunology research has seen a convert. Though I had to leave for a season to acquire another complementary skillset, his constant concern over my progress and future has been a significant source of encouragement through trying times.

My sincere gratitude is also extended to Prof Miranda Yap for her insightful questions that clarified my career path and her astute decision on my laboratory placement when all I had in mind was vague; Dr Wan Hai-Bin for establishing my foundations in analytical chemistry and encouraging me to continue pursuing research and studies; Dr Mao Hai-Quan who taught me to think, learn and work critically and independently; Dr Evelyn Koay in whose laboratory I had a brief respite and honed my molecular biology and biochemical skills; Dr Teo Cheng Peng and Ms Jenny NGAI, in whose clinic and laboratory I spent my formative

years. And all these began with my very first supervisor, Prof Tan Tin Wee, who instilled in me the dire need for researchers to be multi- and cross-disciplinary to meet the challenges facing the scientific community.

It has been a great learning experience at NTU, and I am grateful to Prof Lee Soo Ying for encouraging and helping me affiliate myself with the Royal Society of Chemistry thereby reaping benefit from her resources. Dr Deng Weiqiao and Dr Tan Howe Siang had been instrumental in helping me acquire skills in computational chemistry and molecular modelling which stands me in good stead for my future research. I am also very grateful to Dr Chua Guan Leong for his friendship, advice and access to work in his remarkably well-maintained and safe laboratory. Kudos too to my seniors Chen Shui Ling, Chan Kok Ping, Cheng Hin Soon, Wong Chek Ming, Zhao Yujun, Li Hao, Liu Feng, Sreekumar Pankajakshan, Wang Shunyi and Shen Zhiliang, who each in their own way has made positive impact in these years of my life.

My many friends at NTU should be credited for infusing joy, colour and cheer to my graduate life. Their companionship and support made the going a whole lot easier when times are tough, and burdens easier to bear. My constant meal buddies Choo En, Chok Yew Keong and Ng Eng Chye, with Hendra Widjaya and Ramesh s/o Summugam frequently joining us and adding to the heartening (and fattening) experience. A double honour should be given to Choo En, Yew Keong and Guan Leong for being my chemistry gurus as well. Attapol Pinsa, Rujee Lorpitthaya, Krisada Kittigowittana, Tan Siok Gim, Jenefer Alam, Alni Anita, Chiang Minyi, Joyce Chang, Jocelyn Chan, Yvonne Ling, Lum Tze Keong, Ana Ciric, Mark Dewey, Carolin Ruan, Chen Xiaoping, Celine Hum, Laura Woo, Gladys Lee, Goh Ee Ling, Yeo Siew Ping, Zhu Wenwei, Cheong Shu Qi, Seow Ai Hua, Karis Chiu, Koo Yien Teng, Charlene Poo, Isabelle Wong, Sara Cheung, Damian Chia and Samson Sim — thank you all for the fond memories!

Lastly, I would like to thank Sunil Patel for making freely available a LaTeX thesis template which was modified to adhere to the dissertation format of NTU, and Donald Knuth who created TeX for typesetting beautiful documents.

Soli Deo Gloria

Contents

List of Figures

List of Tables

List of Schemes

Abbreviations

$[\alpha]_D^T$	specific rotation using D-line of sodium; T is in °C
Å	angstrom(s)
Ac	acetyl
acac	acetylacetonate
ADP	adenosine 5'-diphosphate
AIBN	2,2'-azobisisobutyronitrile
AMP	adenosine 5'-monophosphate
Anal.	combustion elemental analysis
anhyd	anhydrous
aq	aqueous
Ar	aryl
atm	atmosphere(s)
ATP	adenosine 5'-triphosphate
ATPase	adenosinetriphosphatase
av	average
9-BBN	9-borabicyclo[3.3.1]nonyl
9-BBN–H	9-borabicyclo[3.3.1]nonane
BINAP	2,2-bis-(diphenylphosphino)-1,1'-binaphthyl
BINOL	1,1'-bi-2-naphthol
Bn, Bzl	benzyl
bpy	2,2'-bipyridyl
BOC, Boc	*tert*-butoxycarbonyl
bp	boiling point, base pair
br	broad (spectral)
Bu, *n*-Bu	normal (primary) butyl
n-BuLi	*n*-butyllithium
s-Bu	*sec*-butyl
t-Bu	*tert*-butyl
t-BuOK	potassium *tert*-butoxide

Bz	benzoyl (not benzyl)
°C	degrees Celsius
calcd	calculated
CAM	ceric ammonium molybdate
cAMP	adenosine cyclic 3',5'-phosphate
CAN	ceric ammonium nitrate
cat	catalytic
CBZ, Cbz	benzyloxycarbonyl
CD	circular dichroism
cDNA	complementary deoxyribonucleic acid
c-Hex, *c*-C_6H_{11}	cyclohexyl
cHPLC	chiral HPLC
CI	chemical ionization; configuration interaction
CIF	crystallographic information file
cm	centimetre(s)
cm^{-1}	wavenumber(s)
cod	1,5-cyclooctadiene
compd	compound
concd	concentrated
concn	concentration
COSY	correlation spectroscopy
cot	1,3,5,7-cyclooctatetraene
Cp	cyclopentadienyl
m-CPBA	*m*-chloroperoxybenzoic acid
δ	chemical shift in parts per million
d	day(s); doublet (spectral); deci
d	density
DABCO	1,4-diazabicyclo[2.2.2]octane dansyl
	5-(dimethylamino)-1-naphthalenesulphonyl
DBN	1,5-diazabicyclo[4.3.0]non-5-ene
DBU	1,8-diazabicyclo[5.4.0]undec-7-ene

DCC	*N,N'*-dicyclohexylcarbodiimide
DCE	1,2-dichloroethane
DDQ	2,3-dichloro-5,6-dicyano-1,4-benzoquinone
de	diastereomeric excess
DEAD	diethyl azodicarboxylate
DEPT	distortionless enhancement by polarization transfer
DFT	density functional theory
DIBAL-H	diisobutylaluminum hydride
DIPEA	diisopropylethylamine
DMA	dimethylacetamide
DMAP	4-(*N,N*-dimethylamino)pyridine
DMDO	dimethyldioxirane
DME	1,2-dimethoxyethane
DMF	dimethylformamide
DMP	Dess-Martin periodinane
DMPU	1,3-dimethyl-3,4,5,6-tetrahydro-2(*1H*)-pyrimidinone
DMSO	dimethyl sulfoxide
DMT	4,4'-dimethoxytrityl (4,4'-dimethoxyltriphenylmethyl)
DNA	deoxyribonucleic acid
2,4-DNP	2,4-dinitrophenylhydrazine
DPS	*tert*-butyldiphenylsilyl
dr	diastereomeric ratio
DTT	dithiothreitol
E1	unimolecular elimination
E2	bimolecular elimination
ED_{50}	dose effective in 50% of test subjects
EDTA	ethylenediaminetetraacetic acid
ee	enantiomeric excess
EI	electron impact
eq	equation
equiv	equivalent

er	enantiomeric ratio
ESI	electrospray ionization
Et	ethyl
FAB	fast atom bombardment
FID	flame ionization detector; free induction decay
Fmoc	9-fluorenylmethoxycarbonyl
FT	Fourier transform
g	gram(s)
GC	gas chromatography
h	hour(s)
HAE	homoenolate anion equivalent
HOMO	highest occupied molecular orbital
HPLC	high-performance liquid chromatography
HRMS	high-resolution mass spectrometry
Hz	hertz
IBX	2-iodoxybenzoic acid
IPA	isopropyl alcohol
IR	infrared
J	coupling constant (in NMR spectrometry)
k	kilo
K	kelvin(s) (absolute temperature)
KHMDS	potassium hexamethyldisilazane, potassium bis(trimethylsilyl)amide
L	litre(s)
LAH	lithium aluminum hydride
LD_{50}	dose that is lethal in 50% of test subjects
LDA	lithium diisopropylamide; local density approximation
LHMDS	lithium hexamethyldisilazane, lithium bis(trimethylsilyl)amide
lit.	literature value (abbreviation used with period)
LTMP	lithium 2,2,6,6-tetramethylpiperidide
LUMO	lowest unoccupied molecular orbital
μ	micro

m	multiplet (spectral); metre(s); milli
M	molar (moles per liter); mega
M^+	parent molecular ion
MAE	Mukaiyama-Aldol-Ene
MALDI	matrix-assisted laser desorption ionization
MAP	Mukaiyama-Aldol-Prins
max	maximum
MCR	multicomponent reaction
MCSCF	multi-configuration self-consistent field
MD	molecular dynamics
Me	methyl
MEM	(2-methoxyethoxy)methyl
Mes	2,4,6-trimethylphenyl (mesityl) [not methylsulphonyl (mesyl)]
MHz	megahertz
min	minute(s); minimum
mM	millimolar (millimoles per liter)
MO	molecular orbital
mol	mole(s); molecular (as in mol wt)
MOM	methoxymethyl
mp	melting point
MP	Møller–Plesset perturbation theory
mRNA	messenger ribonucleic acid
Ms	methylsulphonyl (mesyl)
MS	mass spectrometry; molecular sieves
MW, mol wt	molecular weight
m/z	mass-to-charge ratio (not m/e)
N	normal (equivalents per liter)
NAD^+	nicotinamide adenine dinucleotide
NADH	reduced NAD
NBO	natural bond orbital
NBS	*N*-bromosuccinimide

NCS	*N*-chlorosuccinimide
NICS	nucleus-independent chemical shift
NIS	*N*-iodosuccinimide
nm	nanometre(s)
NMO	*N*-methylmorpholine-N-oxide
NMP	*N*-methylpyrrolidone
NMR	nuclear magnetic resonance
NOE	nuclear Overhauser effect
NOESY	nuclear Overhauser effect spectroscopy
Nu	nucleophile
obsd	observed
OD	optical density
ORD	optical rotary dispersion
PAB	*p*-aminobenzoyl
PCC	pyridinium chlorochromate
PDC	pyridinium dichromate
PES	photoelectron spectroscopy
Ph	phenyl
piv	pivaloyl
pm	picometre(s)
PM3	parametric method 3
PMB	*p*-methoxybenzyl
PNB	*p*-nitrobenzoyl
PNBA	*p*-nitrobenzoic acid
PPA	poly(phosphoric acid)
ppm	part(s) per million
PPTS	pyridinium *para*-toluenesulphonate
PTSA	*para*-toluenesulphonic acid
Pr	propyl
i-Pr	isopropyl
PTC	phase-transfer catalysis

py	pyridine
q	quartet (spectral)
QSAR	quantitative structure–activity relationship
RCM	ring-closure metathesis
redox	reduction–oxidation
rel	relative
R_f	retention factor (in chromatography)
RHF	restricted Hartree–Fock
ROESY	rotating frame Overhauser effect spectroscopy
ROMP	ring-opening metathesis polymerization
rRNA	ribosomal ribonucleic acid
rt	room temperature
s	singlet (spectral); second(s)
SAR	structure–activity relationship
SCF	self-consistent field
SEM	scanning electron microscopy
SET	single electron transfer
S_N1	unimolecular nucleophilic substitution
S_N2	bimolecular nucleophilic substitution
S_N2' or S_N1'	nucleophilic substitution with allylic rearrangement
SOMO	single-occupied molecular orbital
t	triplet (spectral)
t	time; temperature in units of degrees Celsius (°C)
T	absolute temperature in units of kelvins (K)
TBAB	tetrabutylammonium bromide
TBAC	tetrabutylammonium chloride
TBAF	tetrabutylammonium fluoride
TBAI	tetrabutylammonium iodide
TBME	*tert*-butyl methyl ether
TBS	*tert*-butyldimethylsilyl
TBHP	*tert*-butyl hydroperoxide

TCA	trichloroacetic acid
TCNE	tetracyanoethylene
TEAB	tetraethylammonium bromide
TEBA	triethylbenzylammonium chloride
temp	temperature
TES	triethylsilyl
TESCl	chlorotriethylsilane
Tf	trifluoromethanesulphonyl (triflyl)
TFA	trifluoroacetic acid
TFAA	trifluoroacetic anhydride
THF	tetrahydrofuran
THP	tetrahydropyran-2-yl
TIPS	triisopropylsilyl
TLC	thin-layer chromatography
TMAI	tetramethylammonium iodide
TMEDA	*N,N,N',N'*-tetramethyl-1,2-ethylenediamine
TMS	trimethylsilyl; tetramethylsilane
TOF	time-of-flight
Tr	triphenylmethyl (trityl)
tRNA	transfer ribonucleic acid
t_R	retention time (in chromatography)
Ts	*para*-toluenesulphonyl (tosyl)
TS	transition state
UHF	unrestricted Hartree–Fock
UV	ultraviolet
VCD	vibrational circular dichroism
vis	visible
vol	volume
v/v	volume per unit volume (volume-to-volume ratio)
wt	weight
w/w	weight per unit weight (weight-to-weight ratio)

To my family and friends,
without whom all these would not have been possible.

Ἡ χάρις τοῦ κυρίου Ἰησοῦ μεθ᾽ ὑμῶν.
ἡ ἀγάπη μου μετὰ πάντων ὑμῶν ἐν Χριστῷ Ἰησοῦ.

Part I

TOWARDS A TOTAL SYNTHESIS OF PAPULACANDIN D

Chapter 1

Homoenolates In Organic Syntheses

1.1 Introduction

Unmistakably, homoenolates are important armaments in an organic chemists' synthetic repertoire.[1–3] With it, we can perform three-carbon homologations,[4] generate β,γ-unsaturated aldehydes,[5] and more importantly, gain access to 1,4-dissonant systems.[2,6–8] These operations are important as there are numerous natural products incorporating such functionalities. An example of the need for homoenolates would be in the synthesis of homoaldol products **4**. The retrosynthetic analyses comparing the aldol versus the homoaldol synthesis is depicted in Scheme 1.1, where we see that a homoenolate **6** is required.[7]

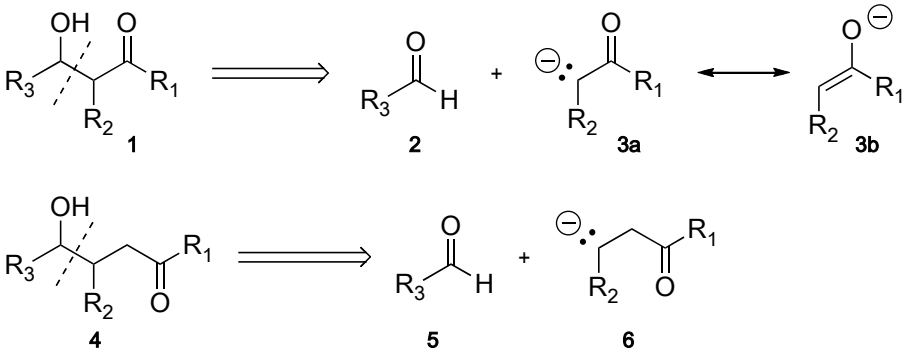

Scheme 1.1: Retrosynthesis of Aldols vs Homoaldols

Compared to enolates (**8**), the formation of homoenolates (**11**) is much more difficult as the β-carbon centre has undergone 'charge inversion' or *umpolung*.[7,9] As can be seen in Scheme 1.2, the formation of a homoenolate would probably entail reagents containing the cyclopropane moiety **10**.[3]

From the reviews by Werstiuk, Hoppe and Martin,[2,6,7] we see that there are several methods for generating homoenolates. Briefly, they can be classified as the 'direct' strategy, the 'offensive' strategy, and the 'defensive' strategy.

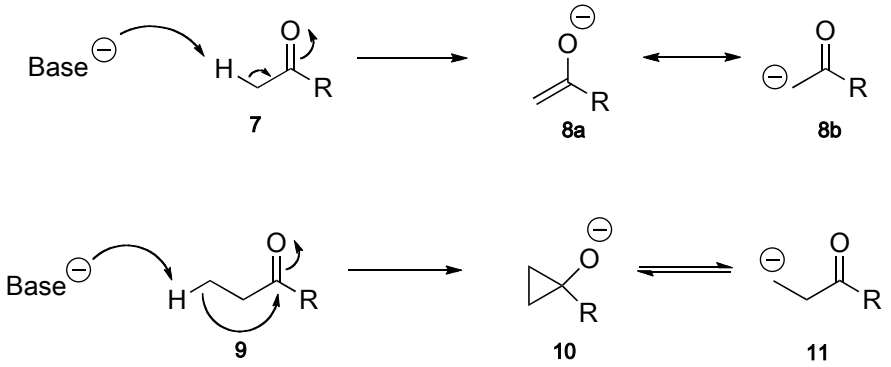

Scheme 1.2: Enolate vs Homoenolate Formation

1.2 Homoenolates By The "Direct" Strategy

As a direct strategy, reagents based on the cyclopropane moiety **10** such as that depicted in Figure 1.1 can be obtained via the metallation of 3-haloacids[10] or, via 3-haloesters first trapped as the cyclopropyl silyl ethers.[11]

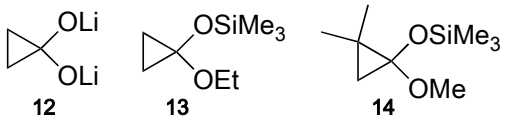

Figure 1.1: Examples of Homoenolates Containing Cyclopropane Moiety

These reagents grant us access to homoenolates such as those seen in Figure 1.2. Investigations done by Nakamura and Kuwajima has shown that the real intermediates are exemplified by the titanium homoenolate **15**, as is the case for those based on zinc or zirconium (**17** and **18** respectively).[11–14]

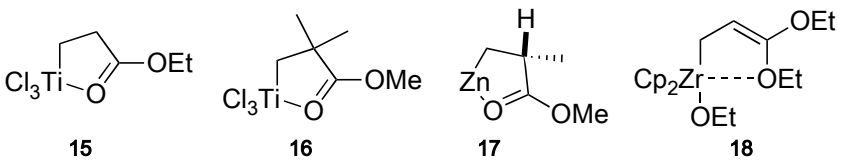

Figure 1.2: Examples of Homoenolates Based On The Direct Strategy

1.3 Homoenolates By The "Offensive" Strategy

As an offensive strategy, the homoenolates are mainly generated from π-allyl complexes **19** or based on allyl anions **20** substituted at one end with heteroatoms such as allyl silanes, sulfides, ethers, amines, or carbamates.[2,7] Unfortunately, a plethora of conditions need to be met as summarised by Werstiuk: "The nature and size of the groups attached to the heteroatom, the counter cation, the solvent including additives, reaction temperature and reaction time are important."

When these conditions are met, electrophiles will primarily react at the γ-position from the heteroatom to give the vinyl derivatives **21** and be easily hydrolysed to form carbonyl compounds **22** as depicted in Scheme 1.3.

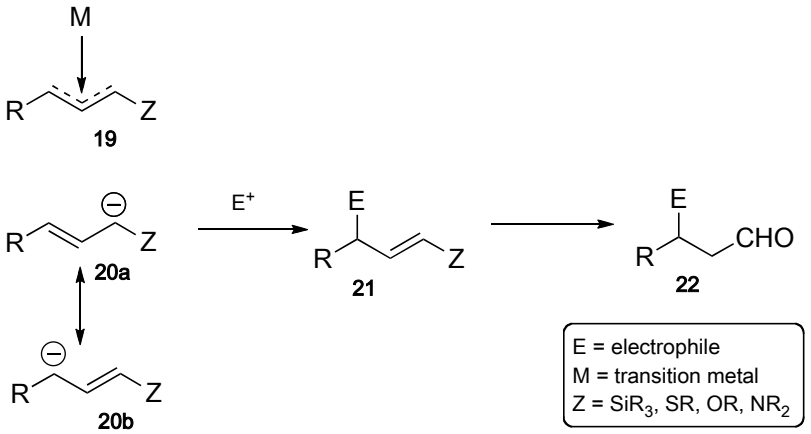

Scheme 1.3: Homoenolates By Offensive Strategy

1.4 Homoenolates By The "Defensive" Strategy

As pointed out by Hoppe, when we compare the carbonyl groups in **3** and **6**, we see that the enolate carbonyl group is protected from nucleophilic attack by resonance.

This is not available for the homoenolate carbonyl group (**6**). As such, in the defensive strategy, acetalization is commonly done to protect this homoenolate carbonyl group. Additional means of protection can be obtained by deactivation via electronic factors such as the incorporation of strongly electron attracting β-substituent Z, or of use of carboxylate resonance as seen in Scheme 1.4.[7]

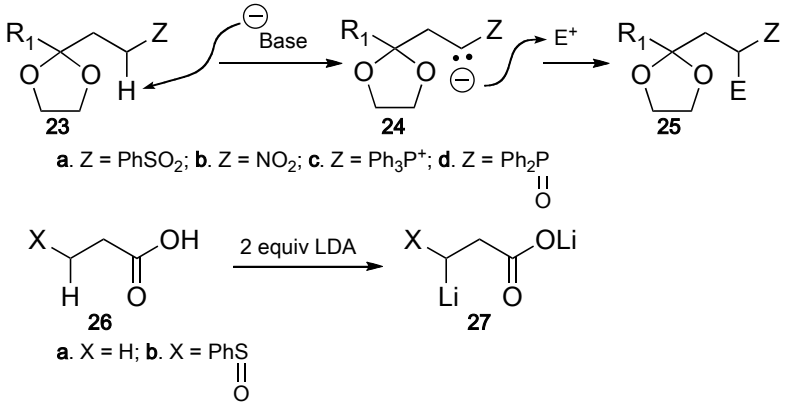

Scheme 1.4: Homoenolates By Defensive Strategy

Several examples of homoenolate reagents generated by the defensive strategy are listed in Figure 1.3.

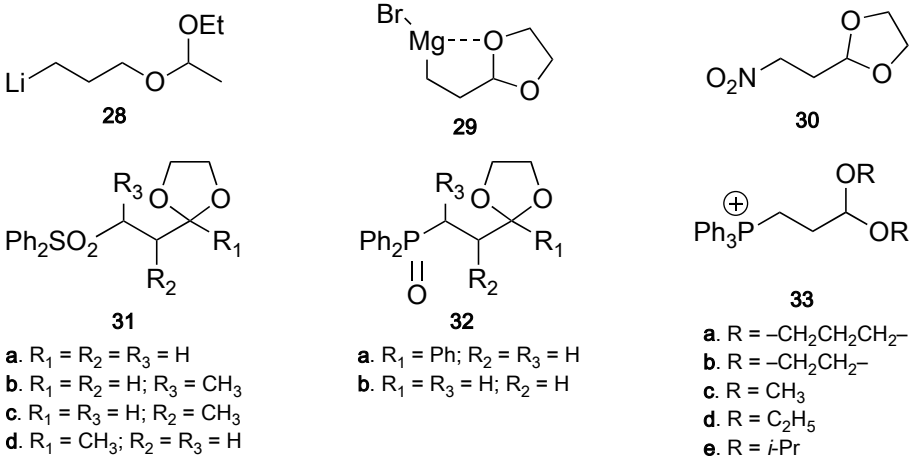

Figure 1.3: Examples of Homoenolate Anion Equivalents Based On The Defensive Strategy

1.5 Phosphonium Salt Homoenolate Anion Equivalents

Homoenolate anion equivalents such as **33** were first reported by Stowell and co-workers.[1] In their paper, they demonstrated the utility of these homoenolate anion equivalents in three-carbon homologations (**39**), and also in the generation of β,γ- and α,β-unsaturated aldehydes (**38** and **37** respectively).

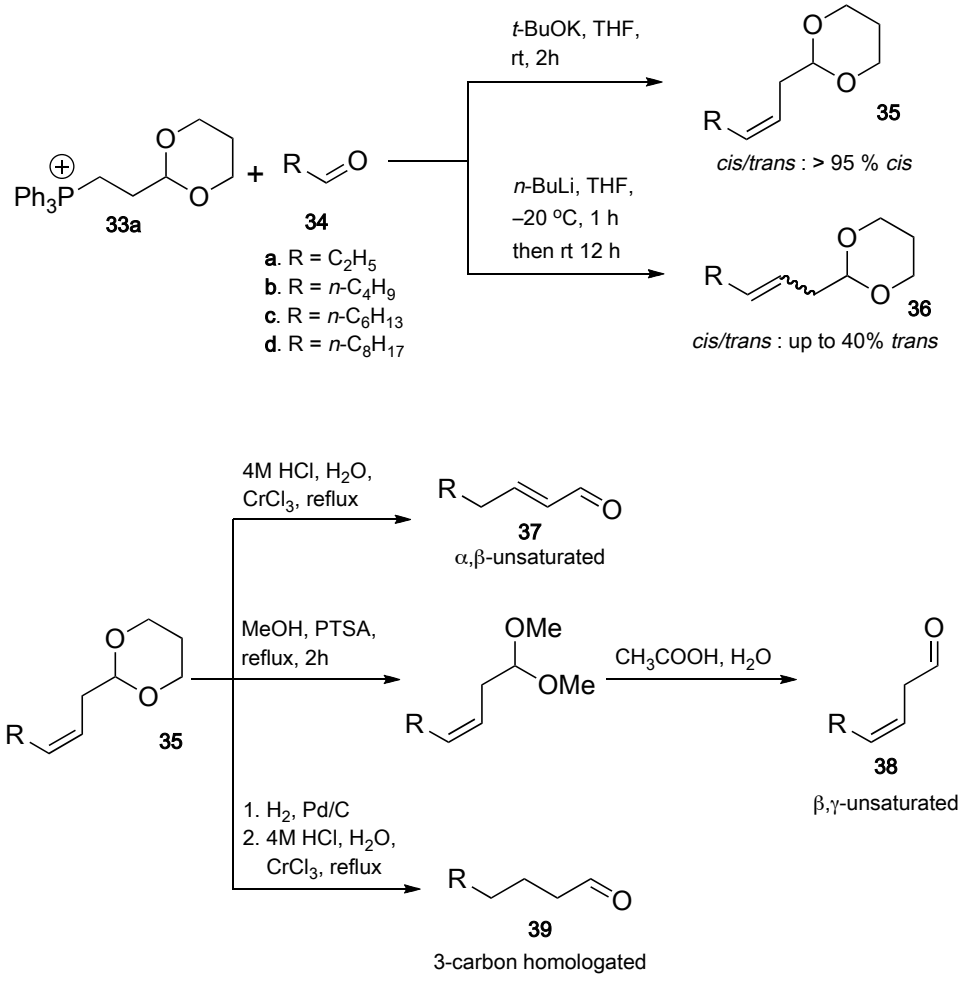

Scheme 1.5: Stowell's Methodology

Homoenolate anion equivalents such as these are very useful synthetically as they give an aldehyde functionality after hydrolysis. Undeniably, carbonyl compounds

are one of the most important functional groups in organic syntheses for carbon-carbon and carbon-heteroatom bond formations and functional group transformations.

As Werstiuk has noted, the chemistry of carbonyl compounds "is rich and varied" since they are "electrophilic, basic, relatively strong carbon acids and contain a π-chromophore".[2] When we couple this information with the possibility of generating either the α,β- or β,γ-unsaturated aldehydes, it immediately becomes apparent that homoenolate anion equivalents such as **33** play important roles in organic syntheses, as the presence of a double-bond offers further avenues for synthetic manipulations while the ability to perform a three-carbon homologation enables us to rapidly extend alkyl chains when done iteratively.

1.5.1 Our Use of Phosphonium Salt Homoenolate Anion Equivalents

In the course of our work on the Mukaiyama-Aldol-Prins (MAP) and Mukaiyama-Aldol-Ene (MAE) cascade reactions,[15,16] we had utilised several homoenolate anion equivalents such as **33a** – **33d** to synthesize highly substituted cyclopentyl building blocks in a regio-, diastereo-, and enantioselective manner with control of up to five stereocenters (Scheme 1.6).

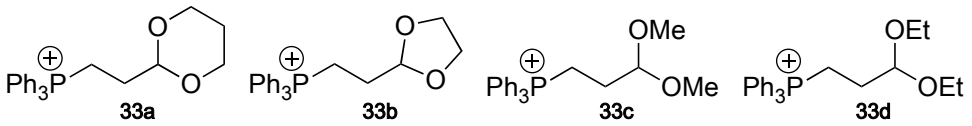

Figure 1.4: Homoenolate Anion Equivalents Used in the MAP Reaction

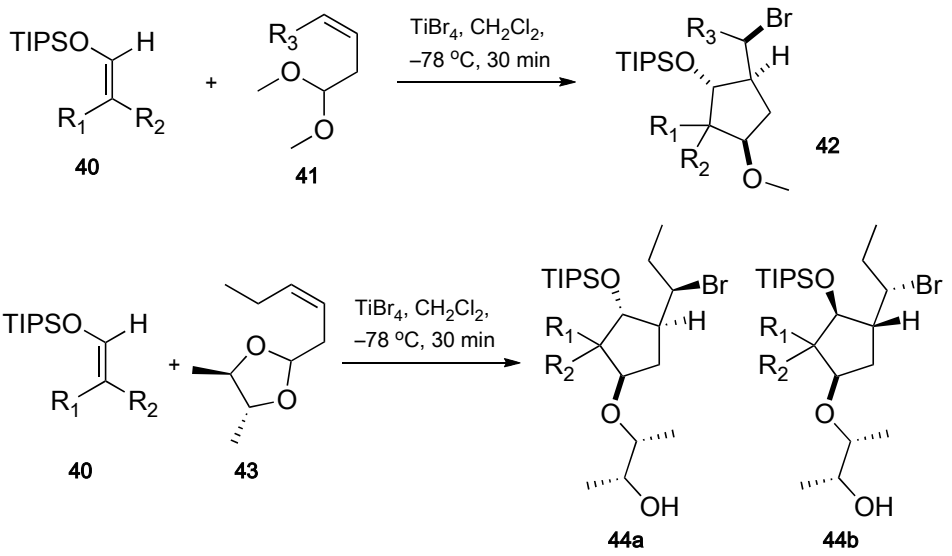

Scheme 1.6: MAP Reactions Using Acyclic and Cyclic Homoenolate Anion Equivalents

These building blocks would allow us to gain access to complex molecules or their analogues, typified by the prostaglandins (**45**), palau'amine (**46**), jatrophane diterpenes (**47**) and ophiobolins (**48**).[17–19] Apart from these, the range of natural products containing the cyclopentyl moiety spans the alkaloids, steroids, mono-, di-, tri- and sesquiterpenoids and marine natural products.[20–25]

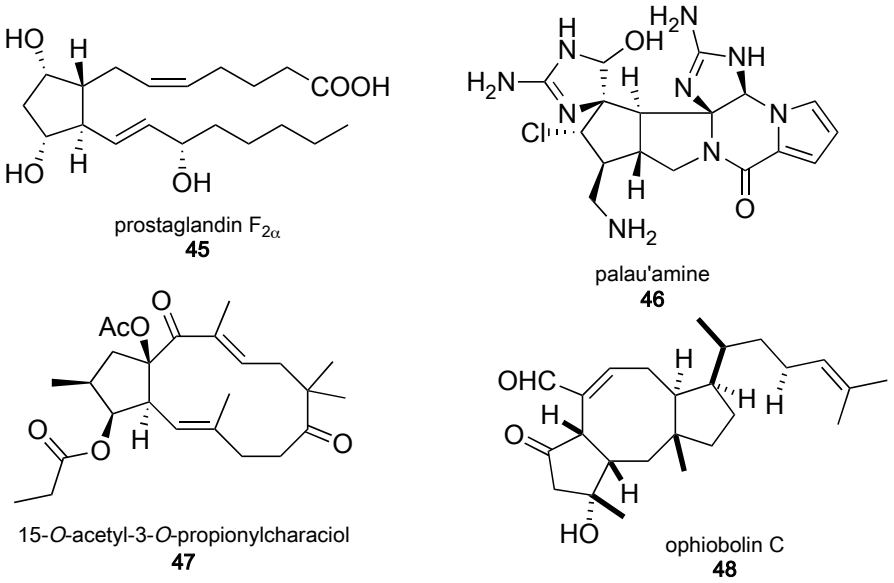

Figure 1.5: Natural Products Containing a Cyclopentane Moiety

1.6 Use of Acetal Phosphonium Salt Homoenolate Anion Equivalents in the Literature

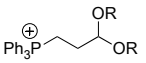

33
a. R = –$CH_2CH_2CH_2$–
b. R = –CH_2CH_2–
c. R = CH_3
d. R = C_2H_5
e. R = *i*-Pr

Because of the versatility and utility of these homoenolate anion equivalents in generating three possible products *viz.*, the plain C3-homologated aldehyde, the β,γ-unsaturated C3-homologated aldehyde, and the α,β-unsaturated C3-homologated aldehydes, we decided to conduct a comprehensive survey of the literature on their applications in organic synthesis. A summary of our findings are presented in Appendix A. In the survey, we classify the usage of **33a** - **33e** into three subcategories as described below:

three-carbon homologations when the Wittig product formed is hydrogenated to remove the unsaturation prior to deprotection;

β,γ-unsaturated aldehydes when the Wittig product is deprotected to give the non-conjugated C3-homologated aldehydes;

other uses when the Wittig products are not manipulated in the two preceding manner.

1.7 Looking Forward

From the survey given in Appendix A, we see that the acetal phosphonium salt homoenolate anion equivalents **33a** – **33e** are indeed of great utility in organic

synthesis. The substrate scope is wide when applied to three-carbon homologations and the generation of β,γ-unsaturated aldehydes, since various functionalities present in the starting material are tolerated. However, we do note the absence of their application to the generation of α,β-unsaturated aldehydes, which is the topic of our discussion in the following chapter.

Chapter 2

Method Development and Substrate Screening

2.1 Conceptualization of Project

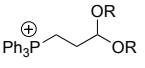

33
a. R = –$CH_2CH_2CH_2$–
b. R = –CH_2CH_2–
c. R = CH_3
d. R = C_2H_5
e. R = *i*-Pr

From the overview given in chapter 1, we were surprised to find that the use of these homoenolate anion equivalents **33a** – **33e** have been limited mainly to either a three-carbon homologating agent, or in the syntheses of β,γ-unsaturated aldehydes. Although the isomerisation of β,γ- to α,β-unsaturated aldehydes is highly favoured due to thermodynamic reasons, and Stowell *et. al.*[1] had demonstrated this use in their paper, yet there is a dearth of information on such application to the synthesis of a complex natural product.

It appears that the general consensus of the synthetic community is to regard this isomerisation as a nuisance in synthesis.[5,26] In fact, the move from initially using dioxan- and dioxolan-based acetals to dimethoxy-, diethoxy- and diisopropoxy-acetals, probably arose due to the need for the Wittig acetal products to be readily deprotected with minimal isomerisation.[27]

We surmised that this facile isomerisation is considered as a side reaction since the goal of most chemists utilising this homoenolate anion equivalent is to generate a β,γ-unsaturated aldehydes. However, we decided to embark on an exploration of the practicality of exploiting this 'side reaction' — the facile isomerisation of the Wittig acetal product after hydrolysis — and investigate the possibility of leveraging on it in natural product synthesis to advantange. What we envisaged is that the three-carbon homologation coupled with the isomerisation to the α,β-unsaturated aldehyde would result in an economy of steps with concomitant increase in product yields.

2.2 Method Development and Substrate Screening

Although Stowell *et. al.*[1] had illustrated the β,γ- to α,β-isomerisation in their paper, only one example was given and the aldehydes he had screened were all simple linear aliphatic aldehydes with no additional functionalities.

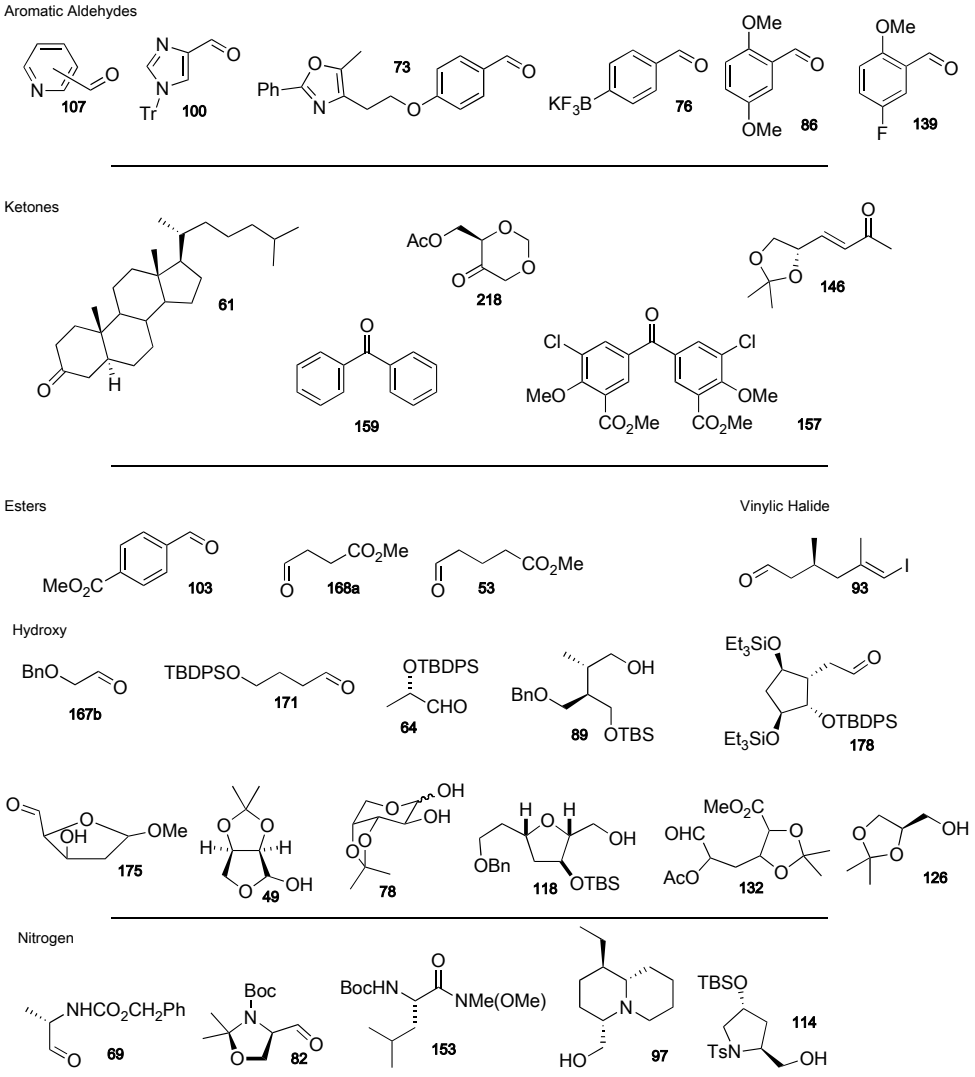

Figure 2.1: Compendium of Reactants Used in the Literature Reviewed

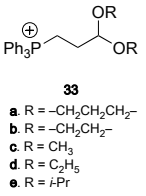

Despite the fact that **33a** – **33e** have been shown to tolerate the presence of various functionalities as can be seen from Figure 2.1, these were mainly in the context of

either three-carbon homologations or the generation of β,γ-unsaturated aldehydes. Hence, we decided to do a more comprehensive screen than that given by Stowell *et. al.*,[1] and fill in the details with a representative set of substrates. We report the results of our findings in Tables 2.1 and 2.2 of the following section.

2.3 Results and Discussion

Generally, the Wittig acetal products are easily formed in good to excellent yields as seen in Table 2.1. As expected from Wittig olefinations with a non-stabilized ylide (**33c**), the *cis*-isomers are obtained predominantly. Straight chain aliphatic aldehydes (**220a**, **220b**, **220f**) and branched aldehydes (**220c**, **220e**) generally give good to excellent yields. Secondary (**220d**) or tertiary aldehydes (**220e**) likewise give excellent yields.

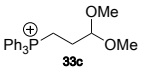

33c

For the case of aromatic aldehydes (**220g** – **220j**), whether they have electron-donating (**220h**) or electron-withdrawing substituents (**220i**), these too give good to excellent yields generally. Likewise, the heteroaromatic aldehyde **220j** gives excellent yield.

We note also that in terms of stereoselectivity, aliphatic aldehydes (**220a**, **220f**) give exclusively the *Z*-isomer when *t*-BuOK was used as the base, as Stowell *et. al.*[1] had demonstrated (Scheme 1.5). Likewise, bulky aliphatic aldehydes (**220d**, **220e**) give purely the *Z*-isomer. On the other hand, the products from aromatic (**220g** – **220j**) or α,β-unsaturated aldehydes (**220b**, **220c**) had poorer *Z*-selectivity. This

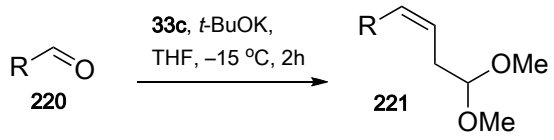

Entry	Aldehyde	Wittig Product	Yield (%)	E/Z^a
1	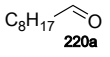	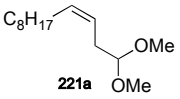	98	0:100
2	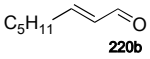	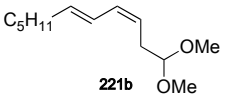	80	15:85
3	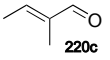	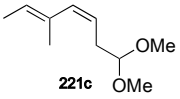	47	25:75
4	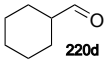	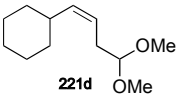	98	0:100
5		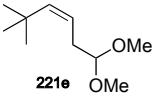	81	0:100
6	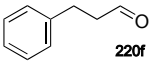	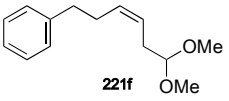	90	0:100
7	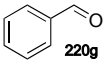	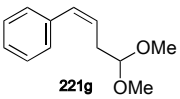	96	11:89
8	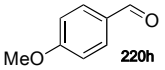	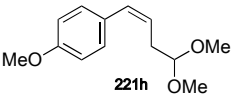	91	12:88
9	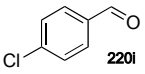	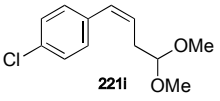	56[b]	38:62
10	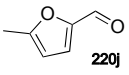	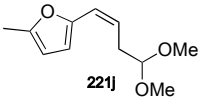	94	11:89

[a] E/Z ratios were determined from crude ^{1}H NMR.
[b] Only E-acetal was obtained after column chromatography.

Table 2.1: Generation of Wittig Acetal Products from (**33c**)

corroborates well with those reported in the literature we surveyed, such as Molander[28] and Voelker[29] (*E*/*Z* 20:80).

For the isomerisation of the products from β,γ- to α,β-unsaturated aldehydes and its application to natural product synthesis, we elected to adopt the procedure from Barbot and Miginiac.[30] This would give us the option of easily switching between obtaining the β,γ- or α,β-product when the need arises.

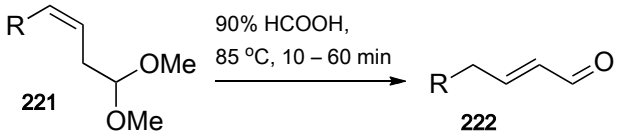

Entry	Wittig Product	Hydrolysis Product	Yield (%)
1	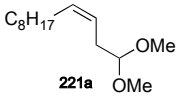	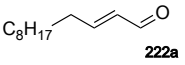	95
2	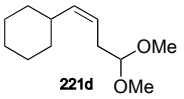	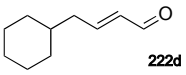	81
3	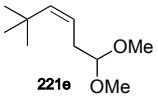	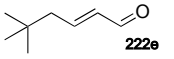	40
4	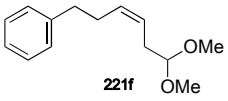	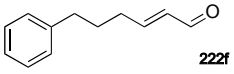	86
5	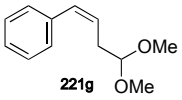	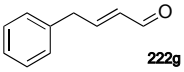	57
6	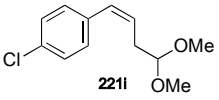	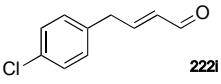	54

Table 2.2: Hydrolysis of Wittig Acetal Products

As can been seen from Table 2.2, by hydrolyzing under hot formic acid, the three-carbon homologated alkenal acetal products readily form the α,β-unsaturated

aldehydes in good to excellent yields under the reaction condition, without any β,γ-products.

Good to excellent yields are generally obtained for alkenal acetals derived from aliphatic aldehydes (**221a**, **221d**, **221f**), while average yields are obtained for those derived from aromatic aldehydes (**221g**, **221i**). We note also that diene acetals such as **221b** and **221c** give poor yields (not reported), perhaps arising from the harsh conditions of the Barbot hydrolysis protocol.

2.4 Looking Forward

Having demonstrated the feasibility of generating the α,β-unsaturated aldehydes via the homoenolate anion equivalent **33c**, and with the substrate scope established, we proposed to implement this methodology to the synthesis of the two natural products listed in Figure 2.2.

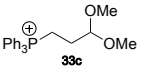

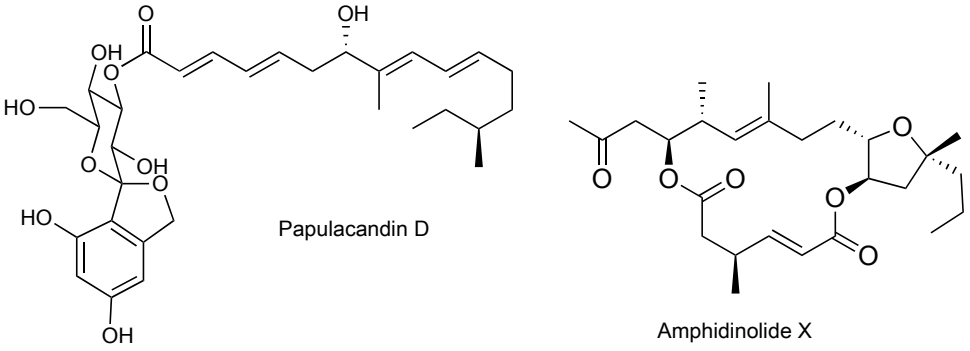

Figure 2.2: Papulacandin D and Amphidinolide X

The first simpler molecule, the acyl side chain of papulacandin D, as proof of concept, while the second more complex molecule, the total synthesis of amphidinolide X, to see if the method stands to scrutiny. This would ratify itself as a

rigorous test of scope and efficiency, as the application of any newly developed methodologies to the syntheses of natural products is the touchstone in discovering the utility, strengths and weaknesses inherent in the method apart from the idealized model studies.

To date, there are only two total synthesis of the antifungal antibiotic papulacandin D by the Barrett[31–33] and Denmark[34] groups, while there are several reports on the total synthesis of amphidinolide X by the groups from Fürstner,[35–37] Vilarassa,[38,39] Dai[40,41] and Lee.[42] These we will delve into in the following chapters.

Chapter 3

Background and Survey of Papulacandin D

3.1 Introduction

Antifungal agents are an important component in our pharmacological arsenal against opportunistic fungal infections. The increase in life expectancy from better healthcare in developed countries,[43,44] and a global increase in incidence of acquired immune-deficiency syndrome or AIDS,[45] has brought invasive fungal infections to the fore.[46] These usually arise in patients who are immunodeficient, immunocompromised or immunosuppressed due to disease or treatment for their diseases. Examples of these are patients with organ transplants, systemic lupus erythematosus, AIDS, or cancer patients undergoing high-dose chemotherapy.[47–49]

Invasive fungal infections often result in high morbidity and high mortality. Unfortunately, drug development in this area has lagged far behind that of antimicrobials,[50] which adds to the challenge for the attending physician in combating nosocomial infections.[51,52] Major opportunistic pathogens are *Candida spp.*, such as *C. albicans*, *C. glabrata*, *C. krusei*, *C. tropicalis*, *Pneumocystis spp.* such as *P. jirovecii* (formerly *P. carinii*) and *Aspergillus spp.* such as *A. fumigatus*, *A. flavus*, and *A. niger*.[51–54] These are currently treated with either amphotericin B as the gold standard, or azole-based drugs which are increasing in importance due to their lower toxicity.

However, a worrying trend is developing with the rapid rise in drug-resistance to antifungal azoles.[55–58] These azole drugs work by inhibiting an enzyme called lanosterol 14α-demethylase which converts lanosterol to ergosterol that is needed in cell membrane construction and for maintaining its integrity. When this occurs,

the amount of ergosterol in the cell is depleted and results in formation of cells with altered membrane structures or function. It also causes a buildup of ergosterol precursors that causes the cell to growth arrest.

The fungi develops resistance to azole drugs via a few main mechanisms. These are variously, the upregulation of genes governing multidrug efflux pumps and mutations to, or overexpression of, the lanosterol 14α-demethylase gene involved in cell membrane construction. By upregulating the efflux pumps, the effective concentration of azole drugs intracellularly is lowered. As such, the drug does not reach therapeutic levels that disrupt cell membrane synthesis or function. Also, when the lanosterol 14α-demethylase gene is either mutated or overexpressed, it results in the azole drug losing its specificity or potency, again overcoming the toxicity of the drug.[56] When azole drugs fail, the more toxic amphotericin B would have to be utilized as the last resort. However, given the high toxicity of amphotericin B, increased efforts into the development of alternative antifungal agents are crucial.[47,59]

A survey of the literature revealed a group of antifungal drugs that is currently under active development.[57,59] They collectively belong to the class called '-*candins*'. As many of these molecules have structural features which can be synthesized using the methodology explored in the previous chapter, we decided to take a closer look at this family of upcoming drugs.

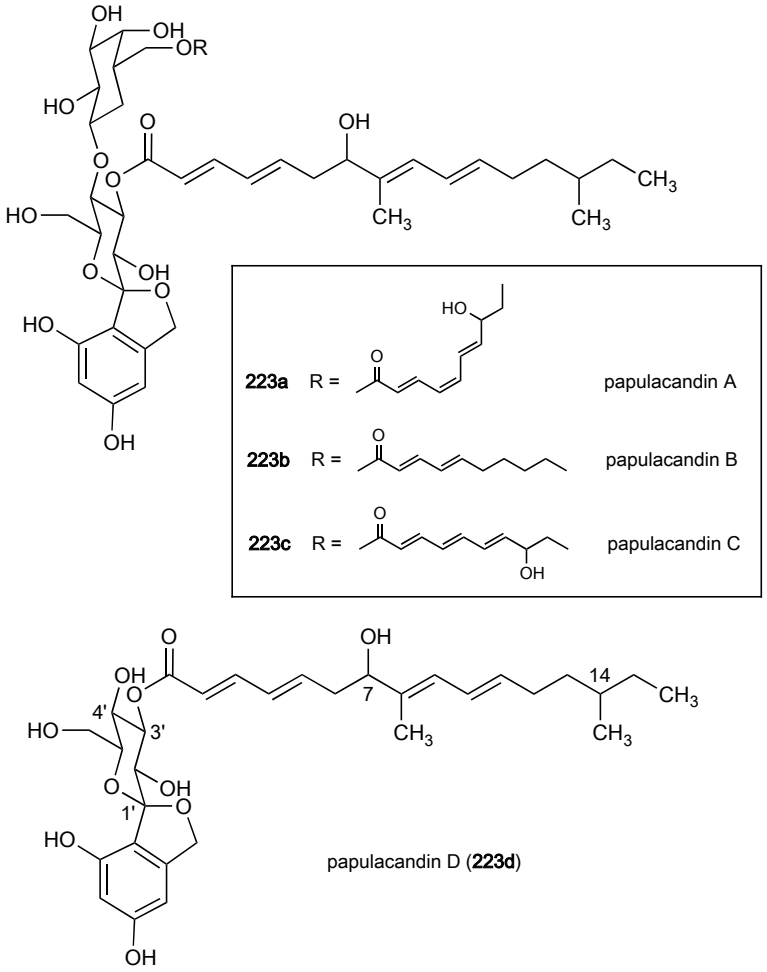

Figure 3.1: Structures of Papulacandins A, B, C and D

3.1.1 Biological Background

One of the first members of the candins to be discovered are the papulacandins. They are a class of glycolipids first isolated from the fermentation broth of *Papularia spherosperma* by Traxler *et. al.*[60,61] in the late 1970's via a routine screening for antibiotics. They were found to be active against *Candida albicans* and further investigations revealed that the mode of action is a non-competitive inhibition of the 1,3-β-D-glucan synthase.[49,62] This synthase is an enzyme important in fungal cell wall assembly, whose inhibition results in the formation of weakened cell walls or even cell lysis through osmotic rupture. This mode of action is distinct from

both the azole antifungals and amphotericin B. The azole antifungals inhibit cell membrane synthesis indirectly by acting on the enzyme needed to convert lanosterol to ergosterol, while amphotericin B, a polyene antifungal, effects its action by directly binding to ergosterol and forming aqueous pores in the cell membrane.

Since the 1,3-β-D-glucan synthase enzyme is only present in fungi but absent in mammals,[63–65] it becomes a significant target as this means that the therapeutic index of any drug based on 1,3-β-D-glucan synthase inhibition will be high i.e. there will be little or no toxicity on the infected host.

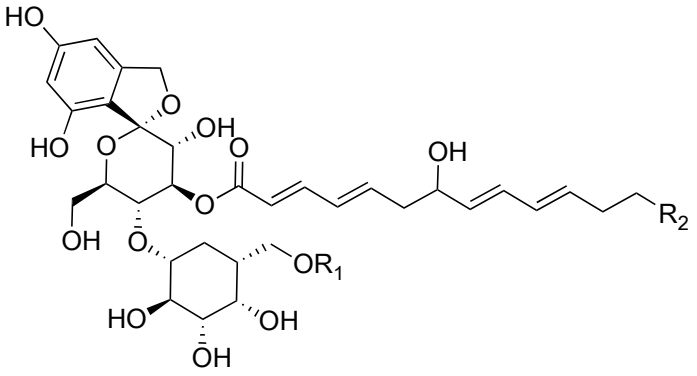

Entry	R_1	R_2
224a Chaetiacandin	–H	$-CH_3$
224b Saricandin	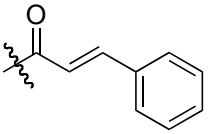	$-CH_2CH_2CH_3$
224c PF-1042	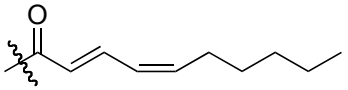	$-CH_2CH_2CH_3$

Figure 3.2: Representative Spiroketal Glycolipid Candins

Other molecules exhibiting the same antifungal activity were subsequently found, all exerting their effects via inhibition of the 1,3-β-D-glucan synthase. However,

structural elucidation reveals that these newer members are different structurally and can be segregated into two broad distinctions: the glycolipids, to which the papulacandins belong, and the lipopeptides. The glycolipids themselves are again separated into those having a spiroketal moiety and those without. A representative selection of these 1,3-β-D-glucan synthase inhibitors are shown in Figures 3.2–3.4.

3.1.2 Structural Features of Candins

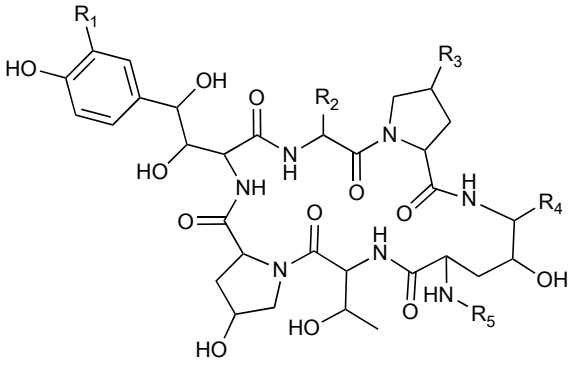

Entry		R_1	R_2	R_3	R_4	R_5
225a	Pneumocandin B_0	H	$NH_2(CO)CH_2CHOH$	H	OH	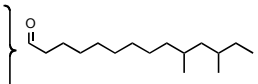
225b	Caspofungin	H	$NH_2(CH_2)_2CHOH$	H	$NH(CH_2)_2NH_2$	
225c	Echinocandin B	H	CH_3CHOH	CH_3	OH	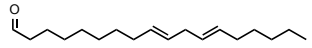
225d	Anidulafungin	H	CH_3CHOH	CH_3	OH	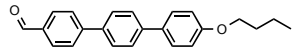
225e	FR901379	$HOSO_3$	$NH_2(CO)CH_2CHOH$	CH_3	OH	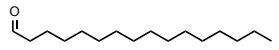
225f	Micafungin	$HOSO_3$	$NH_2(CO)CH_2CHOH$	CH_3	OH	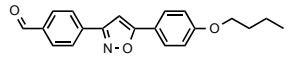

Figure 3.3: Representative Lipopeptide Candins[59]

As mentioned in the previous section, the class of candin antifungals are of two distinct groups. As seen in Figure 3.3, lipopeptide candins have a distinctive cyclic peptide moiety and a fatty acyl side chain.

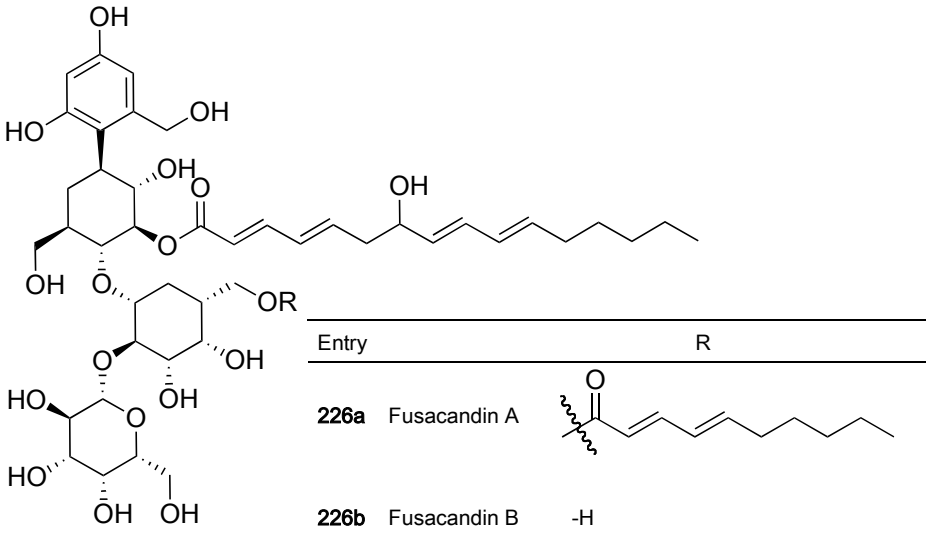

Figure 3.4: Representative Non-spiroketal Glycolipid Candins

The glycolipid candins on the other hand has a glucan moiety that can either be cyclized to form a spiroketal, as in the papulacandins, or left open to give the fusacandins.

3.1.3 Structural Features of Papulacandins

The family of papulacandins isolated are structurally related, and comprises of papulacandins A, B, C, D and E. Except for papulacandin E whose structure has not been reported, the structures of the other family members are shown in Figure 3.1. All members have a distinct spirocyclic glycoside moiety esterified with an acyl side chain at the *O*-C(3') hydroxy position of the glucose unit.[33,34,61,66] These structural motifs give rise to the amphiphilic nature of the molecule. Structure-activity relationship (SAR) studies have shown that deletion of the acyl side chain causes loss of activity. Apart from this, unsaturation of the acyl side chain has

been shown to be of importance for activity, with hydrogenation leading to diminished or no activity.[66] Also, it has been noted that the 5-membered spirocyclic ring is not indispensible for activity.[67,68]

Studies by Römmele *et. al.* thus led them to conclude "that less complex derivatives like papulacandin D may be good starting material for further chemical modifications to obtain more active compounds",[66] which premise is probably the reason why total syntheses of papulacandins to date are based on papulacandin D (**223d**).[31,33,34]

3.2 Reported Total Synthesis of Papulacandin D

In the literature, there are currently only two reported total syntheses of papulacandin D. The first is the pioneering piece of work done by Barrett *et. al.*[31,33] on both the structural elucidation and the total synthesis of papulacandin D, wherein the absolute stereochemistry is established. The other is a more recent work by Denmark *et. al.*. In this synthesis, Denmark's group successfully demonstrated the practicality of silicon-based methodologies they developed, by applying it to the syntheses of both the acyl side chain as well as the spirocyclic *C*-aryl glycopyranoside moiety.[34]

3.2.1 Retrosynthetic Analysis by Barrett *et. al.*

Retrosynthetic analysis of papulacandin D (**223d**) by Barrett *et. al.*[33] suggested to them that the molecule could be synthesized from the esterification of the

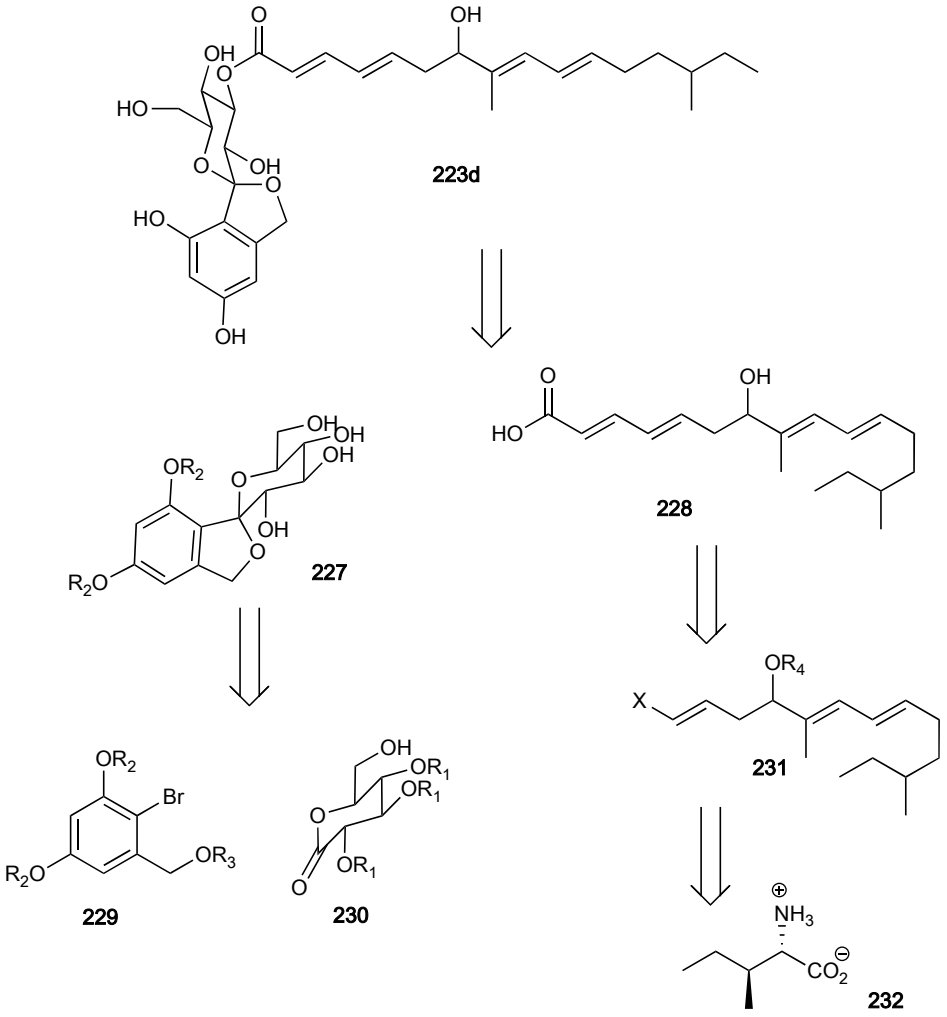

Scheme 3.1: Retrosynthetic Strategy of Barrett *et. al.*

acyl side chain **228** with the *O*-C(3') of the spiroketal moiety **227** as shown in Scheme 3.1. The spiroketal moiety could be assembled from an adaptation of the condensation reaction between β-diketone dianions and lactones, developed in their laboratory.[31,69–72] Given our interest in the application of our recently developed methodology to the synthesis of the acyl side chain of papulacandin D, we will only focus on the discussion of their retrosynthetic analysis of the acyl side chain.

At first glance, the retrosynthetic analysis of the acyl side chain of papulacandin D appears relatively straightforward — a tetra-unsaturated fatty acyl chain, with only two stereogenic centres at C(7) and C(14) to contend with. For the stereogenic considerations at C(14), Barrett's group turned to nature and deliberated on its biosynthesis. Studies in 1983 by Cane, Kaplan and Hensens[73] has provided evidence towards the biosynthetic origins of avermectins, a group of macrolides with a characteristic 16-membered lactone and a spiroketal moiety. In their investigations, L-isoleucine was established to be the biosynthetic precursor of the *sec*-butyl substituent in avermectins A_{1a}, A_{2a}, B_{1a} and B_{2a}. Correspondingly, the Barrett group speculated that in the biosynthesis of papulacandin D, the stereogenic centre at C(14) could be generated from an L-isoleucine subunit. Based on this premise, the forward synthetic design started from the naturally abundant and commercially inexpensive amino acid L-isoleucine.

A sequential series of Wittig olefination reactions to give aldehyde (**236**) set up the stage towards a secure strategy to define the stereogenic centre at C(7). The group sought to do so via an asymmetric propynylation with chiral allenylborane reagents developed by Corey *et. al.*[74] Completion of the synthesis for the acyl side chain was envisioned to be achieved through the organopalladium catalyzed coupling of triene intermediate **231** with either "β-stannylacrylate ester (X = Br or I, etc.) or β-bromoacrylate ester (X = $SnMe_3$ or $ZrCp_2Cl$, etc.)".[33]

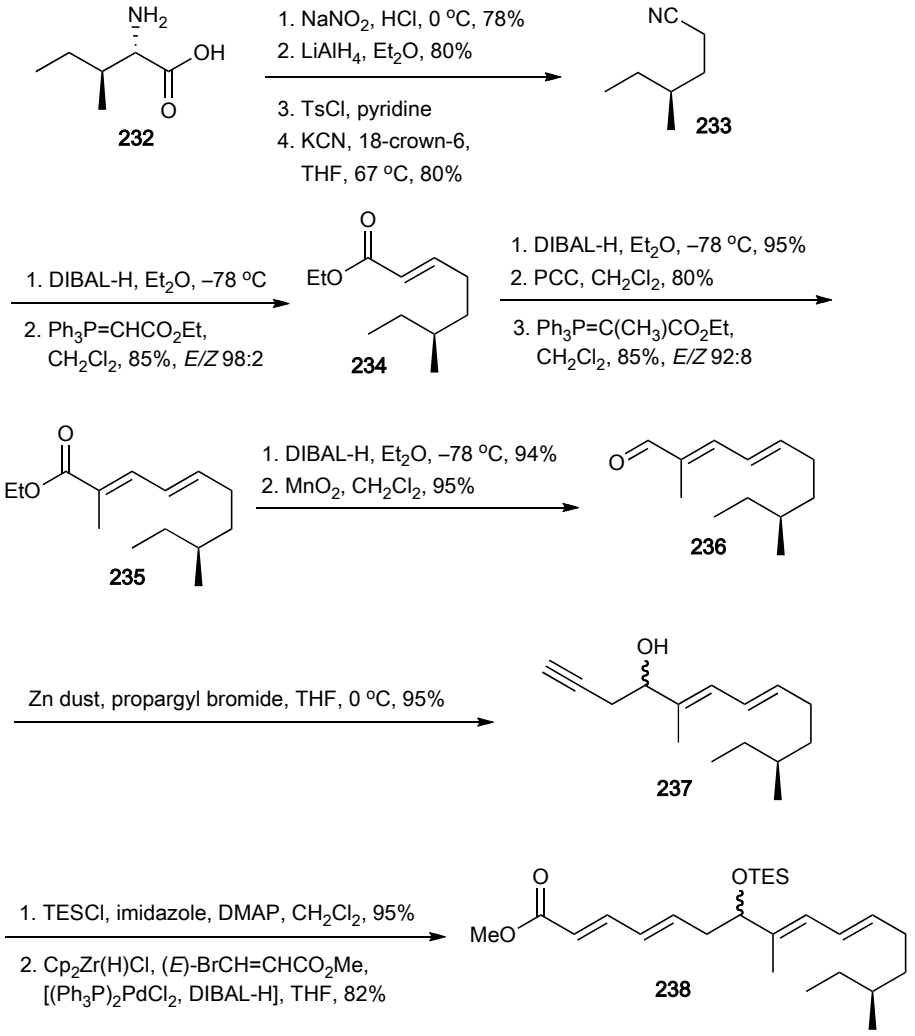

Scheme 3.2: Barrett's Initial Synthesis of Papulacandin D Acyl Side Chain

3.2.2 Synthesis by Barrett *et. al.*

As depicted in Scheme 3.2, the synthesis commenced with procuring the aldehyde **241** from L-isoleucine (**232**) via (3*S*)-methylpentan-1-ol (**239**), a fully characterized compound,[75,76] thereby securing the first stereocentre at C(14).

Interestingly, Barrett[33] proposed two synthetic routes to obtain ester **235**. On a small scale synthesis, transformation of chiral alcohol **239** was carried out using toluene-4-sulphonylation, followed by an S_N2 displacement with lithium bromide

and finally a carbonylation of the Grignard reagent derived from bromide **240** as depicted in Scheme 3.3.

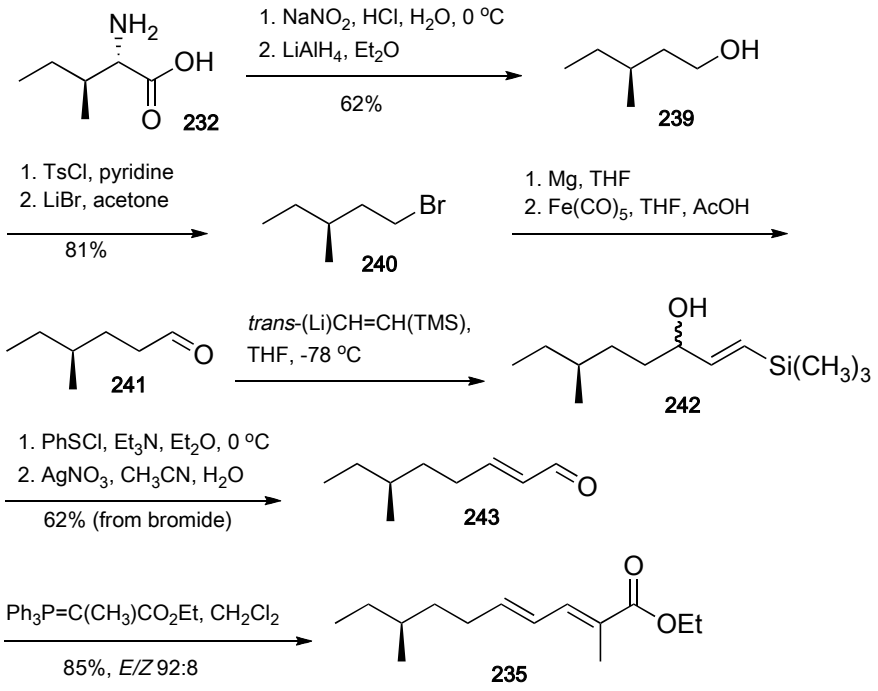

Scheme 3.3: Small Scale Synthesis of Ester **235**

For ease of handling in large scale synthesis, the second proposed synthetic route begins with a one-carbon homologation of the chiral alcohol **239**. This involved the reaction of the 4-toluenesulphonate derivative of chiral alcohol **239** with potassium cyanide. Subsequently, a DIBAL-H reduction provided aldehyde **241**. This was then put through two Wittig olefinations with an intervening reduction/oxidation sequence to obtain the diene ester **235**. Another reduction/oxidation to obtain aldehyde **236** set the stage for installation of the last stereogenic centre on C(7), generating homopropargylic alcohol **237**.

Initial plans for defining the C(7) stereochemistry were to carry out an asymmetric propynylation of aldehyde **236** with chiral allenylborane reagents.[74] However, attempts to do so were only moderately successful with a diastereoselectivity of

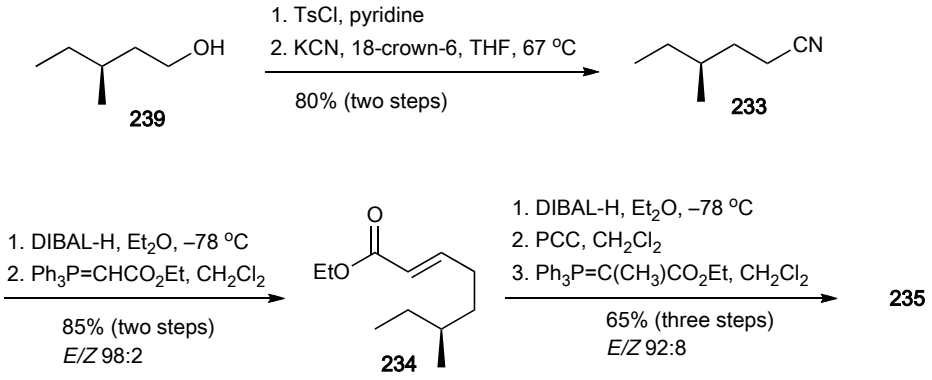

Scheme 3.4: Large Scale Synthesis of Ester **235**

less than 62%. As the group was not only concerned with the total synthesis of papulacandin D but more importantly, the elucidation of the actual stereochemistry of the side chain of the target molecule, it was essential that they obtain the tetraene ester **238** in very high diastereoisomeric purity. However, their efforts to derivatize the alcohol **237** for separation by chromatography proved to be unproductive unfortunately. Hence, as an alternative strategy, the group decided to employ kinetic resolution under Sharpless epoxidation[77–80] conditions to attain the desired unreacted alchohol **237a** in 45% yield, 90% theoretical yield.

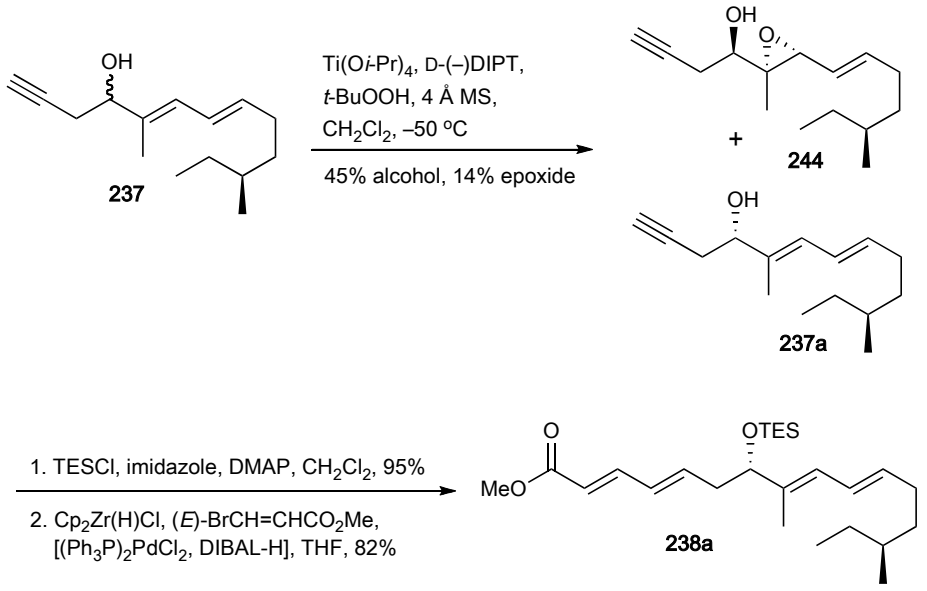

Scheme 3.5: Sharpless Epoxidation

With the desired homopropargylic alcohol in hand, completion of the synthesis of the acyl side chain via an alkyne hydrometalation and palladium(0)-catalyzed coupling was expected to be a straightforward and secure strategy. Unexpectedly, a few complications arose in the final assembly of the delicate tetraene ester side chain.

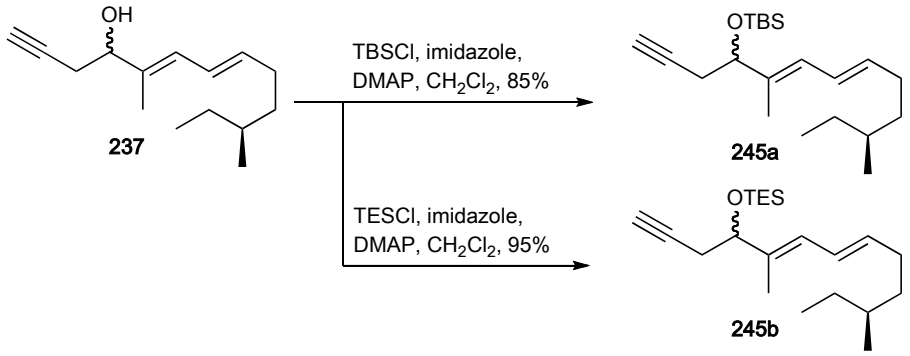

Scheme 3.6: Protected Alkyne **237** for Hydrozirconation

Hydrozirconation of TBS-protected alkyne **245a** followed by iodolysis provided an unstable vinyl iodide which was not isolated. Instead, the reaction mixture was passed through a short alumina column. This was used directly for coupling with methyl (3*E*)-(tributylstannyl)acrylate in the presence of bis(triphenylphosphine)-palladium(II) dichloride. The reaction mixture was observed to turn black immediately and subsequent attempts at purification yielded the desired tetraene ester in low and variable yields (<30%).

In view of these failings, the group examined alternative coupling conditions. The vinyl zirconocene obtained from TES-protected alkyne **245b** after hydrozirconation was allowed to react with zinc chloride to obtain a vinyl zinc transmetallated product. Again, without isolation, the vinyl zinc reagent was reacted with (3*E*)-bromoacrylate in the presence of tetrakis(triphenylphosphine)palladium(0). Under

such conditions, the desired tetraene ester was obtained in good yield (64%). While the coupling between the vinyl zinc reagent and (3*E*)-bromoacrylate provided the desired ester in good yield, it was uncertain whether the transmetallation step was essential.

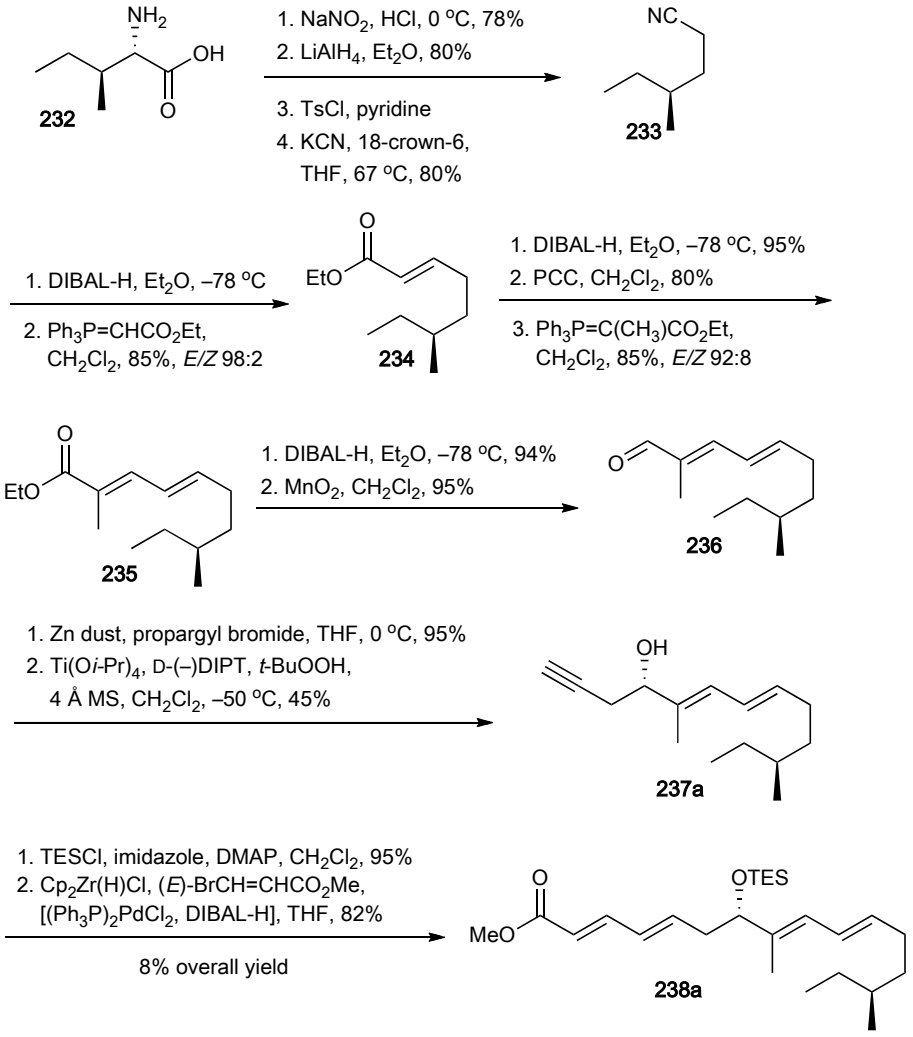

Scheme 3.7: Barrett's Eventual Synthetic Scheme for Papulacandin D Acyl Side Chain

According to a report by the Negishi group,[81] it is possible to perform a direct coupling of the vinyl zirconium reagent with methyl (3*E*)-bromoacrylate and a catalytic amount of a palladium-phosphine complex that is generated from bis(triphenylphosphine)palladium(II) dichloride using DIBAL-H. Using Negishi's

coupling conditions, the Barrett group was rewarded with a superior yield of the desired tetraene ester **238a** in 82% yield.

At this point, the synthesis of the acyl side chain was successfully completed by the Barrett group, over 15 steps with an overall yield of 8%.

3.2.3 Retrosynthetic Analysis by Denmark *et. al.*

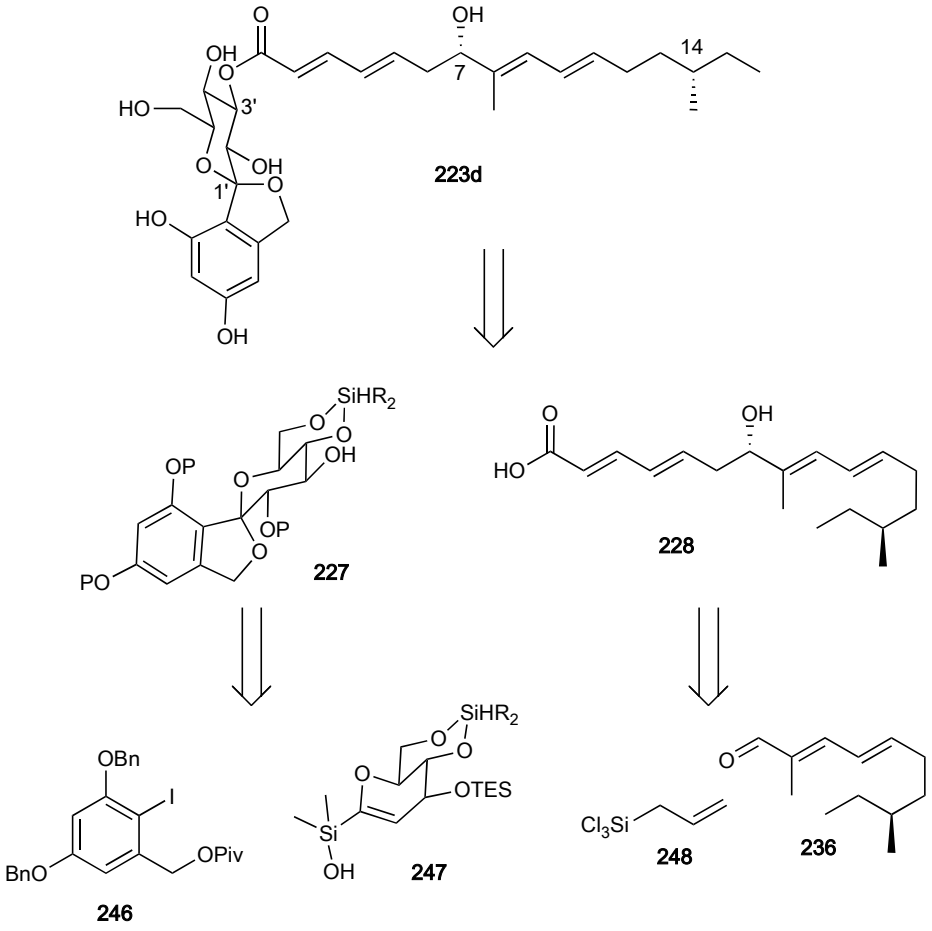

Scheme 3.8: Retrosynthetic Strategy of Denmark *et. al.*

The retrosynthetic strategy of Denmark *et. al.*[34] is shown in Scheme 3.8. They first disconnected the molecule into two fragments at the *O*-C(3') ester linkage, to give the unsaturated acyl side chain **228** and the spiroketal moiety **227**.

They initially envisaged that **227** could be obtained via the synthesis of C-aryl-2*H*-pyrans by utilizing the palladium-catalyzed cross-coupling reaction of the 2-pyranylsilanol **247** and the aryl iodide **246** — a methodology their group had previously developed.[82]

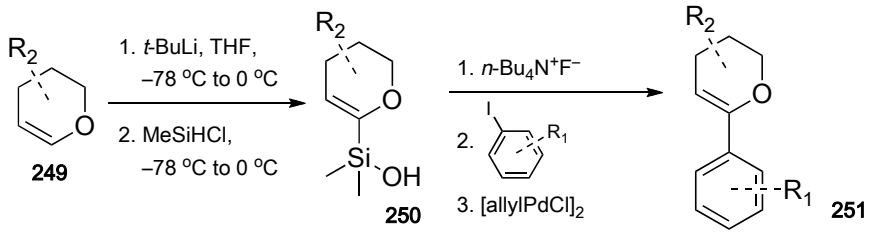

Scheme 3.9: Denmark's Coupling

However, a major drawback of that transformation was the limited applicability of the methodology to simple substrates and the incompatibility of the fluoride activation required with commonly employed silicon protecting groups in total syntheses. As such, they were eager to challenge themselves with their newly developed "fluoride-free variant" that was more recently reported.[83]

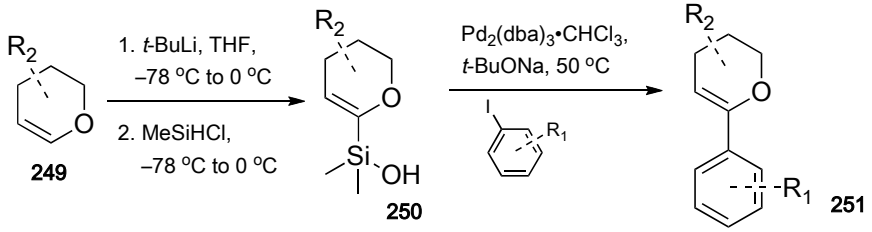

Scheme 3.10: Denmark's Fluoride-Free Coupling

The key chemistry involved in the synthesis of the spiroketal moiety in papulacandin D is the adaptation of this methodology and the demonstration of its compatibility in the context of a natural product synthesis.

In the retrosynthetic analysis of the acyl side chain **228**, the Denmark group's strategy was to construct the chiral centre at C(7) through the use of their chiral bisphosphoramide catalyst **252**[84,85] in an enantioselective addition of allyltrichlorosilane to dienal **236**.

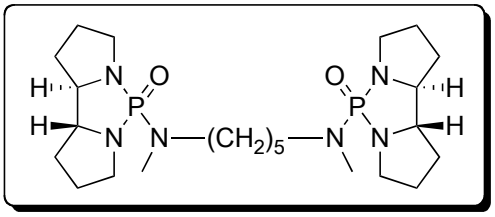

Figure 3.5: Denmark's Chiral Bisphosphoramide Catalyst

This dienal **236** could be further derived from geraniol (**253**) with a series of straightforward chemical transformations in addition to a crucial asymmetric hydrogenation to provide (*S*)-citronellol (**254**), thus establishing the chiral centre on C(14). To complete the synthesis of the acyl side chain, elongation of dienal **236** to generate unsaturated carboxylic acid **228**, was perceived to be easily obtained, via olefin metathesis and Wittig olefination.

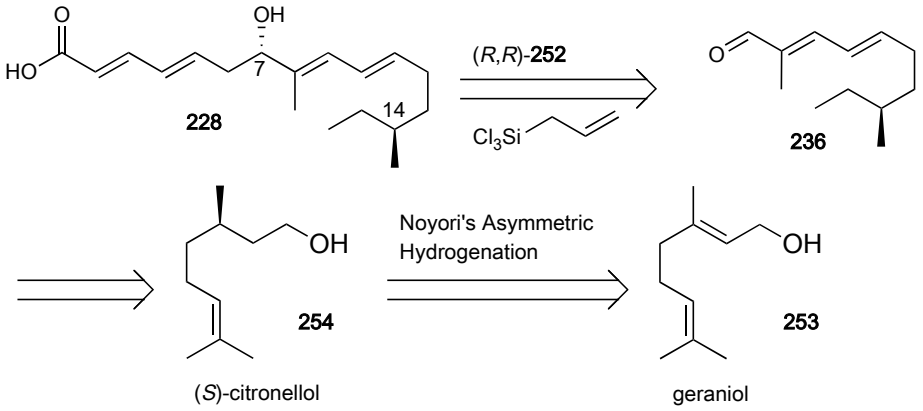

Scheme 3.11: Denmark's Retrosynthetic Analysis of Papulacandin D Acyl Side Chain

3.2.4 Synthesis by Denmark *et. al.*

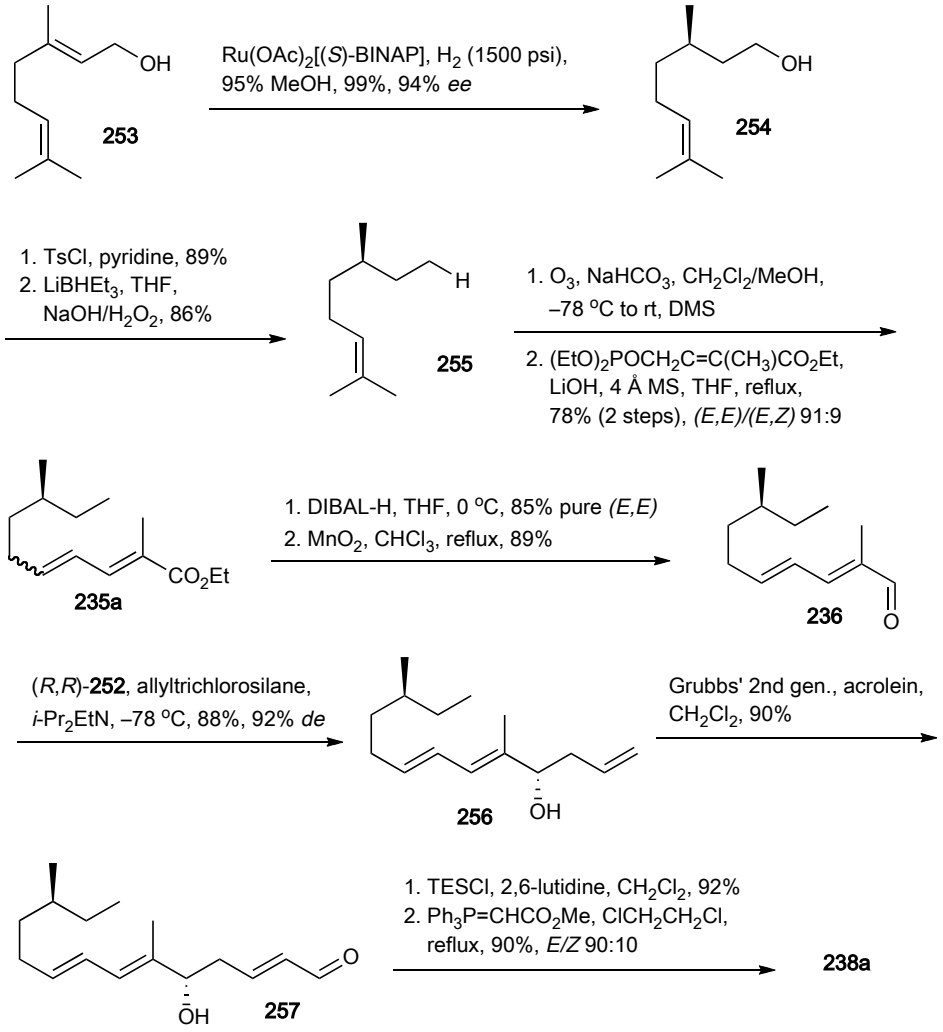

Scheme 3.12: Denmark's Synthesis of Papulacandin D Acyl Side Chain

Starting with commercially available geraniol (**253**) that was enriched by spinning-band distillation, Denmark *et. al.* carried out Noyori's asymmetric hydrogenation with catalytic $Ru(OAc)_2[(S)\text{-BINAP}]$[86,87] to obtain (*S*)-citronellol (**254**) in excellent yield and enantiomeric excess (99%, 94% *ee*). This then underwent tosylation, followed by an S_N2 attack with superhydride $LiBHEt_3$ to provide the deoxygenated hydrocarbon **255** in good yield (88%, over two steps). The stable intermediate ethyldienoate ester **235a** was readily procured by ozonolysis followed by a Horner-Wadsworth-Emmons olefination. This unsaturated ester **235a** was found to be

an inseparable mixture of isomers ($\Delta^{10,11}$ *E:Z*=91:9). However, these geometrical isomers were readily resolved by column chromatography in the subsequent DIBAL-H reduction to the corresponding alcohol (85%, pure *E,E*). Oxidation with manganese oxide then afforded aldehyde **236** in good yield (89%).

With dienal **236** in hand, the group proceeded with their key step — a Lewis base-catalyzed enantioselective allylation methodology developed by their group, utilizing chiral bisphosphoramide (*R,R*)-**252**. This went on uneventfully to give the desired homoallylic alcohol **256a** in good yield and excellent diastereoselectivity (88%, 92% *de*). Subsequent olefin metathesis with Grubb's second generation catalyst, protection of the C(7) hydroxyl group with chlorotriethylsilane and a final Wittig olefination furnished the desired methyl ester of the papulacandin D acyl side chain (**238a**) in an overall yield of 29% over 11 steps.

Chapter 4

Synthesis of Papulacandin D Acyl Side Chain

4.1 Introduction

With the importance of antifungal drug development delineated in the previous chapter and our brief survey therein of the only two total syntheses of papulacandin D, we expectantly applied the methodology we had developed in chapter 2 to the synthesis of its acyl side chain. To facilitate our discussion, the numbering of the carbon skeletons in the following schemes will be based on that for papulacandin D.

Returning to the examination of the acyl side chain of papulacandin D, we propose the following retrosynthetic plan as depicted in Scheme 4.1

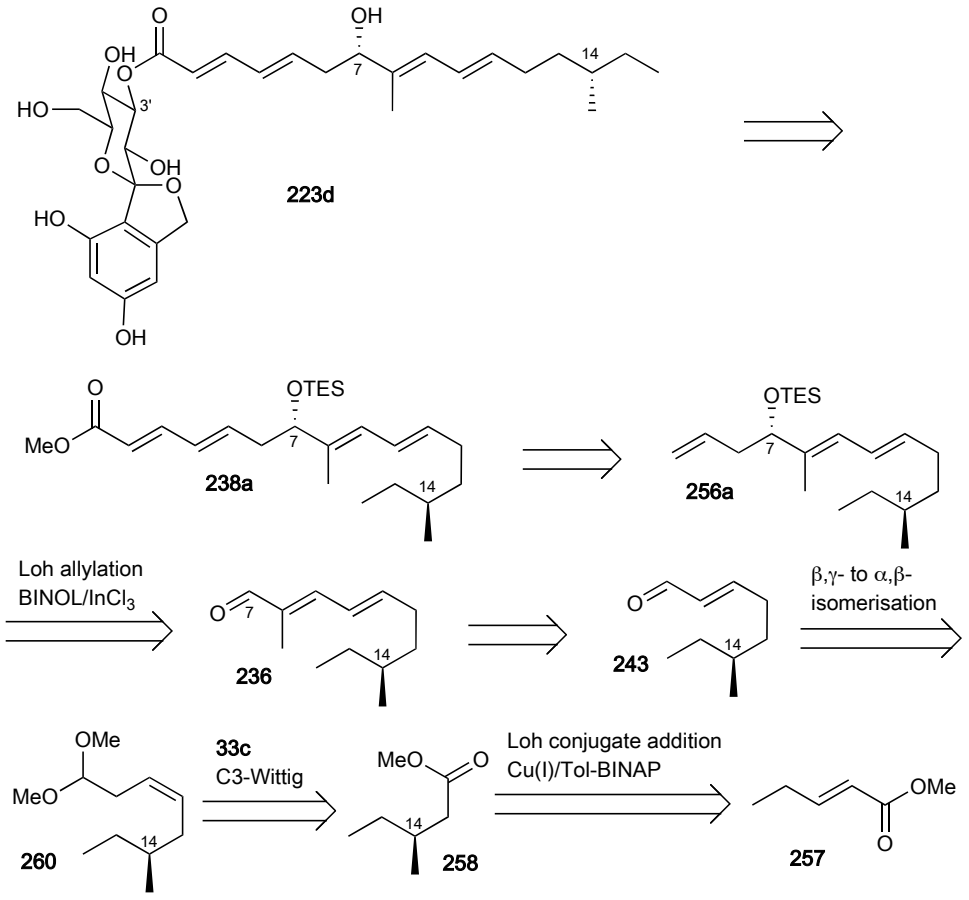

Scheme 4.1: Papulacandin D Retrosynthetic Analysis

As with Barrett *et. al.*, and Denmark *et. al.*, the first obvious disconnection was at the *O*-C(3') ester bond, establishing the two main fragments — the spiroketal moiety **227** and the acyl side chain **228**. In like manner, this acyl side chain would be synthesized as the methyl ester **238a** where the hydroxy group is triethylsilyl-protected.

4.2 Key Considerations on Our Retrosynthetic Strategy

Given the relatively simple features present in the acyl side chain, with only two chiral centres to contend with, our first consideration was the generation of the C(7)-hydroxy chiral centre. As mentioned previously in subsection 3.2.2, the strategy employed by Barrett *et. al.* to access this chiral alcohol **237a** involved an initial zinc mediated propargylation to give racemic allylic alcohol **237**, followed by resolution under Sharpless epoxidation conditions to recover the desired alcohol (**237a**) (Schemes 3.7 and 3.5). Such a strategy was evidently tortuous and inefficient, as in theory 50% of the yield would immediately be lost by kinetic resolution via Sharpless epoxidation.

Denmark's strategy was much more elegant and efficient, choosing instead to generate the chiral alcohol **256** in one step, using a methodology developed in-house. This Lewis base-catalyzed asymmetric allylation involves the use of their chiral phosphoramide catalyst **252** that enantioselectively adds allyl trichlorosilane to aldehyde **236**.

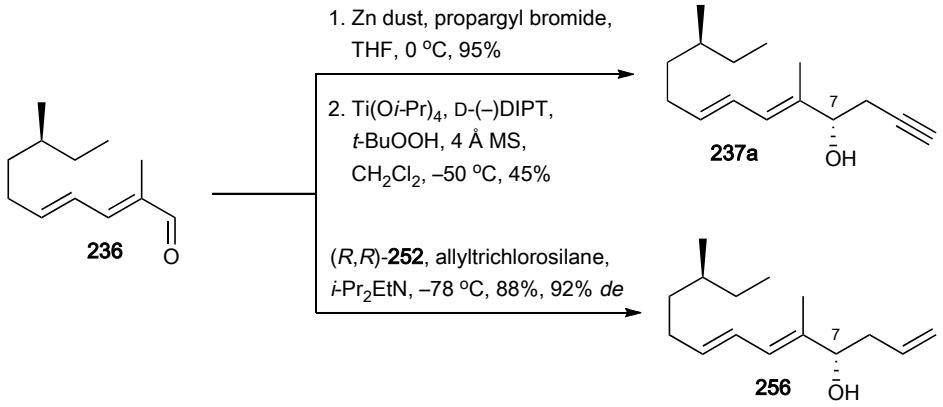

Scheme 4.2: Comparison of Barrett's and Denmark's Strategy for C(7)-hydroxy Generation

As our group too has been involved in the area of catalytic asymmetric allylation, specifically via chiral indium(III) complexes,[88–91] we were inclined to shadow Denmark's approach. In our case, we will apply our own asymmetric allylation methodology that is Lewis acid-based, to obtain the C(7)-hydroxy chiral centre.

For the other chiral center at C(14), Barrett considered its biosynthesis and thus accessed it through the cheap and readily available enantiopure (L)-isoleucine (**232**), using a diazotization followed by a reduction to the (3*S*)-methylpentan-1-ol (**239**) (Schemes 3.3 and 3.4). Incidentally, this chiral alcohol is also commercially available.

Denmark *et. al* on the other hand, chose to gain access to this chiral center by building it through the asymmetric hydrogenation of the commercially available geraniol (**253**) using Noyori's catalyst. This was followed by a reduction with the superhydride $LiBHEt_3$ before an ozonolysis is executed to generate the requisite aldehyde **241**, in the process also removing three carbons as acetone. Through a judicious choice of starting material and methodologies, Denmark again procures higher yields through efficient and effective strategies.

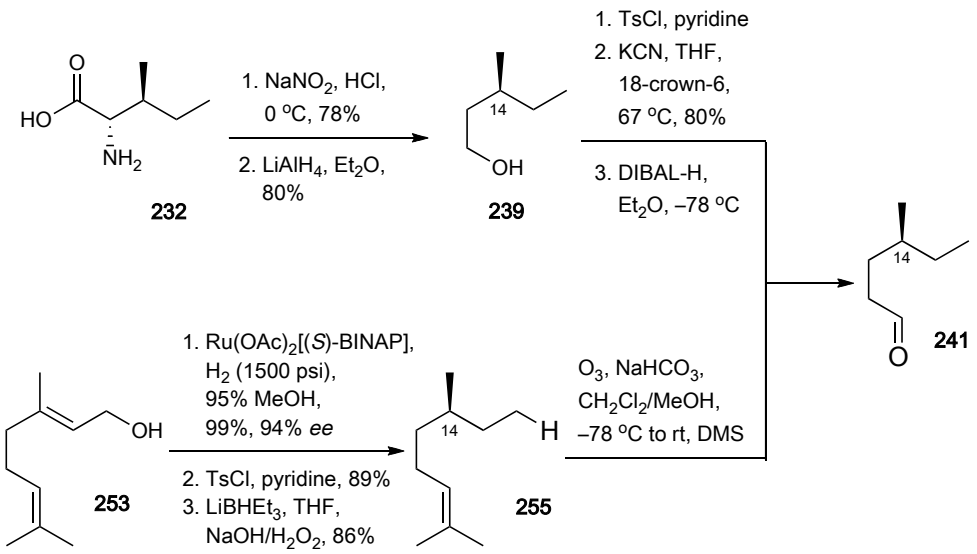

Scheme 4.3: Comparison of Barrett's and Denmark's Strategy for C(14) Chiral Center

For our case, we have recently developed a means to achieve an asymmetric conjugate addition to α,β-unsaturated esters through the use of Cu(I)/Tol-BINAP with Grignard reagents.[92,93] This has been applied to the syntheses of the natural products siphonarienal, siphonarienone and iriomoteolide 1a.[92–96] Here, we would like to demonstrate its utility again, by installing the chiral center at C(14), using methyl 2-pentenoate as starting material. This is shown in our retrosynthetic analysis (Scheme 4.1) and in the forward synthesis in Scheme 4.9. Thereafter, the product would be put through the three-carbon Wittig homologation with **33c** and hydrolyzed to form the conjugated α,β-unsaturated aldehyde via isomerization. Having laid these out, we proceed to an in-depth discussion of these key steps.

4.2.1 Asymmetric Allylation Reaction

In a review by Denmark and Fu,[97,98] they had attributed the popularity of metal-based allylation of aldehydes in the construction of acyclic systems carrying controlled sequences of stereocenters to the following factors:

1. Acquisition of highly diastereo- and enantioselective products is possible;
2. Judicious employment of different metals proffers the ability to fine-tune reagent reactivities;
3. Potential for further diverse chemical transformations on the homoallylic alcohol product formed aids synthetic planning.

Given the cornucopian methods available for the catalytic enantioselective addition of allylic organometallic reagents to aldehydes, a classification system which groups reagents into three main categories is generally subscribed to:[97,98]

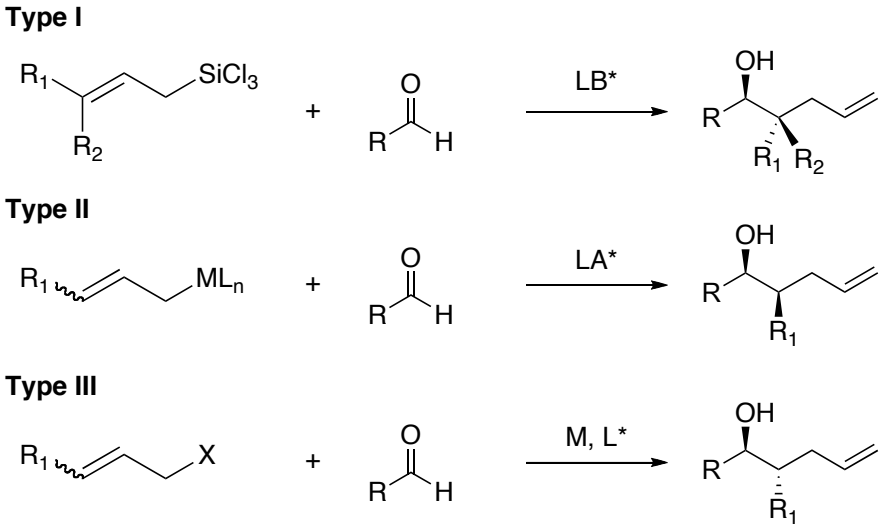

Scheme 4.4: Classification of Allylation Reactions

Type I reactions Where the addition of allylic trichlorosilanes are catalyzed by chiral Lewis bases and the *syn-/anti-* diastereoselectivity is reflected by the *Z-/E-* ratio of the allylic geometry.

Type II reactions Where the addition of allylic organometallic reagents (Si, Sn, B) are catalyzed by chiral Lewis acids and predominantly *syn-* diastereoselectivity is observed, independent of the starting allylic geometry.

Type III reactions Where the addition of allylic organometallic reagents (Cr, Zn, In) are generated *in situ* from the corresponding allylic halides and are catalyzed by chelating ligands. This type of reaction leads to predominantly *anti-* diastereoselectivity that is independent of the starting allylic geometry.

In the total synthesis of papulacandin D, Denmark *et. al.*[34] employed chiral bisphosphoramide (*R,R*)-**252** to achieve the enantioselective allylation of aldehyde **236**. This chiral Lewis base-catalyzed allylation reaction is of Type I (Scheme 4.4), a methodology specifically designed to overcome the problems associated with Type II catalysis involving the use of Lewis acids with allylic silanes and stannanes.[97,98] The general scheme by which Lewis base-promoted allylation gives rise to improved diastereoselectivity can be attributed to the more rigid, closed transition state as shown in Scheme 4.5.[97–101]

This is in contrast to Lewis acid-catalyzed allylation, which goes through a more flexible open transition state mechanism and hence gives poorer diastereocontrol. Here, we see that in cases when γ-substituted allylic reagents are employed, the *syn-* homoallylic alcohol is the major product, independent of the geometry of the

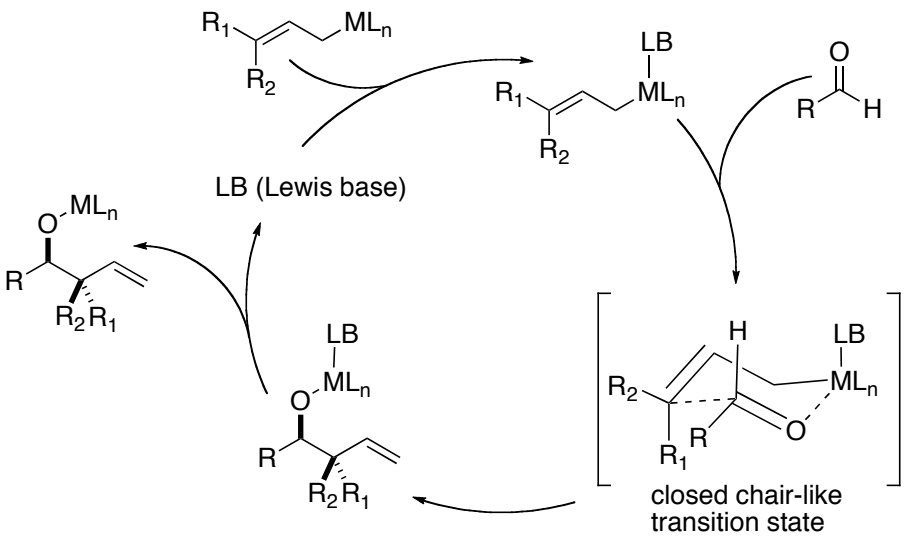

Scheme 4.5: Lewis Base-Promoted Allylation

starting allylic reagent. It is proposed that the anti-periplanar transition structure is favoured because of the minimization of the steric interactions between the aldehyde R group and the γ-R' group of the allylic reagent. Such a Type II reaction involves the use of Lewis acids and proceeds via an open transition state model as depicted in Scheme 4.6.[97–101]

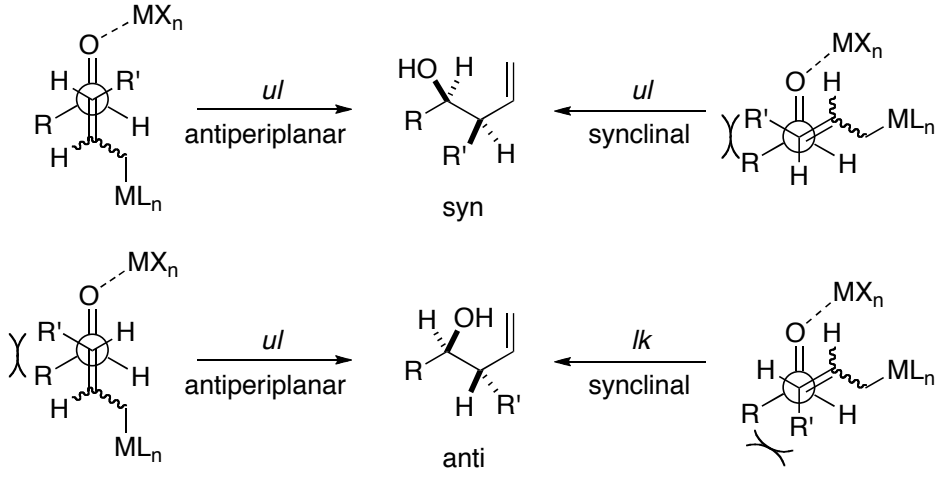

Scheme 4.6: Lewis Acid-Promoted Allylation

Although this may be the case, yet it is our intention to generate the C(7)-hydroxy chiral centre by means of a catalytic asymmetric allylation via the chiral indium

complex developed by our group.[88] Even though our methodology falls into the class of Type II catalysis, it generally serves admirably for simple allylation reactions where diastereoselectivity is not an issue, as is the case with the synthesis of papulacandin D. Here, the C(7)-hydroxy chiral center is obtained using a simple allylation with no diasteroselectivity issues to consider.

4.2.2 Asymmetric Conjugate Addition

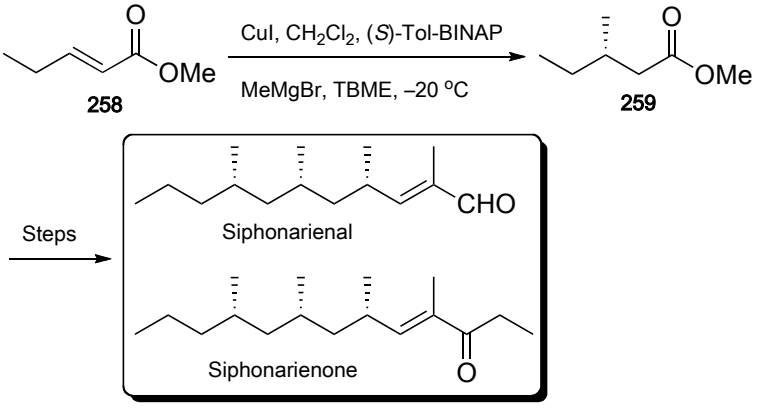

Scheme 4.7: Synthesis of Siphonarienal and Siphonarienone

The asymmetric conjugate addition of a methyl group to the α,β-unsaturated methyl ester **258** to generate methyl (3*S*)-methylpentanoate (**259**) has been applied by our group to the synthesis of siphonarienal and siphonarienone.[92,93,95] Since the required chiral alcohol **239** can be procured using a DIBAL-H reduction on **259**, we do not foresee any issues complicating this step of the synthesis.

4.2.3 Wittig Three-carbon Homologation/Isomerisation

In Chapter 2, we have demonstrated via our panel of substrates that simple aliphatic aldehydes give excellent yields for the three-carbon homologation with

the phosphonium salt based homoenolate anion equivalent **33c**. We also showed that these products undergo the subsequent hydrolysis-isomerization readily to give the desired α,β-unsaturated aldehyde with excellent yields. As such, we do not foresee any issues with the generation of the requisite α,β-unsaturated aldehyde **243**.

4.3 Synthesis of Papulacandin D Acyl Side Chain

Our forward synthesis of the acyl side chain of papulacandin D is depicted in scheme 4.8. Since the chiral alcohol (3*S*)-methylpentan-1-ol (**239**) is commercially

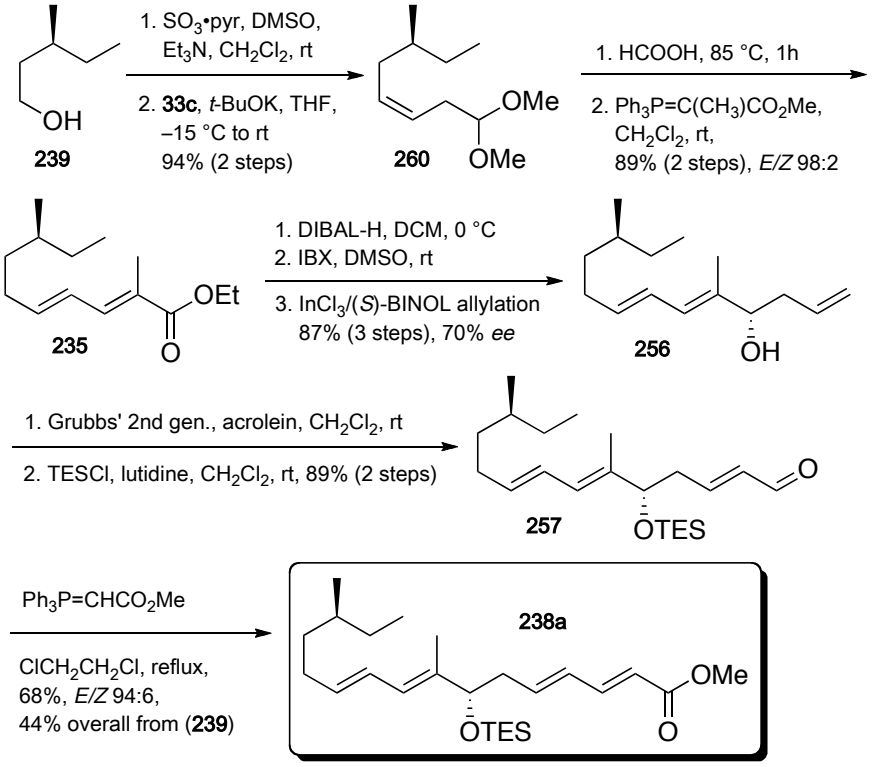

Scheme 4.8: Papulacandin D Synthesis

available, we opted to begin our synthesis from it. However, as a proof-of-concept

of the applicability of our asymmetric conjugate addition, we performed a small-scale synthesis of **239** from *trans*-methyl pentenoate (**258**), using Cu(I)/(*S*)-Tol-BINAP with the Grignard reagent methyl magnesium bromide. The product **259** was then reduced to the coveted chiral alcohol **239** using DIBAL-H in an overall yield of 62% and 96% *ee* over two steps.

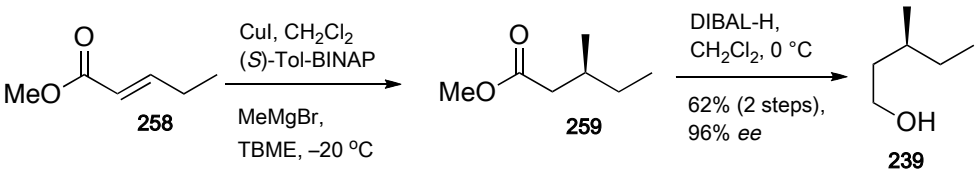

Scheme 4.9: Synthesis of (3*S*)-methylpentan-1-ol from *trans*-methyl pentenoate

Beginning from the alcohol **239**, we implemented an adapted Ireland's procedure as a one-pot Parikh-Doering oxidation/Wittig olefination,[102–104] to obtain the three-carbon homologated aldehyde as an exclusively *cis*-acetal (**260**). This was then deprotected by hydrolysing in neat hot formic acid to give the desired α,β-unsaturated aldehyde **243** arising from facile concomitant isomerisation.[30] The crude aldehyde was then submitted to Wittig olefination to give the ester **235** as a predominantly *trans*-product after chromatographic purification (89% yield, *E*/*Z* 98:2).

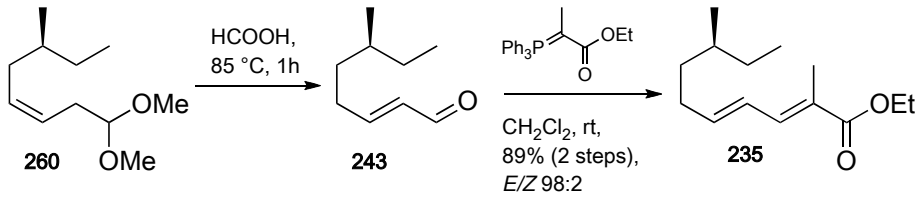

Scheme 4.10: Hydrolysis With Concomitant Isomerization

To obtain the diene aldehyde **236**, the ester was first reduced to the allylic alcohol using DIBAL-H (1.0 M in heptanes) and then reoxidised to the aldehyde

with IBX. This crude aldehyde **236** was then used in our Lewis acid-catalyzed enantioselective allylation to yield the homoallylic alcohol with our indium(III) chloride/(*S*)-BINOL methodology[88] in good yield and satisfactory enantioselectivity (87% yield, 70% *ee*) as shown in Scheme 4.12.

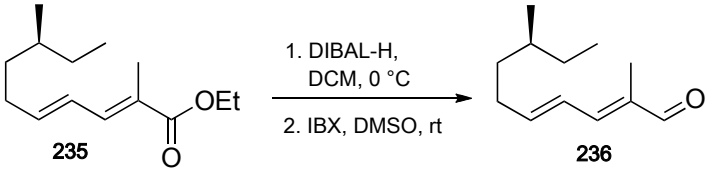

Scheme 4.11: Preparation of Aldehyde **236** for Asymmetric Allylation

At this juncture, we became ambitious and wanted to know if it was possible to shorten our synthesis using our one-pot asymmetric allylation/Grubbs' olefin cross-metathesis procedure developed previously.[105] This procedure utilizes our camphor-based allyl-transfer methodology for the asymmetric allylation[106] and is coupled with a subsequent Grubbs' olefin cross-metathesis. The challenge for us in using this methodology is that the use of α,β-unsaturated aldehydes as substrates for this allyl-transfer procedure has not been investigated before. We were also concerned that the presence of an α-methyl group in the substrate may contribute to undesirable steric hindrance. Yet, the rewards to be gleaned from a successful reaction were too tempting to resist.

Unfortunately, after stirring for one week at –20 °C, unreacted **236** was recovered. We increased the temperature to 0 °C for four days, but the reaction was still sluggish. When the temperature was raised to room temperature, we recovered mainly a side product that appears to be the dehydration product of **256** after

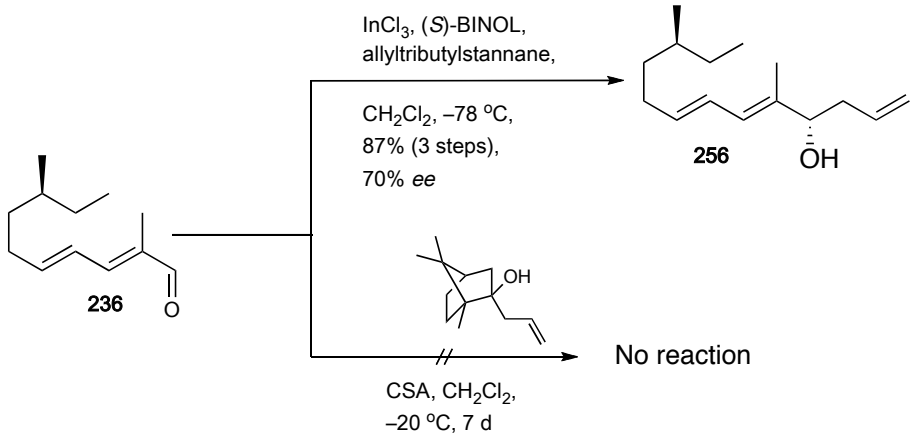

Scheme 4.12: Loh's Asymmetric Allylation

another three days. With this failure, we abandoned the camphor-based allyl-transfer procedure and continued with our initial synthetic plans.

We then attempted to do a one-pot cross-metathesis/Wittig olefination[107] on **256** to procure the unprotected methyl ester of the acyl side chain of papulacandin D (**228a**). We tested this reaction on a small-scale and were able to isolate the desired product through preparative TLC, from among a few other bands visible under UV light visualization. However, when the purified product was kept at 4 °C for a few days, the same bands were again observed after TLC. As such, we abandoned this procedure as well.

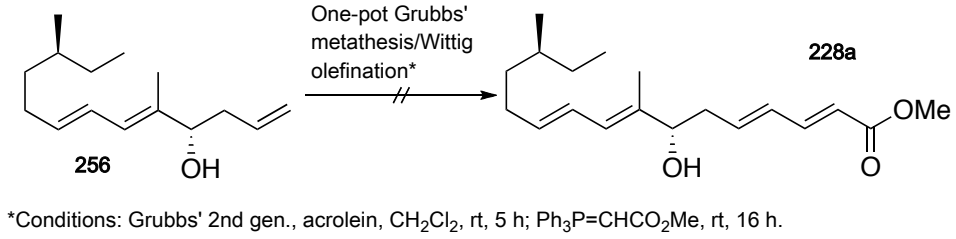

Scheme 4.13: One-pot Grubbs' Metathesis/Wittig Olefination

Thus, we protected homoallylic alcohol **256** obtained from the $InCl_3$/(*S*)-BINOL asymmetric allylation as the triethylsilyl ether and attempted to perform Grubb's

metathesis on it. To our dismay, the reaction refused to proceed even after stirring overnight. When the reaction time was extended to two days, only trace amounts of the aldehyde product was obtained.

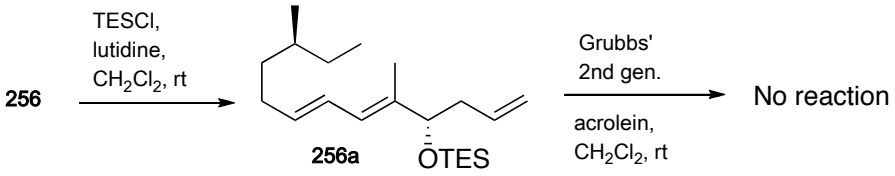

Scheme 4.14: TES-protection Before Grubbs' Metathesis

Hence, we reverted back to performing a Grubbs' metathesis on **256**, prior to protecting the alcohol moiety with chlorotriethylsilane and finishing up the synthesis with a Wittig olefination. Thus, the desired methyl ester **238a** of the acyl side chain of papulacandin D was obtained in an overall yield of 44% from the chiral alcohol **239**.

4.4 Conclusion

Hitherto, as depicted in Scheme 4.8, the synthesis of papulacandin D acyl side chain is accomplished. We have successfully applied the methodology developed in chapter 2 and demonstrated its utility in forming α,β-unsaturated aldehydes via the facile isomerization of the hydrolysis product of the three-carbon homologated acetal generated from the homoenolate anion equivalent **33c**.

We have also successfully demonstrated the application of two other methodologies developed in our group to the synthesis of **238a**, vis-à-vis the asymmetric conjugate

addition of a methyl group to an α,β-unsaturated ester and the $InCl_3$/(*S*)-BINOL-based asymmetric allylation reaction.

With this successful demonstration of the practicality of utilizing the facile isomerization of β,γ-unsaturated aldehyde to the α,β-unsaturated aldehyde after hydrolysis of the three-carbon homologated dimethoxy acetal, we look forward with keen anticipation to its application to a more challenging molecule in the subsequent chapters.

Chapter 5

Experimental Section

5.1 General Procedures

All experiments were conducted in oven-dried round-bottom flasks equipped with an elliptical Teflon coated magnetic stirrer bar and was stirred using a Heidolph MR3001K magnetic hotplate stirrer unless otherwise noted. Heating when required was via a water or silicone oil bath thermostated with the Heidolph EKT 3001 temperature controller.

Experiments involving air- and/or moisture-sensitive reagents were conducted in glassware dried for at least two hours in a 125 °C oven, and kept under a positive pressure with a nitrogen balloon via a rubber septum inlet. For reactions requiring more stringent conditions, a Schlenk-line was utilized under positive pressure of argon gas, together with flame-dried glassware.[108] Vacuum source was supplied using an Edwards RV3 oil pump equipped with a dry-ice/acetone cold trap.

5.2 Solvents and Reagents

All commercially available reagents and solvents were used as received without purification, unless otherwise stated. Technical grade hexane and ethyl acetate were distilled before use. Diethyl ether, dichloromethane and tetrahydrofuran were obtained from a PureSolv MD5 solvent purification system from Innovative Technologies. For more stringent requirements, tetrahydrofuran was freshly distilled over sodium sand with benzophenone as indicator to a purple colour, while

dichloromethane and *tert*-butyl methyl ether (TBME) were freshly distilled over CaH_2.[109]

Anhydrous solvents and liquid reagents were transferred using oven-dried needles and glass syringes which had been cooled to ambient temperature in a dessicator or via cannulation. Moisture from reagents were removed azeotropically with anhydrous THF prior to use where feasible.

5.3 Chromatography

Reaction progress was monitored using thin layer chromatography (TLC).

Analytical TLC was performed with Merck 60 F_{254} pre-coated silica gel plates (4 cm × 1 cm). After development, the plates were visualized with λ_{254} UV lamp and/or stained with 2,4-dinitrophenylhydrazine (2,4-DNP) or I_2. Staining with alkaline $KMnO_4$, ceric ammonium molybdate (CAM), vanillin or 50% H_2SO_4 was followed by heating using a Bosch GHG 500-2 heatgun or over a hotplate.

Preparative TLC was performed using Merck 60 F_{254} pre-coated silica gel plates (20 cm × 20 cm). The sample was applied as a narrow band (18 cm × 0.5 cm) after being dissolved in a minimal amount of solvent, 2 cm above the solvent level. After development, the plate was visualized under λ_{254} UV light, and isolated by scraping off the desired band. This was loaded into a pasteur pipette and eluted with chloroform and dried *in vacuo* to obtain the desired compound.

Flash column chromatography was carried out using SiliCycle SiliaFlash F60, 40–63 μm 60 Å silica gel powder, packed as a slurry and pre-equilibrated with the appropriate solvent system before use.

Low boiling point solvents were removed *in vacuo* with a Heidolph Laborota 4000 Efficient rotary evaporator, equipped with an Eyela A-3S recirculating water aspirator and chilled with an Eyela CCA-1110. High boiling point solvents were removed with a similar setup using a Vacuubrand MZ2C or MD1C oil-free diaphram pump as vacuum source.

5.4 Physical Characterization

^{1}H NMR and ^{13}C NMR (400 MHz and 100 MHz respectively) were acquired using either JEOL ECA 400 or JEOL ECA 400SL. Unless otherwise stated, the samples were dissolved in $CDCl_3$ and chemical shifts are reported in δ units with reference to the residual proton peak from $CDCl_3$ as the internal standard (^{1}H: δ 7.26 ppm; ^{13}C: δ 77.00 ppm). Data acquisition and processing were done with the supplied JEOL Delta software. The coupling constants (J) were recorded in Hz. Abbreviations for the multiplicity of the peaks are: s (singlet), d (doublet), t (triplet), q (quartet), qn (quintet), dd(doublet of doublets), dt(doublet of triplets), br (broad), m (multiplet) and app (apparent).

FTIR spectra were acquired either neat, as Nujol mulls or KBr plates using the IRPrestige-21 spectrometer from Shimadzu, with data acquisition and processing using the supplied IRsolution software v1.21. Abbreviations for the peaks are: s

(strong), br (broad), m (medium) and w (weak) and are reported in wavenumbers (cm^{-1}).

Optical rotation data were acquired using the Jasco P-1030 polarimeter in a 1 cm × 1 cm cell with the sodium D-line at the stated ambient temperature using Spectra Manager v1.53.01 (Build 1).

Mass spectra were obtained on a Finnigan Surveyor LCQ DECA XP MAX in ESI mode with data processed using Xcalibur software v1.4SR1. High resolution mass spectra were obtained using a Waters Acquity UPLC Q-ToF Premier in ESI mode, with data processed using MassLynx v4.1 (SCN639).

GC-FID data were acquired with Agilent 6890N using helium as carrier gas, nitrogen as makeup gas and hydrogen generated from a Parker Balston H2PD-3000K hydrogen generator. HPLC data were acquired on an Agilent 1100 system equipped with a multiwavelength UV detector and fluorescence detector. Both GC and LC machines were running Chemstation software Rev.A.10.02 (1757).

Chiral GC separations were done using the Astec Chiraldex G-TA column. Chiral HPLC separations were done using Daicel OD-H, AS-H, AD-H, OJ-H or OB-H as stated. Separation parameters used were from the cited literature. For compounds where no prior literature on separation are available, method development was done in-house by the author.

5.5 Software

Chemical structures were drawn using the ChemBioOffice suite (v12.0) from CambridgeSoft. Nomenclature for compounds were obtained using MarvinSketch (Marvin v5.2.6) from ChemAxon.

Computational calculations and 3D molecular modelling were done on an 8-core Mac Pro (2 × 2.8 GHz Quad-Core Intel Xeon processors) equipped with 10 GB of 800 MHz DDR2 FB-DIMM memory. Computations were done using Gaussian for Windows (G03), with structure preparation/visualization using GaussView (GV03W). Both programs were run in Microsoft Windows XP under the virtualization software VMWare Fusion version 3.1.0 (261058) for Mac OSX (10.5.8). Computational calculations and 3D modelling were also done using Spartan '08 for Mac (v1.2.1) from Wavefunction Inc.

NMR, LC/GC/MS data were processed using the instrument specific software supplied by the vendor, or using the MNova suite v6.1.1-6384 with the NMR and MS plugins from Mestrelab Research S. L.

Document preparation was done using TeXShop v2.33 (2.33) for LaTeX from the MacTeX 2009 distribution with the *achemso* style package from the American Chemical Society. Reference management and citation were done using BibDesk v1.5.2 (1854).

5.6 Experimental Procedures

5.6.1 Synthesis of Three-carbon Homologated Dimethoxy Acetal Products

Representative procedure for the Wittig olefination of carbonyl compounds using (3,3-dimethoxypropyl)triphenylphosphonium chloride (33c)

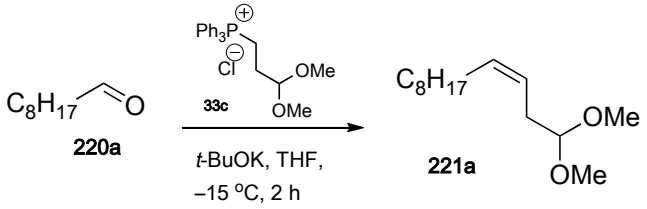

Scheme 5.1: Three-carbon Homologation

The ylide from homoenolate anion equivalent **33c** was first formed by dissolving the crude phosphonium chloride (2.2 mmol) in anhydrous THF. To this was added potassium *tert*-butoxide in THF (2.6 mL, 2.6 mmol, 1.2 equiv, 1.0 M *t*-BuOK/THF). This was stirred at room temperature to form a bright orange solution which was then cooled to –15 °C using an acetone-ice bath. Aldehyde (2 mmol) was then added and the solution stirred at this temperature for 2 h or until consumption of starting material as shown by TLC. The reaction mix was quenched with saturated NH_4Cl solution and extracted with ethyl acetate (3 × 5 mL). The pooled organic phase was washed with water, followed by brine, dried over anhydrous $MgSO_4$ and solvent was removed *in vacuo*. The crude product was then purified via flash column chromatography.

(3*Z*)-1,1-dimethoxydodec-3-ene (**221a**)

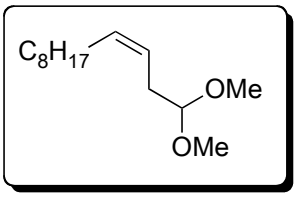

Figure 5.1: (3*Z*)-1,1-dimethoxydodec-3-ene

Appearance: Clear viscous oil.

Yield: 98% (purely *Z*).

TLC: R_f 0.56 (hexane/ethyl acetate 90:10).

^{1}H NMR (400 MHz, $CDCl_3$):

δ 5.50–5.43 (m, 1H), 5.36–5.29 (m, 1H), 4.33 (t, J = 5.8 Hz, 1H), 3.29 (s, 6H), 2.35–2.32 (m, 2H), 2.03–1.98 (m, 2H), 1.45–1.15 (m, 12H), 0.86–0.81 (m, 3H).

^{13}C NMR (100 MHz, $CDCl_3$):

δ 132.59, 123.22, 104.19, 52.81, 31.85, 30.89, 29.52, 29.46, 29.27, 27.43, 22.64, 14.06.

FTIR (neat): 2924, 1466, 1123.

HRMS (ESI): *m/z* $[C_{14}H_{28}O_2Na]^+$ 251.1987 (calculated), 251.1989 (found).

(3*Z*,5*E*)-1,1-dimethoxyundeca-3,5-diene (**221b**)

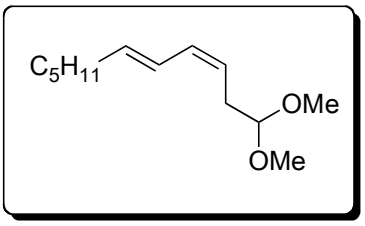

Figure 5.2: (3*Z*,5*E*)-1,1-dimethoxyundeca-3,5-diene

Appearance: Pale yellow viscous oil.

Yield: 80% (*E/Z* 15:85).

TLC: R_f 0.42 (hexane/ethyl acetate 90:10).

^{1}H NMR (400 MHz, $CDCl_3$):

δ 6.31–6.24 (m, 1H), 6.09–6.03 (m, 1H), 5.70 (dt, J = 15.1, 7.32 Hz, 1H), 5.31–5.25 (m, 1H), 4.40 (t, J = 5.9, 1H), 3.33 (s, 6H), 2.52–2.49 (m, 2H), 2.10–2.04 (m, 2H), 1.42–1.25 (m, 6H), 0.88 (t, J = 7.4 Hz, 3H).

^{13}C NMR (100 MHz, $CDCl_3$):

δ 136.05, 130.89, 125.20, 122.87, 103.96, 52.88, 32.83, 31.41, 38.94, 22.51, 14.03.

FTIR (neat): 2926, 1653, 1458, 1122.

HRMS (ESI): *m/z* $[C_{13}H_{24}O_2Na]^+$ 235.1674 (calculated), 235.1671 (found).

(2*E*,4*Z*)-7,7-dimethoxy-3-methylhepta-2,4-diene (**221c**)

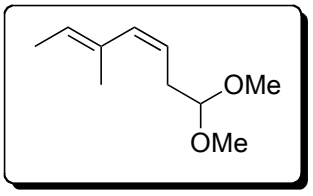

Figure 5.3: (2*E*,4*Z*)-7,7-dimethoxy-3-methylhepta-2,4-diene

Appearance: Clear viscous oil.

Yield: 47% (*E/Z* 25:75).

TLC: R_f 0.39 (hexane/ethyl acetate 90:10).

^{1}H NMR (400 MHz, $CDCl_3$):

δ 5.92 (d, J = 11.9 Hz, 1H), 5.51–5.41 (m, 1H), 5.27 (dt, J = 11.9, 6.9 Hz, 1H), 4.39 (t, J = 6.4 Hz, 1H), 3.33 (s, 6H), 2.60–2.56 (m, 2H), 1.75 (s, 3H).

^{13}C NMR (100 MHz, $CDCl_3$):

δ 135.03, 133.14, 125.08, 122.30, 104.31, 52.86. 32.20, 16.29, 13.57.

FTIR (neat): 2932, 2916, 1641, 1445, 1126.

HRMS (ESI): *m/z* $[C_{10}H_{18}O_2Na]^+$ 193.1204 (calculated), 193.1204 (found).

[(1*Z*)-4,4-dimethoxybut-1-en-1-yl]cyclohexane (**221d**)

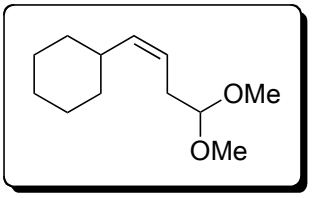

Figure 5.4: [(1*Z*)-4,4-dimethoxybut-1-en-1-yl]cyclohexane

Appearance: Clear viscous oil.

Yield: 98% (purely *Z*).

TLC: R_f 0.42 (hexane/ethyl acetate 90:10).

^{1}H NMR (400 MHz, $CDCl_3$):

δ 5.36–5.21 (m, 2H), 4.35 (t, J = 5.9 Hz, 1H), 3.33 (s, 6H), 2.38 (t, J = 7.3 Hz, 2H), 2.30–2.18 (m, 1H), 1.71–1.58 (m, 5H), 1.32–1.00 (m, 5H).

^{13}C NMR (100 MHz, $CDCl_3$):

δ 138.55, 121.34, 104.32, 52.85, 36.51, 33.10, 31.09, 25.98, 25.88.

FTIR (neat): 2924, 2849, 1647, 1449, 1125, 1064.

HRMS (ESI): *m/z* $[C_{12}H_{22}O_2Na]^+$ 221.1517 (calculated), 221.1523 (found).

(3*Z*)-1,1-dimethoxy-6,6-dimethylhept-3-ene (**221e**)

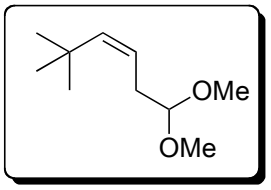

Figure 5.5: (3*Z*)-1,1-dimethoxy-6,6-dimethylhept-3-ene

Appearance: Clear viscous oil.

Yield: 81% (purely *Z*).

TLC: R_f 0.40 (hexane/ethyl acetate 90:10).

^{1}H NMR (400 MHz, $CDCl_3$):

δ 5.46–5.42 (m, 1H), 5.17 (dt, J = 11.9, 7.3 Hz, 1H), 4.37 (t, J = 6.0 Hz, 1H), 3.33 (s, 1H), 2.54–2.50 (m, 2 H). 1.10 (s, 9H).

^{13}C NMR (100 MHz, $CDCl_3$):

δ 142.19, 121.94, 104.59, 53.04, 33.43, 31.86, 31.09.

FTIR (neat): 2955, 1651, 1463, 1126, 1063.

HRMS (ESI): *m/z* $[C_{12}H_{22}O_2Na]^+$ 195.1361 (calculated), 195.1361(found).

(3*Z*)-(6,6-dimethoxyhex-3-enyl)benzene (**221f**)

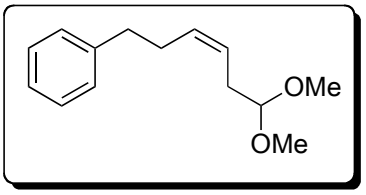

Figure 5.6: (3*Z*)-(6,6-dimethoxyhex-3-enyl)benzene

Appearance: Pale yellow viscous oil.

Yield: 90% (purely *Z*).

TLC: R_f 0.36 (hexane/ethyl acetate 90:10).

^{1}H NMR (400 MHz, $CDCl_3$):

δ 7.29–7.24 (m, 3H), 7.18 (d, J = 6.9 Hz, 2H), 5.58–5.51 (m, 1H), 5.43–5.36 (m, 1H), 4.22 (t, J = 5.9 Hz, 1H), 3.29 (s, 6H), 2.67 (t, J = 7.3 Hz, 2H), 2.37 (q, J = 7.8 Hz, 2H), 2.30 (t, J = 6.0 Hz, 2H).

^{13}C NMR (100 MHz, $CDCl_3$):

δ 141.83, 131.22, 128.46, 125.76, 124.18, 104.04, 52.86, 35.68, 30.84, 29.37.

FTIR (neat): 2932, 1603, 1452, 1125, 1061.

HRMS (ESI): *m/z* $[C_{14}H_{20}O_2Na]^+$ 243.1361 (calculated), 243.1368 (found).

(1*Z*)-(4,4-dimethoxybut-1-en-1-yl)benzene (**221g**)

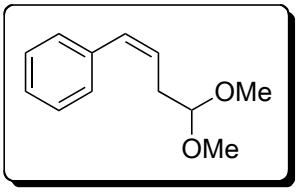

Figure 5.7: (1*Z*)-(4,4-dimethoxybut-1-en-1-yl)benzene

Appearance: Clear viscous oil.

Yield: 96% (*E*/*Z* 11:89).

TLC: R_f 0.26 (hexane/ethyl acetate 90:10).

^{1}H NMR (400 MHz, $CDCl_3$):

δ 7.41–7.22(m, 3H), 6.59 (d, J = 11.9 Hz, 2H), 5.73 (dt, J = 11.9, 7.3 Hz, 1H), 4.51 (t, J = 5.9 Hz, 1H), 3.36 (s, 6H), 2.73–2.70 (m, 2H).

^{13}C NMR (100 MHz, $CDCl_3$):

δ 137.29, 131.20, 128.81, 128.30, 126.88, 126.31, 104.05, 53.02, 32.29.

FTIR (neat): 2936, 1738, 1447, 1125, 1059.

HRMS (ESI): *m/z* $[C_{12}H_{17}O_2]^+$ 215.1048 (calculated), 215.1051 (found).

1-[(1*Z*)-4,4-dimethoxybut-1-en-1-yl]-4-methoxybenzene (**221h**)

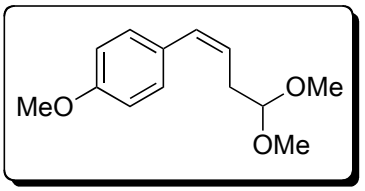

Figure 5.8: 1-[(1*Z*)-4,4-dimethoxybut-1-en-1-yl]-4-methoxybenzene

Appearance: Clear viscous oil.

Yield: 91% (*E/Z* 12:88).

TLC: R_f 0.26 (hexane/ethyl acetate 90:10).

^{1}H NMR (400 MHz, $CDCl_3$):

δ 7.23 (d, J = 8.7 Hz, 2H), 6.87 (d, J = 8.7 Hz, 2H), 6.48 (d, J = 11.4 Hz, 1H), 5.59 (dt, J = 11.4, 7.3 Hz, 1H), 4.47 (t, J = 6.0 Hz, 1H), 3.80 (s, 3H), 3.32 (s, 6H), 2.68–2.65 (m, 2H).

^{13}C NMR (100 MHz, $CDCl_3$):

δ 158.33, 130.45, 129.88, 124.49, 113.56, 103.97, 55.19, 52.86, 32.14.

FTIR (neat): 2936, 1607, 1510, 1462, 1252, 1125.

HRMS (ESI): *m/z* $[C_{10}H_{18}O_2Na]^+$ 245.1154 (calculated), 245.1158 (found).

1-chloro-4-[(1*Z*)-4,4-dimethoxybut-1-en-1-yl]benzene (221i)

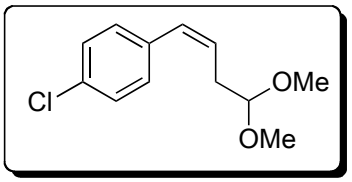

Figure 5.9: 1-chloro-4-[(1*Z*)-4,4-dimethoxybut-1-en-1-yl]benzene

Appearance: Clear viscous oil.

Yield: 56% (*E/Z* 38:62).

TLC: R_f 0.31 (hexane/ethyl acetate 90:10).

^{1}H NMR (400 MHz, $CDCl_3$):

δ 7.29 (d, J = 8.7 Hz, 2H), 7.21 (d, J = 8.2 Hz, 2H), 6.49 (d, J = 11.9 Hz, 1H), 5.71 (dt, J = 11.9, 7.3 Hz, 1H), 4.46 (t, J = 6.0 Hz, 1H), 3.32 (s, 6H), 2.64–2.60 (m, 2H).

^{13}C NMR (100 MHz, $CDCl_3$):

δ 135.51, 132.43, 129.91, 129.85, 128.27, 126.85, 103. 75, 52.93, 32.12.

FTIR (neat): 2937, 1703, 1491, 1364, 1125.

HRMS (ESI): *m/z* $[C_{10}H_{18}O_2Na]^+$ 249.0653 (calculated), 249.0664 (found).

2-[(1*Z*)-4,4-dimethoxybut-1-en-1-yl]-5-methylfuran (221j)

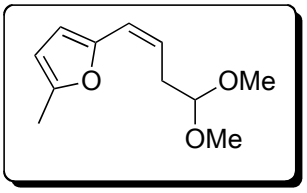

Figure 5.10: 2-[(1*Z*)-4,4-dimethoxybut-1-en-1-yl]-5-methylfuran

Appearance: Clear viscous oil.

Yield: 94% (*E/Z* 11:89).

TLC: R_f 0.50 (hexane/ethyl acetate 90:10).

^{1}H NMR (400 MHz, $CDCl_3$):

δ 6.23–6.15(m, 2H), 5.98–5.97 (m, 1H), 5.46 (dt, J = 11.9, 7.3 Hz, 1H), 3.36 (s, 6H), 2.83–2.79 (m, 2H), 2.29 (s, 3H).

^{13}C NMR (100 MHz, $CDCl_3$):

δ 151.73, 122.56, 119.32, 110.70, 107.38, 104.25, 53.12, 32.97, 13.93.

FTIR (neat): 2936, 1740, 1447, 1242, 1125, 1056.

HRMS (ESI): m/z $[C_{10}H_{18}O_2Na]^+$ 197.1178 (calculated), 197.1184 (found).

5.6.2 Hydrolysis of Three-carbon Homologated Dimethoxy Acetal Products

Representative procedure for the hydrolysis of dimethoxy acetal (3*Z*)-1,1-dimethoxydodec-3-ene (221a) to give the α,β-unsaturated aldehyde (2*E*)-undec-2-enal (222a)

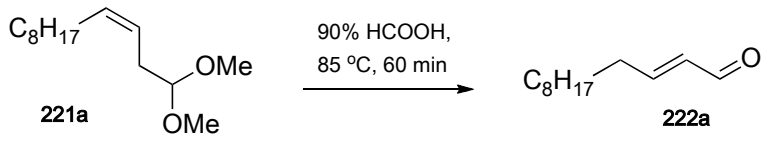

Scheme 5.2: Hydrolysis of 3-alkenal Acetal

The 3-alkenal acetal product (2 mmol) from the Wittig olefination was added to hot formic acid (90% HCOOH, 5 mL) at 85 °C in a 25 mL round-bottom flask

equipped with a magnetic stirrer bar. The solution was stirred for up to 60 mins. As the hydrolysis progresses, the solution colour deepens to a dark orange. The solution was then quickly cooled in ice water and extracted with hexane (5 × 10 mL). This was washed with water, followed by brine, and dried over anhydrous $MgSO_4$. The solvent was removed *in vacuo* to yield the crude product. The crude product was then purified via flash column chromatography with (hexane/ethyl acetate 95:5).

(2*E*)-dodec-2-enal (**222a**)

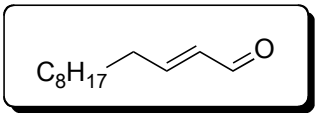

Figure 5.11: (2*E*)-dodec-2-enal

Appearance: Clear viscous oil.

Yield: 95%.

TLC: R_f 0.44 (hexane/ethyl acetate 90:10).

^{1}H NMR (400 MHz, $CDCl_3$):

δ 9.51 (d, J = 7.8 Hz, 1H), 6.86 (dt, J = 15.6, 6.8 Hz, 1H), 6.12 (dd, J = 15.6, 8.2 Hz, 1H), 2.33 (q, J = 7.3 Hz, 2H), 1.53–1.49 (m, 2H), 1.31–1.27 (m, 12H), 0.88 (t, J = 6.0 Hz, 3H).

^{13}C NMR (100 MHz, $CDCl_3$):

δ 194.17, 159.09, 132.93, 32.71, 31.83, 29.43, 29.31, 29.23, 29.11, 27.81, 22.63, 14.07.

FTIR (neat): 2926, 1694, 1466, 1141, 976.

HRMS (ESI): *m/z* $[C_{12}H_{23}O]^+$ 183.1749 (calculated), 183.1747 (found).

(2*E*)-4-cyclohexylbut-2-enal (**222d**)

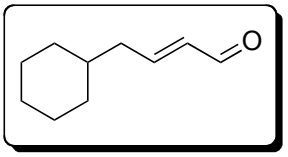

Figure 5.12: (2*E*)-4-cyclohexylbut-2-enal

Appearance: Clear viscous oil.

Yield: 81%.

TLC: R_f 0.16 (hexane/ethyl acetate 90:10).

^{1}H NMR (400 MHz, $CDCl_3$):

δ 9.49 (d, J = 7.8 Hz, 1H), 6.87– 6.79 (m, 1H), 6.09 (dd, J = 15.6, 7.8 Hz, 1H), 2.22 (t, J = 8.2 Hz, 2H), 1.72–1.64 (m, 4H), 1.54–1.44 (m, 1H), 1.26–1.12 (m, 4H). 1.00–0.94 (m, 2H).

^{13}C NMR (100 MHz, $CDCl_3$):

δ 194.08, 157.91, 133.96, 40.61, 37.24, 33.09, 26.22, 26.11.

FTIR (neat): 2924, 1690, 1449, 1155, 978.

HRMS (ESI): *m/z* $[C_{10}H_{17}O]^+$ 153.1279 (calculated), 153.1275 (found).

(2*E*)-5,5-dimethylhex-2-enal (**222e**)

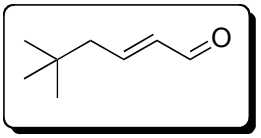

Figure 5.13: (2*E*)-5,5-dimethylhex-2-enal

Appearance: Clear viscous oil.

Yield: 40%.

TLC: R_f 0.20 (hexane/ethyl acetate 90:10).

^{1}H NMR (400 MHz, $CDCl_3$):

δ 9.49 (d, J = 8.24, 1H), 7.86–6.80 (m, 1H), 6.08 (dd, J = 15.6, 7.8 Hz, 1H), 2.2 (d, J = 7.6 Hz, 2H), 0.94 (s, 9H).

^{13}C NMR (100 MHz, $CDCl_3$):

δ 194.02, 156.41, 135.12, 47.17, 29.45.

FTIR (neat): 2957, 1728, 1694, 1366, 1167, 1115, 978.

HRMS (ESI): m/z $[C_8H_{15}O]^+$ 127.1123 (calculated), 127.1115 (found).

(2*E*)-6-phenylhex-2-enal (**222f**)

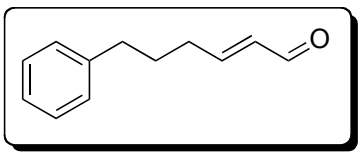

Figure 5.14: (2*E*)-6-phenylhex-2-enal

Appearance: Clear viscous oil.

Yield: 86%.

TLC: R_f 0.31 (hexane/ethyl acetate 90:10).

^{1}H NMR (400 MHz, $CDCl_3$):

δ 9.50 (d, $J = 7.8$ Hz, 1H), 7.31–7.16 (m, 5H), 6.84 (dt, $J = 15.6$, 6.9 Hz, 1H), 6.13 (dd, $J = 15.6$, 7.8 Hz, 1H), 2.67 (t, $J = 7.3$ Hz, 2H), 2.40–2.34 (m, 2H), 1.89–1.82 (m, 2H).

^{13}C NMR (100 MHz, $CDCl_3$):

δ 194.02, 158.28, 141.32, 133.19, 128.43, 128.39, 126.05, 35.18, 32.07, 29.38.

FTIR (neat): 2934, 1689, 1454, 1122, 700.

HRMS (ESI): *m/z* $[C_{12}H_{15}O]^+$ 175.1123 (calculated), 175.1123 (found).

(2*E*)-4-phenylbut-2-enal (**222g**)

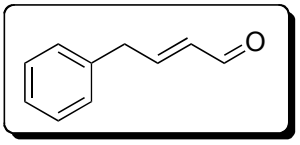

Figure 5.15: (2*E*)-4-phenylbut-2-enal

Appearance: Clear viscous oil.

Yield: 57%.

TLC: R_f 0.24 (hexane/ethyl acetate 90:10).

^{1}H NMR (400 MHz, $CDCl_3$):

δ 9.54 (d, $J = 8.2$ Hz, 1H), 7.36–7.18 (m, 5H), 7.01–6.94 (m, 1H), 6.15–6.09 (m,1H), 3.66 (d, $J = 6.9$ Hz, 2H).

^{13}C NMR (100 MHz, $CDCl_3$):

δ 193.79, 156.40, 133.54, 128.87, 126.99, 39.01.

FTIR (neat): 2959, 1691, 1454, 1122.

HRMS (ESI): *m/z* $[C_{10}H_{11}O]^+$ 147.0800 (calculated), 147.0805 (found).

(2*E*)-4-(4-chlorophenyl)but-2-enal (**222i**)

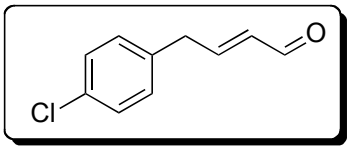

Figure 5.16: (2*E*)-4-(4-chlorophenyl)but-2-enal

Appearance: Yield: 54%.

TLC: R_f 0.22 (hexane/ethyl acetate 90:10).

^{1}H NMR (400 MHz, $CDCl_3$):

δ 9.54 (d, J = 8.2 Hz, 1H), 7.31 (d, J = 8.7 Hz, 2H), 7.12 (d, J = 8.7 Hz, 2H), 6.96–6.89 (m, 1H), 6.09 (dd, J = 15.6, 7.8 Hz, 1H), 3.62 (d, J =6.4 Hz, 2H).

^{13}C NMR (100 MHz, $CDCl_3$):

δ 193.53, 155.45, 135.41, 133.74, 132.89, 130.13, 128.99, 38.23.

FTIR (neat): 1686, 1491, 1406, 1124, 1092, 812.

HRMS (ESI): *m/z* $[C_{10}H_{10}ClO]^+$ 181.0420 (calculated), 181.0417 (found).

5.6.3 Synthesis of the Acyl Side Chain of Papulacandin D

methyl (3*S*)-methylpentanoate (259)

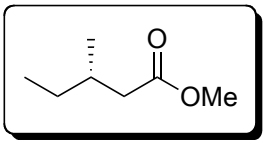

Figure 5.17: methyl (3*S*)-methylpentanoate

(*S*)-Tol-BINAP (1.03 g, 1.52 mmol) and CuI (0.19 g, 1.00 mmol) were added to an oven dried 250 mL two-necked round bottom flask equipped with septa and stirring bar. This was stirred in anhydrous CH_2Cl_2 (100 mL) for 20 minutes, concentrated *in vacuo* and then stirred in 200 mL of *tert*-butyldimethyl ether to form a bright yellow suspension. The mixture was then cooled to –20 °C and MeMgBr (85 mL, 3.0 M solution in Et_2O, 255 mmol) was added. After stirring for 15 minutes, a pre-cooled solution of methyl trans-2-pentenoate (5.71 g, 50 mmol) in *tert*-butyldimethyl ether (60 mL) was added over 10 h using a syringe pump. This was then stirred at –20 °C for another 1 h. The reaction mixture was then quenched with methanol (50 mL) and saturated ammonium chloride solution (150 mL). The aqueous layer was extracted with diethyl ether (200 mL × 3) and the combined organic extracts were dried over anhydrous Na_2SO_4, filtered and concentrated *in vacuo*. The resulting residue was purified by flash chromatography (pentane/Et_2O 99:1) to afford the desired product as a colourless oil.

Appearance: Clear viscous oil.

Yield: 67%.

^{1}H NMR (400 MHz, $CDCl_3$):

δ 3.65 (s, 3H), 2.30 (dd, J = 14.8, 6.0 Hz, 1H), 2.09 (dd, J = 14.8, 8.4 Hz, 1H), 1.87–1.85 (m, 1H), 1.34–1.32 (m, 1H), 1.24–1.17 (m, 1H), 0.91 (d, J = 6.4 Hz, 3H), 0.87 (t, J = 7.6 Hz, 3H).

^{13}C NMR (100 MHz, $CDCl_3$):

δ 173.8 , 51.3, 41.2, 31.9, 29.3, 19.2, 11.2.

FTIR (neat): 2961, 1740, 1462, 1194.

HRMS (ESI): m/z $[C_7H_{14}O_2]^+$ 130.0994 (calculated), 130.0983 (found).

cGC: 96%*ee* (Chiraldex G-TA; 30 m × 0.25 mm; FID; 60 °C; τ_{maj} = 11.9 min, τ_{min} = 11.1 min).

$[\alpha]_D^{20}$ = +6.0 (c = 1.2, $CHCl_3$).

(3*S*)-methylpentan-1-ol (**239**)

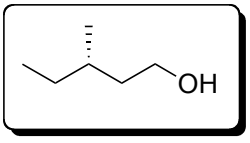

Figure 5.18: (3*S*)-methylpentan-1-ol

Appearance: Clear viscous oil.

Yield: 93%.

^{1}H NMR (400 MHz, $CDCl_3$):

δ 3.71–3.61 (m, 2H), 1.64–1.43 (m, 2H), 1.41–1.30 (m, 2H), 1.22–1.11 (m, 1H), 0.88–0.85 (m, 6H) .

^{13}C NMR (100 MHz, $CDCl_3$):

δ 61.2, 39.5, 31.0, 29.5, 19.1, 11.2.

FTIR (neat): 3329,1460, 1061.

(3*Z*,6*S*)-1,1-dimethoxy-6-methyloct-3-ene (**260**)

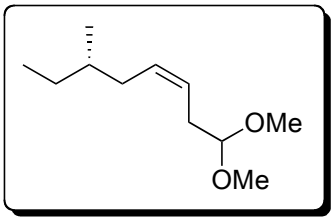

Figure 5.19: (3*Z*,6*S*)-1,1-dimethoxy-6-methyloct-3-ene

A one-pot modified Parikh-Doering oxidation/three-carbon Wittig olefination was done.[102–104] In a 500 mL round-bottom flask, pyridine·SO_3 (4.84 g, 30 mmol) was dissolved in CH_2Cl_2 (20 mL) to form a white suspension. To this was added pyridine (3.3 mL, 41 mmol), and then triethylamine (8.5 mL, 61 mmol) to give a clear amber solution. This was cooled to –15 °C using an acetone-ice bath. (3*S*)-3-methylpentan-1-ol (1.7 mL, 13.8 mmol) was dissolved in 1:2 DMSO/CH_2Cl_2 (15 mL v/v) and transferred to the cooled pyridine·SO_3 solution. The reaction was stirred at –15 °C to rt over 6 hours.

The ylide from the homoenolate anion equivalent **33c** was formed by dissolving the crude phosphonium chloride (40 mmol) in anhydrous THF (40 mL). To this was added potassium *tert*-butoxide in THF (60 mL of 1.0 M *t*-BuOK/THF, 60 mmol, 1.5 equiv). This was stirred at room temperature to form a bright orange solution which was then cooled to –15 °C using an acetone-ice bath.

The round-bottom flask containing the crude aldehyde from the Parikh-Doering oxidation was cooled to –15 °C, upon which the ylide solution was then transferred

and stirred at –15 °C for 16 hours in a cryobath. Thereafter, the reaction mix was brought to rt, diluted with an equal volume of CH_2Cl_2 (150 mL), washed with small volumes of water (5 × 50 mL) to remove the DMSO and concentrated *in vacuo*. This was passed through a short plug of SiO_2 before purification using flash column chromatography (hexane/ethyl acetate 98:2).

Appearance: Clear viscous oil.

Yield: 94% (purely *Z*).

TLC: R_f 0.29 (hexane/ethyl acetate 96:4).

^{1}H NMR (400 MHz, $CDCl_3$):

δ 5.59–5.46 (m, 1H), 5.46–5.31 (m, 1H), 4.37 (t, J = 5.8 Hz, 1H), 3.33 (s, 6H), 2.37 (t, J = 6.3 Hz, 2H), 2.09–1.76 (m, 2H), 1.44–1.29 (m, 2H), 1.13 (dq, J = 14.6, 7.3 Hz, 1H), 0.87 (t, J = 7.3 Hz, 7H).

^{13}C NMR (100 MHz, $CDCl_3$):

δ 131.40, 124.15, 104.35, 77.48, 77.16, 76.84, 52.99, 35.14, 34.51, 31.16, 29.34, 19.23, 11.67.

FTIR (neat): 2958, 2928, 1462, 1375, 1360, 1190, 1123, 1059.

HRMS (ESI): *m/z* $[C_{11}H_{22}O_2Na]^+$ 209.1517 (calculated), 209.1515 (found).

ethyl (2*E*,4*E*,8*S*)-2,8-dimethyldeca-2,4-dienoate (235)

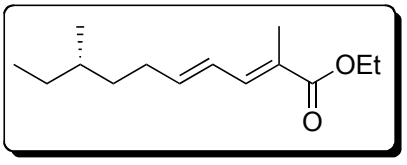

Figure 5.20: ethyl (2*E*,4*E*,8*S*)-2,8-dimethyldeca-2,4-dienoate

The 3-alkenal acetal product **260** (1.46 g, 7.9 mmol) from the Wittig olefination was added to hot formic acid (90% HCOOH, 15 mL) at 85 °C in a 25 mL round-bottom flask equipped with a magnetic stirrer bar. The solution was stirred for 45 mins. The solution was then quickly cooled in ice water and extracted with hexane (5 × 10 mL). This was washed with water, followed by brine, and dried over anhydrous $MgSO_4$. The solvent was removed *in vacuo* to yield the crude product which was used directly in the next step.

[(Ethoxycarbonyl)ethylidene]triphenylphosphorane (3.70 g, 10.2 mmol) was dissolved in CH_2Cl_2 (25 mL) and transferred to a solution of the crude aldehyde in CH_2Cl_2 (25 mL). This was stirred at room temperature for 16 h. Thereafter, the solvent was removed *in vacuo* and the residue was dissolved in diethyl ether and passed through a short plug of SiO_2. This was concentrated and purified using flash column chromatography (hexane/ethyl acetate 98:2) to give the desired ester **235** as a colourless oil.

Appearance: Colourless oil.

Yield: 89% (2 steps) (*E/Z* 98:2).

TLC: R_f 0.38 (hexane/ethyl acetate 96:4).

^{1}H NMR (400 MHz, $CDCl_3$):

δ 7.16 (d, J = 11.4 Hz, 2H), 6.37–6.28 (m, 2H), 6.12–6.02 (m, 2H), 4.20 (q, J = 7.1 Hz, 5H), 2.27–2.08 (m, 5H), 1.92 (s, 6H), 1.49–1.10 (m, 23H), 0.91–0.80 (m, 18H).

^{13}C NMR (100 MHz, $CDCl_3$):

δ 168.84, 143.60, 138.75, 125.92, 125.11, 77.48, 77.16, 76.84, 60.57, 35.87, 34.09,

31.06, 29.47, 19.14, 14.48, 12.69, 11.46.

FTIR (neat): 2861, 1705, 1640, 1240.

HRMS (ESI): *m/z* $[C_{14}H_{25}O_2]^+$ 225.1855 (calculated), 225.1857 (found).

(4*S*,5*E*,7*E*,11*S*)-5,11-dimethyltrideca-1,5,7-trien-4-ol (**256**)

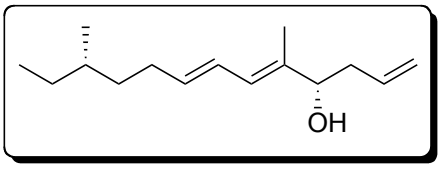

Figure 5.21: (4*S*,5*E*,7*E*,11*S*)-5,11-dimethyltrideca-1,5,7-trien-4-ol

The ester **235** (1.45 g, 6.5 mmol) was dissolved in anhydrous THF (15 mL) and cooled to 0 °C. DIBAL-H (15 mL, 15 mmol, 2.3 equiv, 1.0 M in THF) was added slowly and stirred at rt for 30 min. This was quenched with ice-cold MeOH (0.2 mL) and stirred with twice its volume of a saturated Rochelle salt solution for 1 h. This was then extracted with ethyl acetate (3 × 5 mL), dried *in vacuo*, and the crude alcohol used directly in the next step.

A solution of IBX/DMSO (3.66 g, 13 mmol, 2 equiv, 1 M) was added to the crude allylic alcohol and stirred at rt for 5 h. Thereafter, the reaction was diluted with ethyl acetate (13 mL) and water was added. This was filtered through a sintered glass funnel, and the organic phase was washed with small volumes of water (5 × 4 mL) to remove DMSO, then concentrated *in vacuo* to give the crude aldehyde. This was dried azeotropically with anhydrous THF (5 mL × 2) before being dissolved in anhydrous CH_2Cl_2 (5 mL) and used in the next step directly.

To an oven dried 10 mL round-bottom flask equipped with a magnetic stirring bar was added $InCl_3$ (0.29 g, 1.3 mmol). Using a Schlenck line, the solid was dried azeotropically with anhydrous THF (5 mL × 2), before dissolving in anhydrous CH_2Cl_2 (5 mL). To another oven-dried 10 mL round-bottom flask was added (*S*)-BINOL (0.41 g, 1.4 mmol). This was similarly dried azeotropically and dissolved in anhydrous CH_2Cl_2 (5 mL). Into a 100 mL oven-dried round-bottom flask equipped with a magnetic stirrer, 3 Å powdered molecular sieves (194 mg) was weighed and purged several times with Ar/vacuum for 15 min. Subsequently, the $InCl_3$ and (*S*)-BINOL solutions were transferred with washings to this 100 mL flask using anhydrous CH_2Cl_2 to a total volume of 20 mL.

The mixture was then stirred under argon at rt for 2 h to afford a white suspension. Subsequently, allyltributylstannane (4.27 g, 4 mL, 12.9 mmol) was added to the suspension and stirred for 10 mins. The mixture was then cooled to –78 °C for 15 mins followed by slow addition of the aldehyde (5 mL in CH_2Cl_2) via a syringe pump over 4 h. The reaction mixture was stirred at –78 °C for 16 h and then at rt for 5h. Thereafter, the reaction mix was filtered through a short plug of SiO_2 and purified using flash column chromatography (hexane/ethyl acetate 95:5) to give the desired homoallylic alcohol as a pale yellow oil.

Appearance: Pale yellow oil.

Yield: 87%.

TLC: R_f 0.14 (hexane/ethyl acetate 96:4).

^{1}H NMR (400 MHz, $CDCl_3$):

δ 6.30–6.19 (m, 2H), 5.96 (d, J = 10.8 Hz, 2H), 5.76 (ddd, J = 17.1, 10.1, 7.1 Hz,

2H), 5.66 (dt, J = 14.5, 5.5 Hz, 2H), 5.08–4.94 (m, 4H), 4.00 (t, J = 6.8 Hz, 2H), 2.30 (t, J = 6.9 Hz, 4H), 2.23–2.03 (m, 4H), 1.71 (s, 6H), 1.45–1.27 (m, 7H), 1.26–1.08 (m, 5H), 0.91–0.79 (m, 12H).

^{13}C NMR (100 MHz, $CDCl_3$):

δ 137.65, 136.31, 135.87, 127.18, 127.02, 116.91, 78.07, 40.80, 37.57, 35.20, 31.58, 30.46, 19.45, 12.05, 11.70.

FTIR (neat): 3377, 2959, 2924, 2872, 2855, 1462, 964.

HRMS (ESI): m/z $[C_{15}H_{27}O]^+$ 223.2062 (calculated), 223.2064 (found).

cHPLC: 70 %*ee* (Daicel Chiralpak AD-H; 0.2% *i*-PrOH/hexane; 0.5 mL/min; λ = 220, 260 nm; τ_{maj} = 50.1 min, τ_{min} = 52.0 min).

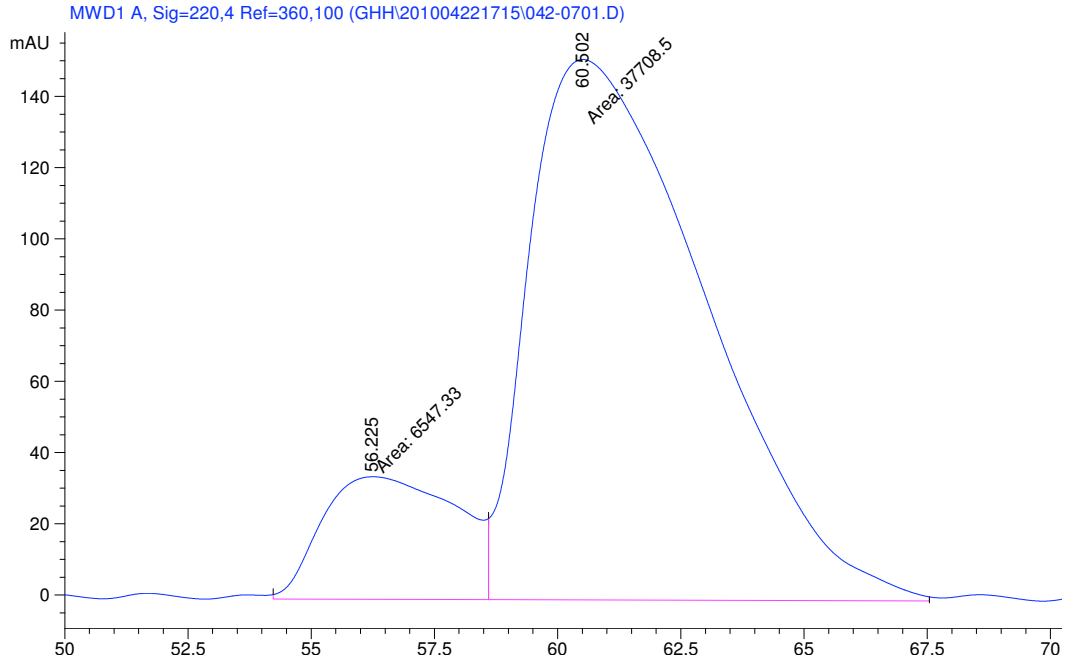

Figure 5.22: cHPLC of **256**

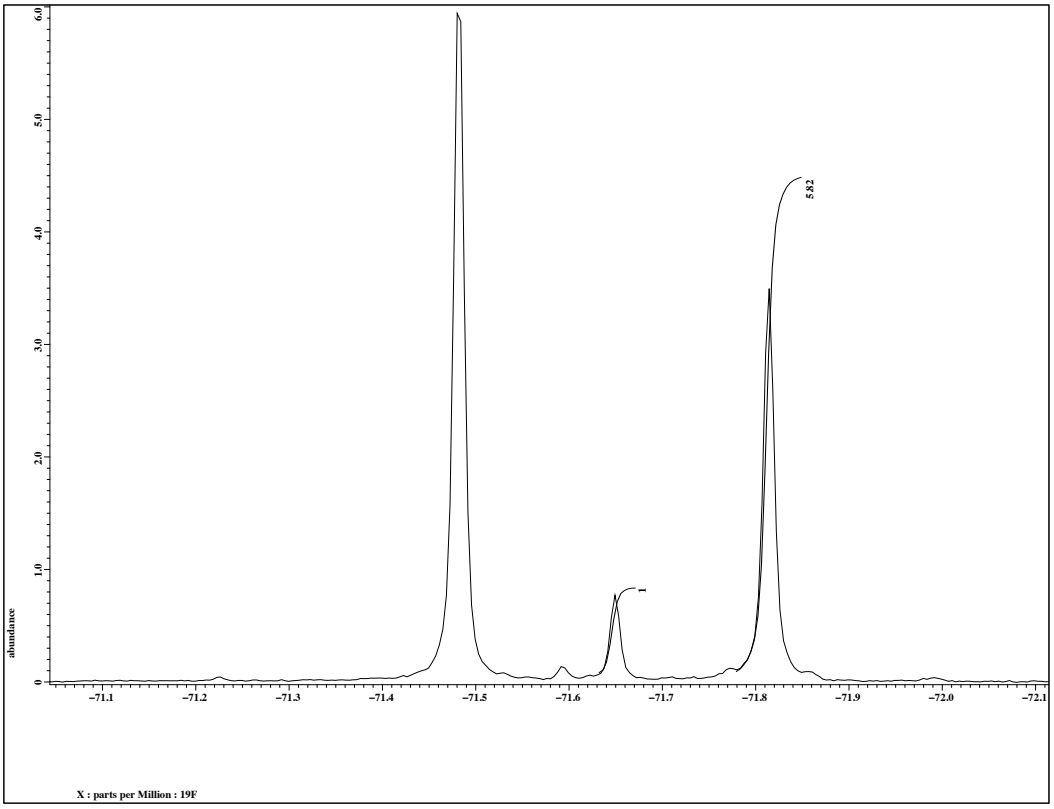

Figure 5.23: ^{19}F NMR of the Mosher's Ester of **256**

(2*E*,5*S*,6*E*,8*E*,12*S*)-6,12-dimethyl-5-[(triethylsilyl)oxy]tetradeca-2,6,8-trienal (**257**)

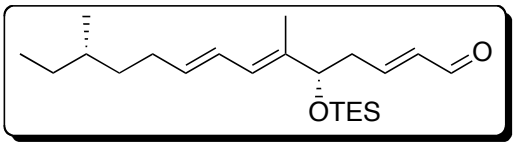

Figure 5.24: (2*E*,5*S*,6*E*,8*E*,12*S*)-6,12-dimethyl-5-[(triethylsilyl)oxy]tetradeca-2,6,8-trienal

To a 10-mL oven-dried two-necked round-bottom flask equipped with a magnetic stirrer bar, was added Grubbs' 2nd generation catalyst (99.6 mg, 0.1 mmol, 0.05 equiv) under Ar via a Schlenck line. Anhydrous CH_2Cl_2 (2 mL) and acrolein (1.7 mL, 25 mmol, 13 equiv) were then transferred.

The homoallylic alcohol **256** (0.44 g, 2.0 mmol) was weighed into an oven-dried 5mL round-bottom flask under an Ar balloon, then purged and flushed with argon/vacuum several times before filling with Ar. This was then diluted with CH_2Cl_2 (1 mL) and transferred with washings to the Grubbs' catalyst suspension. The reaction was stirred under Ar at room temperature for 5 h, then filtered through a short SiO_2 plug to remove the catalyst, dried *in vacuo*, and redissolved in CH_2Cl_2 (24 mL). Thereafter, 2,6-lutidine (1.4 mL, 12 mmol) was added followed by TESCl (1 mL, 6 mmol) and the reaction stirred for 16 h at rt. The reaction was quenched with saturated aqueous sodium bicarbonate and aqueous workup was done using CH_2Cl_2 (3 × 10 mL). The pooled organic phase were washed with water, then brine.This was dried over anhydrous $MgSO_4$, and the solvent removed *in vacuo* to give the crude product. This was purified using flash column chromatography to yield the desired TES-protected aldehyde **257**.

Appearance: Pale yellow oil.

Yield: 89%.

TLC: R_f 0.69 (hexane/ethyl acetate 90:10).

^{1}H NMR (400 MHz, $CDCl_3$):

δ 9.48 (dd, J = 7.8 Hz, 1H), 6.80 (dt, J = 7.8, 7.3 Hz, 1H), 6.23–6.09 (m, 2H), 5.95 (d, J = 13.3 Hz, 1H), 5.67 (dt, J = 15.1, 8.3 Hz, 1H), 4.15 (t, J = 6.4 Hz, 1H), 2.62–2.45 (m, 2H), 2.19–2.02 (m, 2H), 1.45–1.29 (m, 2H), 1.25–1.11 (m, 2H), 0.92 (t, J = 7.8 Hz, 9H), 0.88–0.84 (m, 9H), 0.56 (q, J = 7.8 Hz, 6H).

^{13}C NMR (100 MHz, $CDCl_3$):

δ 194.03, 155.49, 135.92, 135.73, 134.40, 125.87, 125.40, 76.61, 39.99, 36.15, 34.01,

30.58, 29.34, 19.05, 11.92, 11.32, 6.79, 4.72.

FTIR (neat): 2936, 1694, 1462, 1080, 1005, 745.

HRMS (ESI): *m/z* $[C_{22}H_{41}O_2Si]^+$ 365.2876 (calculated), 365.2868 (found).

methyl (2*E*,4*E*,7*S*,8*E*,10*E*,14*S*)-8,14-dimethyl-7-[(triethylsilyl)oxy]hexadeca-2,4,8,10-tetraenoate (**238a**)

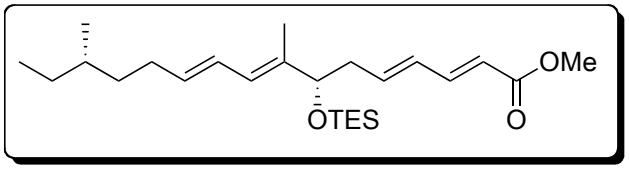

Figure 5.25: methyl (2*E*,4*E*,7*S*,8*E*,10*E*,14*S*)-8,14-dimethyl-7-[(triethylsilyl)oxy]hexadeca-2,4,8,10-tetraenoate

Aldehyde **257** (0.42 g, 1.3 mmol) was dissolved in DCE (5 mL) in a 25 mL round-bottom flask equipped with a magnetic stirrer bar. To this was added a solution of (triphenylphosphoranylidene)acetate (0.66 g, 2.0 mmol, 1.5 equiv) in dichloroethane (5 mL). The reaction mix was then refluxed for 16 h. Thereafter, the reaction was cooled to rt, transferred to a 125 mL separatory funnel containing 30 mL of water. The aqueous layer was extracted with CH_2Cl_2 (3 × 15 mL), and the pooled organic phase were washed with brine (10 mL). This was then dried over anhydrous $MgSO_4$, filtered, and concentrated to an orange syrup. The crude product was purified using flash column chromatography (hexane/ethyl acetate 95:5) to afford a clear, yellow oil.

Appearance: Clear yellow oil.

Yield: 68% (E/Z 94:6).

TLC: R_f 0.48 (hexane/ethyl acetate 95:5).

^{1}H NMR (400 MHz, MeOD):

δ 7.26 (dd, J = 15.6, 11.0 Hz, 1H), 6.32–6.24 (m, 2H), 6.17–6.10 (m, 1H), 5.99 (d, J = 11 Hz, 1H), 5.86 (d, J = 15.6 Hz, 1H), 5.68 (dt, J = 15.1, 6.8 Hz, 1H), 4.17 (t, J = 6.4 Hz, 1H), 3.75 (s, 3H), 2.49–2.36 (m, 2H), 2.23–2.07 (m, 2H), 1.50–1.32 (m, 3H), 1.28–1.13 (m, 2H), 0.97 (t, J = 8.2 Hz, 9H), 0.93–0.90 (m, 9H), 0.61 (q, J = 8.2 Hz, 6H).

^{13}C NMR (100 MHz, MeOD):

δ 170.19, 147.44, 143.35, 138.60, 136.99, 132.22, 127.90, 120.91, 79.78, 52.85, 42.25, 38.36, 36.06, 32.47, 31.32, 20.33, 12.93, 12.59, 8.07, 6.56.

FTIR (neat): 2934, 1722, 1645, 1263, 1001, 745.

HRMS (ESI): m/z $[C_{25}H_{44}O_3Si]^+$ 421.3138 (calculated), 421.3137 (found).

$[\alpha]_D^{21}$ = +8.3 (c = 0.198, $CHCl_3$).

Part II

TOWARDS A TOTAL SYNTHESIS OF AMPHIDINOLIDE X

Chapter 1

Background and Survey of Amphidinolide X

1.1 Introduction

Apart from being a highly stimulating and satisfying intellectual endeavour, the work of a synthetic organic chemist also serves to achieve a higher goal by its application to translational medicine — in bringing and bridging treatments from the laboratory bench to the patient's bedside. This aspect is and will always continue to play an important role in society, as we continue to strive for respite from diseases.

In view of this, research in natural products has continually uncovered and recapitulated the abundant wealth nature has in store for us, both in material and in design. It is to these that synthetic organic chemists perpetually find recourse, in the discovery and development of new drugs, and intellectual stimulation towards mimicking or even attempting to outdo nature in synthetic methodology. This fertile ground presents such a bewildering myriad of fascinating and complicated structures derived from permutations and combinations of simple precursors, that it has often challenged chemists to demonstrate their ingenuity to construct similar structures through efficient and elegant synthetic pathways.

This part of the thesis will present a brief introduction to the amphidinolides, which belong to a class of marine macrolide natural products. Thereafter, focus will be placed on the molecule of interest to us — amphidinolide X. There, emphasis will be given to the discussion of the methods used for macrocycle formation and for oxacycle synthesis, *i.e.*, the formation of the oxolane (tetrahydrofuran)

moiety that is a common feature in many members of the amphidinolide family. We will then present our strategy towards the total synthesis of amphidinolide X.

The key methodologies developed by our group that will be employed in the synthesis will be highlighted. In particular, the methodology developed in Part I Chapter 2 using the homoenolate anion equivalent **33c** to generate a three-carbon homologated acetal product, which will be put through hydrolysis conditions that generate the isomerized α,β-unsaturated aldehyde, will be undertaken. Hopefully this will provide further attestation to the utility of the methodology in natural product synthesis.

1.2 Biological Background

The amphidinolides are a class of cytotoxic polyene macrolides isolated from dinoflagellates of the genus *Amphidinium*, which are symbionts of Okinawan marine acoel flatworm *Amphiscolops sp.* All of these compounds exhibit significant *in vitro* activity against murine leukaemia cells, and some congeners also display activity toward rabbit skeletal muscle actomyosin ATPase.[110–112]

Much of the earlier work on the isolation and determination of the gross chemical structures of the various members of the amphidinolide family have been performed by Kobayashi and co-workers. Their search for bioactive substances from marine organisms, particularly secondary metabolites from symbiotic marine microorganisms, can be traced back to the early 1980s. To date, more than thirty members of the amphidinolide family have been isolated and characterized.[110,113–118]

Vested by interest in the cytotoxic potency of the amphidinolides against human cancer cell lines, the total syntheses for many of the members of this family have been reported. In some cases, this has resulted in a reassignment of stereochemistries.[119] Nested away in this big family of amphidinolides is our target molecule amphidinolide X — a fairly recent addition to the family. Isolated in 2003, there already exists an impressive number of reports of both its total synthesis and that of the fragment containing the tetrahydrofuran ring in a relatively short span of time.[35–42,120]

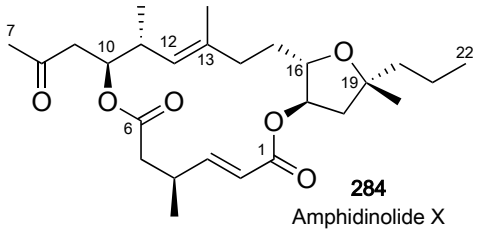

Figure 1.1: Amphidinolide X

1.3 Isolation, Family Members and Structural Aspects

Structural features of the amphidinolides are unique. Members of the amphidinolide family gleaned from Kobayashi's reviews[110,113–118] are illustrated in Figures 1.2 to 1.4. As can be seen from the figures, amphidinolides show a wide variation in the size of the macrocyclic lactone rings. As an illustration, we see that they can be 16-membered, amphidinolide X; 19-membered, amphidinolide E; 20-membered, amphidinolide A; 25-membered, amphidinolides C and F; 26-membered, amphidinolides B, D and H; 27-membered, amphidinolide G. A notable feature in the

family members of the amphidinolide class is the presence of an odd-numbered macrocyclic lactone ring in many of them.[110] This is in stark contrast to macrolides derived from terrestrial microorganisms, which cannot be explained via the classical polyketide biosynthetic pathway.[112,121]

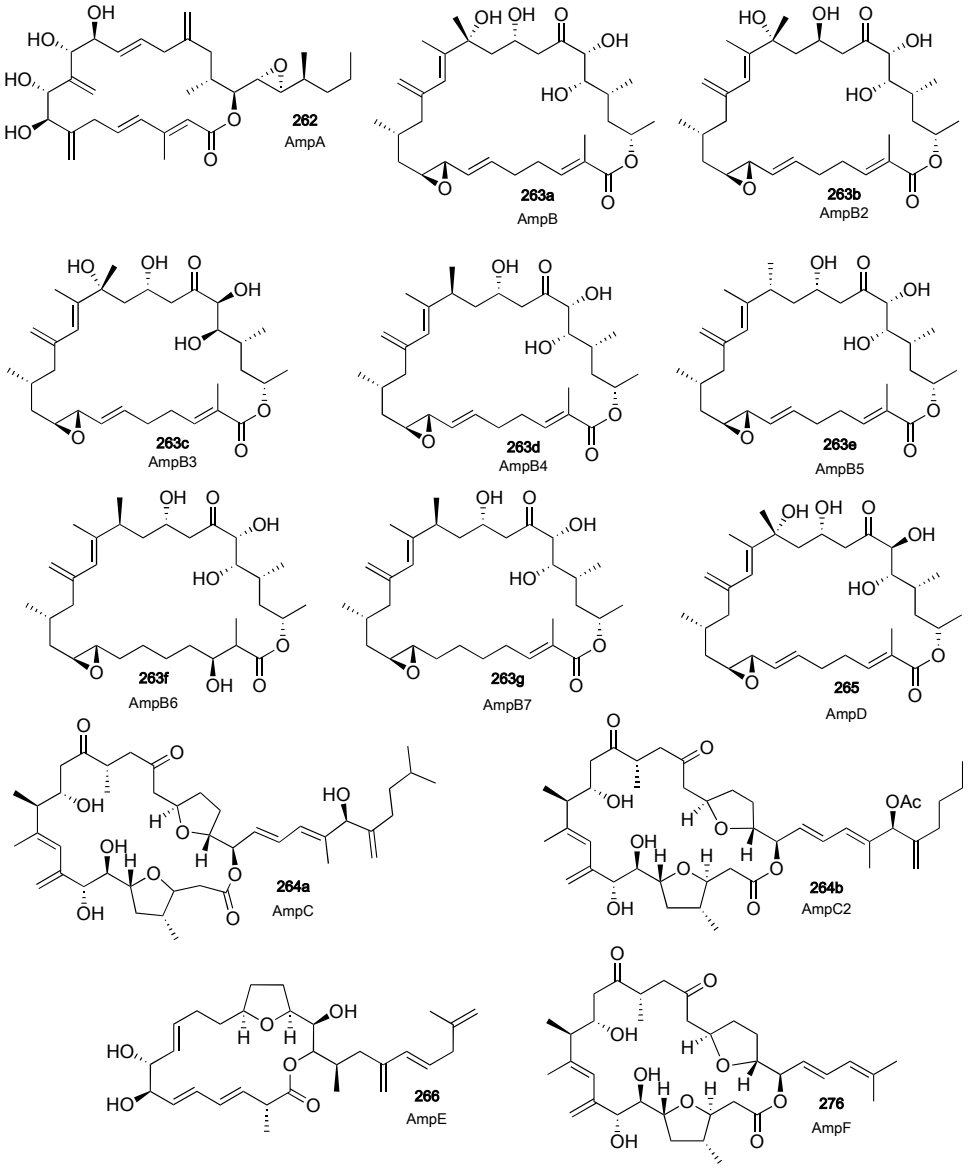

Figure 1.2: Amphidinolide Family — A to F

It should be noted that the cytotoxic activity of amphidinolide B and its related compounds (amphidinolides D, G and H) are extremely strong. Amphidinolide D, an epimer of amphidinolide B at the C(21) position was however, about 100 times

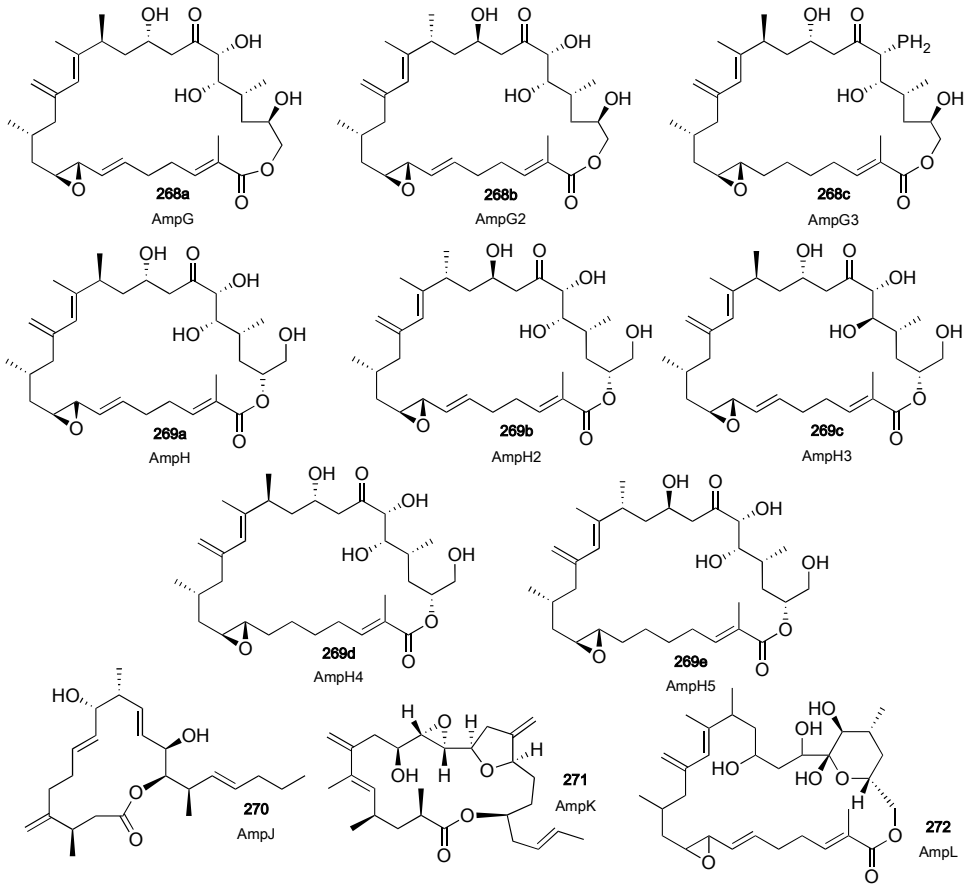

Figure 1.3: Amphidinolide Family — G to L

less cytotoxic than the latter. Epoxide opening with methanol generated an alcohol whose IC_{50} value against L1210 cell was considerably weaker. These results suggest that the stereochemistry on C(21), as well as the epoxide functionality are important features contributing to the cytotoxicity of amphidinolides. Similarly, the cytotoxicities of amphidinolides C and F were markedly different although these two members vary only in the length of the side chain. Amphidinolide C was tested to be approximately 250 times more potent when compared to amphidinolide F. Given the structural similarities in these two congeners, it is thought to be very likely that amphidinolide F could be the biological precursor to amphidinolide C.[110]

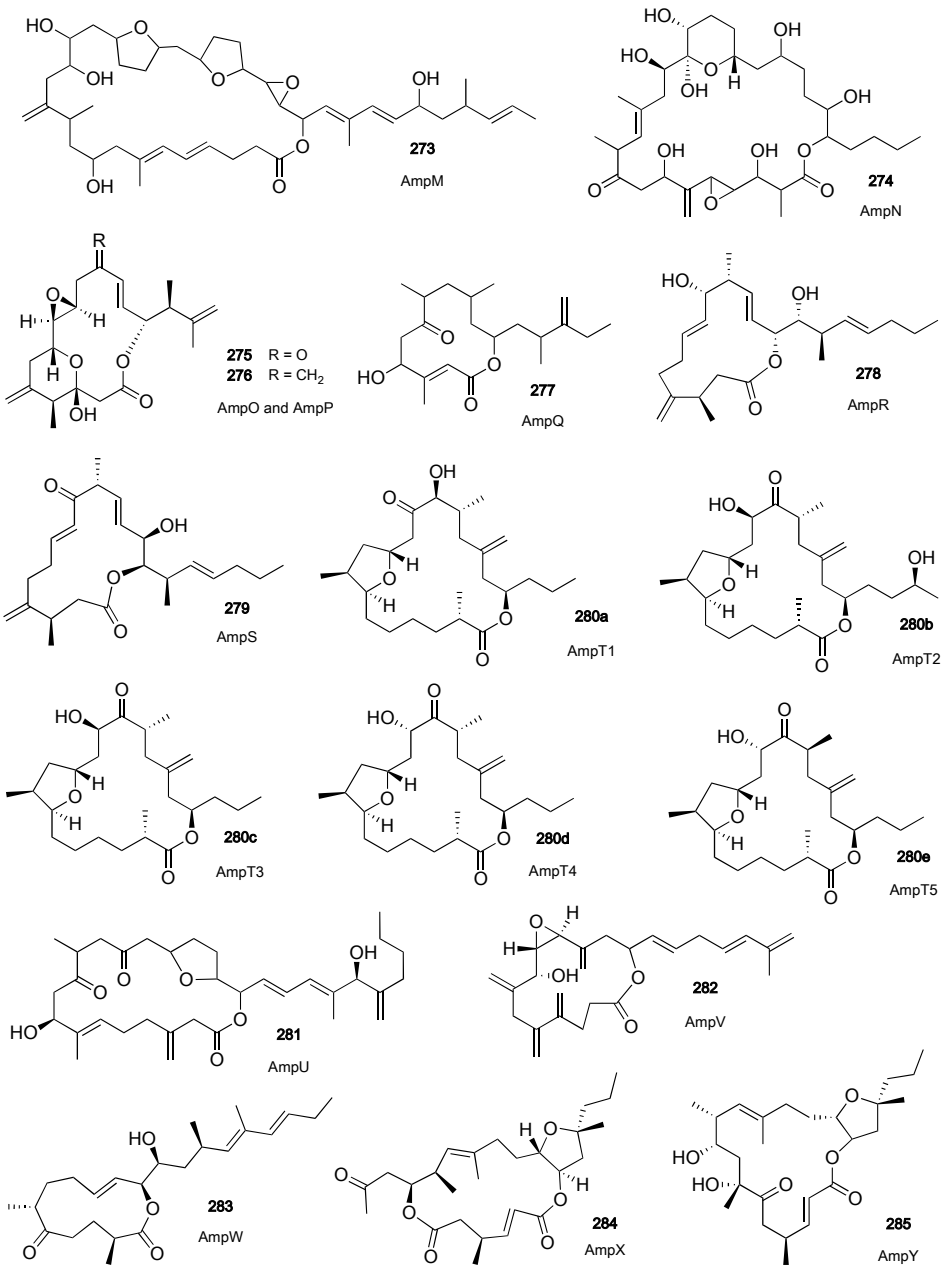

Figure 1.4: Amphidinolide Family — M to Y

Amongst all the amphidinolides, amphidinolide N exhibits the most potent cytotoxicity against human cancer cell lines, with IC_{50} values of 50 pg/mL and 60 pg/mL against murine lymphoma L1210 cell and human epidermoid carcinoma KB cells respectively. Amphidinolide N is a 26-membered macrolactone, possessing the characteristic *exo*-methylene, alkyl chain and epoxide functionality described in the other cogeners above. In addition, amphidinolide N possesses a

tetrahydropyran ring with a sterically demanding quarternary chiral centre and two other chiral centres on the ring system, making the synthesis of this molecule a challenging endeavour.[110]

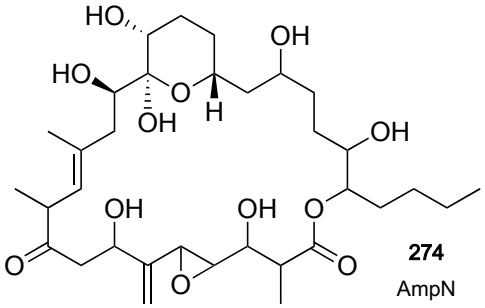

Figure 1.5: Amphidinolide N

Amphidinolide X, the target molecule of interest to us has its own exclusive set of structural uniqueness. Amphidinolide X has an intermediate, 16-membered lactone ring size as family members possess lactone ring sizes ranging from 12- to 29-membered. It has the distinction of being the first macrodiolide obtained from natural sources to be made up of polyketide-derived diacid and diol structural subunits.[118,121] Another distinguishing structural feature possessed by amphidinolide X resides in the absence of an *exo*-methylene functionality. Most of the members making up this family of macrodiolides possess one or more *exo*-methylene groups, with the exceptions of amphidinolides W and Y.

1.4 Importance for Drug Discovery and Development

Marine macrolides have commanded a considerable amount of scrutiny for its seemingly limitless source and range of diverse and highly complex secondary metabolites, exhibiting a wide range of desirable biological properties such as cytotoxicity, neurotoxicity, antiviral, and antifungal activities. In particular, the amphidinolides have demonstrated their immense potential as chemotherapeutic agents.[122]

Arising from their ability to interfere with the polymerization dynamics of two major components of the cellular cytoskeleton, amphidinolides and the majority of the marine macrolides proffer potential as potent chemotherapeutics. This is due to the inhibition of cytoskeletal actin and tubulin subunits which polymerize into microfilaments and microtubules respectively.[122]

Since the cytoskeleton plays a critical role in the determination of cell shape and the normal functioning of a range of cellular processes such as cell motility, division, adhesion and intracellular transportation, small molecules interacting with the cytoskeleton when used as therapeutics, can alter the abnormal growth properties of tumour cells, influence their ability to adhere to tissues and decrease their ability to metastasize. Thus they present themselves as attractive leads for the development of new chemotherapeutic agents.[122]

1.4.1 Actin Interaction Probes

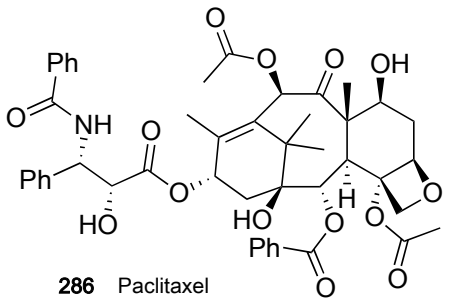

Figure 1.6: Paclitaxel

One of the major components found in the cytoskeleton of eukaryotic cells is actin. Like tubulin, the other major component of the cytoskeleton, it has important cellular functions. Whilst the chemistry community may be more familiar with tubulin primarily due to the successes of paclitaxel in the treatment of cancer and the subsequent discovery of a number of other natural products (Figure 1.7) such as the epothilones (**287**), discodermolide (**291**), laulimalide (**289**), eleutherobin (**290**) and sarcodictyins (**288**) which share paclitaxel's microtubule-stabilizing properties, there is growing interest amongst the scientific community to investigate the detailed interactions of the actin cytoskeleton and its cellular function.[123,124]

Molecular genetic approaches are often used to study the highly complex and dynamic actin cytoskeleton and its associated cellular functions. However more recently, marine macrolides such as the amphidinolides have gained credibility in serving as novel molecular probes to help elucidate the cellular functions of actin.[111]

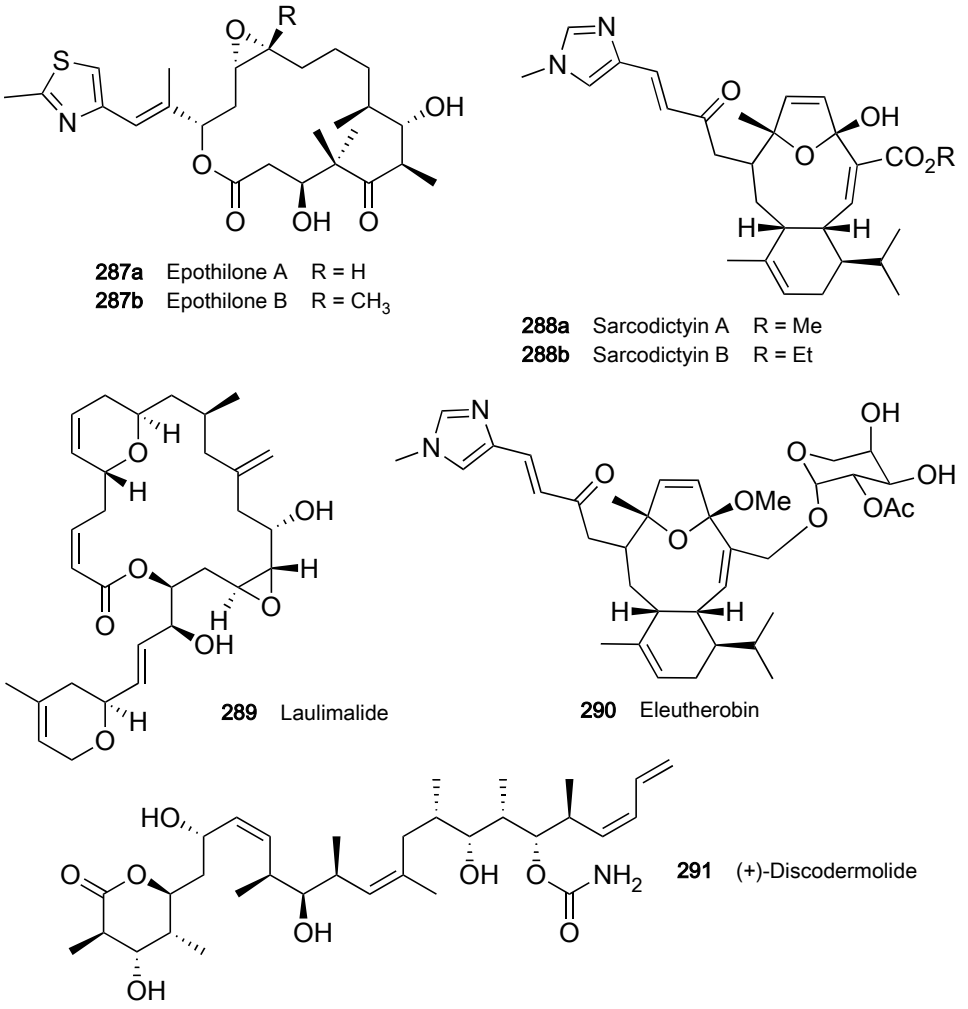

Figure 1.7: Other Microtubule Stabilizers

1.4.2 Chemotherapeutic Agents Targeting the Actin Cytoskeleton

Actin filaments (F-actin) are formed by the assembly of globular (G-actin) monomer subunits in a head-to-tail orientation, forming a right handed double-stranded helix. This assembly and disassembly of the actin cytoskeleton is controlled by special regulatory proteins. The rate limiting step for the formation of F-actin is the formation of a stable nucleus. When two G-actin monomers collide, they form a dimer. However this dimer is unstable and readily comes apart. In order for

filamentous actin to grow, three or four G-actin monomers must collide simultaneously. In cells, spontaneous nucleation is rare and F-actin formation is regulated by a complex library of over 100 actin-binding proteins. It has been recognized that in numerous disease states, abnormal release of actin filaments into extracellular space and normal actin cytoskeleton functionality has been compromised.[122,125]

Given the critical role of the cytoskeleton in many pathogenic cellular processes such as angiogenesis, cell adhesion, intracellular transportation, cytokinesis and metastasis, it is not surprising that nature has its own mechanisms to ensure proper functioning. Investigation by Gachet and Hyams *et. al.*,[126] have unveiled an actin dependent cell cycle checkpoint that ensures the proper orientation of microtubule spindles during metaphase.[111]

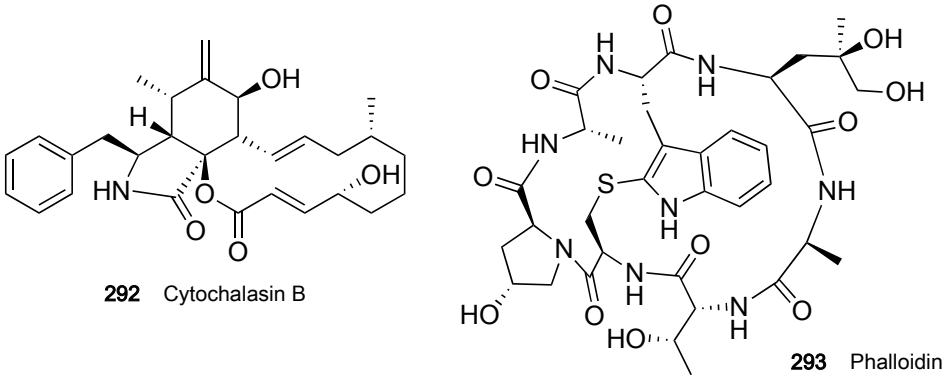

Figure 1.8: Actin Destabilizer and Stabilizer

Compounds that are able to influence the polymerization and depolymerization kinetics of actin are hence potentially powerful chemotherapeutics. Such compounds that inhibit actin are classified into two types: destabilizers and stabilizers of actin filaments.[127] Actin destabilizers such as cytochalasin B (**292**) destroys the actin cytoskeleton by severing or sequestering actin. Actin stabilizers such as phalloidin (**293**) stabilizes filamentous actin by binding at the junction of two or three

monomeric actin along the actin filament. To gain better understanding behind the mechanisms of action of these drugs and to develop specific inhibitors, it is crucial to determine the binding site and binding mode of these drugs to their target proteins.

Amphidinolides belong to this class of marine natural products with the latent potential of development into new chemotherapeutical agents. Pioneering the isolation, characterization and biological studies on the amphidinolides, Kobayashi *et. al.* have laid the foundation towards investigations of developing chemotherapeutic drugs from this family of natural products. The group has shown that amphidinolide H (AmpH) is a novel actin inhibitor that binds covalently to actin.[127] The AmpH binding site has been determined to be Tyr200 of the actin subdomain 4. AmpH has been shown to disrupt actin organization in cells by inducing formation of small actin patches, followed by aggregation of F-actin rearrangement into aggregrates via retraction of actin fibres.[127] Burgeoning interest into employing marine macrolides such as the amphidinolides as therapeutic drugs targeting the actin cytoskeleton has gain momentum with the discovery that certain bacterial and viral pathogens have been found to exploit the actin cytoskeleton during their lifecycle of infection.

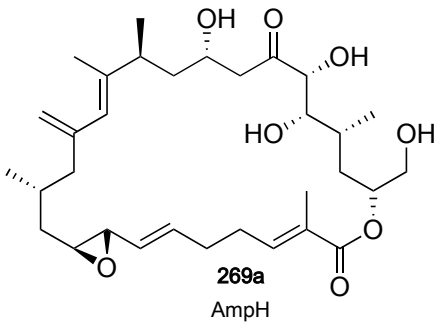

Figure 1.9: Amphidinolide H

1.5 Contributions from Organic Synthesis

Synthetic interests in these marine macrolides stem from the quandary that most of these natural products can be isolated in only microscopic quantities from the biological sources. For instance, amphidinolide X is extremely rare making up only 0.001% wet weight of the algae. Organic synthesis thus serves as a practical and ecologically sensible alternative to the large scale harvesting of marine organisms. In cases such as the amphidinolides, the desired natural products are in fact produced by symbiotic organisms living in close association with the marine hosts, which presents specific cell culture difficulties. Microbial fermentation may then be a potential means of obtaining significant quantities of the macrolide. However, it should be noted that to date, this approach has met with limited success, since the identification and isolation of the genes involved in the biosynthesis have not been fully characterized. Hence, chemical total synthesis still remains the more viable option.

Also, *de novo* chemical synthesis provides the possibility of deriving non-natural analogues which might exhibit better therapeutic indices. Fürstner *et. al.* recognized the value of such "molecular editing" and have embarked on a series of "diverted total synthesis" on the amphidinolides to obtain insights into the structural-activity relationships governing the cytotoxicity profile of this family of natural products.[37] Deviations from the total synthesis of amphidinolide X generated a library of seven designed analogues that showed better activity than the natural product, albeit showing a moderate averaged cytotoxicity.[37]

Chapter 2

Syntheses of Amphidinolide X in the Literature

2.1 Introduction

As we have noted in Section 1.2 (page 91), within a relatively short timespan after its discovery in 2003, amphidinolide X has already attracted an impressive number of total syntheses of the molecule itself, synthesis of the tetrahydrofuran ring, and amphidinolide X analogues.[35–42,120]

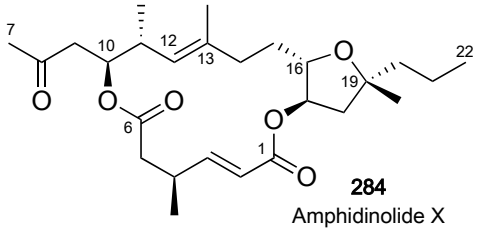

Figure 2.1: Amphidinolide X

The very first total synthesis of amphidinolide X was done by Fürstner *et. al.*[35] This was followed by the groups from Dai,[40,41] Vatèle,[120] Vilarrasa[38,39] and Lee.[42] During this period, Fürstner went on to publish two other papers on the convergent syntheses of amphidinolides X and Y and their analogues.[36,37] It is to these that we turn our attention to in the next section, with a discussion of their retrosynthetic analyses and forward syntheses.

In the subsequent discussions, we will see that one of the main concerns in the synthesis of amphidinolide X lies in the generation of the fragment containing the oxolane ring. If that can be dealt with, the ancillary concern would then be the assembly of the fragments making up the molecule into the macrocycle. With this in mind, we will proceed to our survey in the next section. To facilitate our discussions, the numbering of the carbon skeletons of the fragments in the schemes will be based on that for amphidinolide X.

2.2 Reported Total Synthesis of Amphidinolide X

2.2.1 Retrosynthetic Analysis by Fürstner *et. al.*

Given that amphidinolide X (**284**) has two ester linkages, retrosynthetic analysis by Fürstner made these first two obvious disconnections to the macrolactone ring.[35–37] For the fragment C(7)–C(22), a further disconnection between C(13)–C(14) was envisaged to proceed through a metal-catalyzed alkyl-alkenyl cross-coupling reaction, hence generating the three main fragments as shown in Scheme 2.1. These three similarly sized fragments ensure a highly convergent synthesis, and also allow them to utilize the methodology their group has developed in the formation of the oxolane ring.

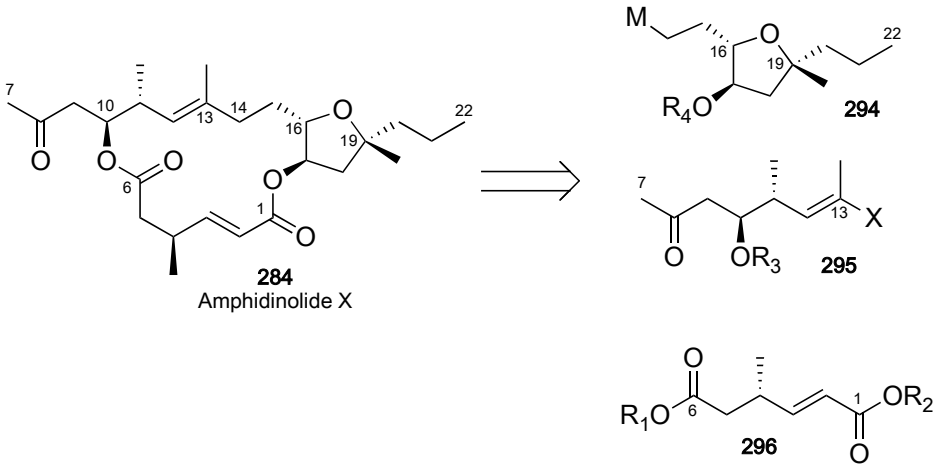

Scheme 2.1: Fürstner's Retrosynthetic Analysis of Amphidinolide X

To Fürstner, the key synthetic transformation that has to be addressed first would be the construction of the synthetically challenging tetrahydrofuran ring system which bears three chiral centres. But this was secondary to his main concern of

wanting to form the tetrasubstituted chiral center at C(19) residing at the ether bridge as early in the synthesis as possible.

To gain access to this key structural element, it is their intention to use a chiral allene as the 'latent progenitor' of the THF ring with a methodology their group has developed.[128] This THF ring can be formed in a stereoselective manner via an iron-catalyzed Grignard reaction on a propargyl epoxide. As Scheme 2.2 shows, this sequence should be able to transfer the central chirality of the epoxide via the relay from the axial chirality of the allene to the C(19) chiral center.

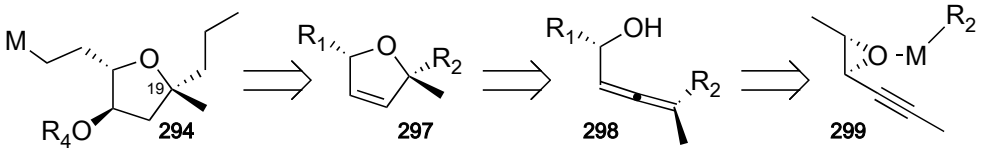

Scheme 2.2: Fürstner's Retrosynthetic Analysis of the THF Ring

2.2.2 Synthesis by Fürstner *et. al.*

As seen in Scheme 2.3, the crucial THF ring was first synthesized using Fürstner's methodology by starting from the monoprotected allylic alcohol **300** to secure the epoxide **301**. This was generated in excellent yield and good optical purity, and was followed by a Swern oxidation to form the aldehyde before reacting with the Ohira–Bestmann reagent to give alkyne **302**. This terminal alkyne was then end-capped with a methyl group using MeOTf, before reaction with propyl magnesium chloride using $Fe(acac)_3$ as a precatalyst to generate the allene **304** as an 89:11 *syn-/anti*-mixture — the major product being the desired allene. Fürstner surmised that the good selectivity most likely arises from precoordination of the oxophilic

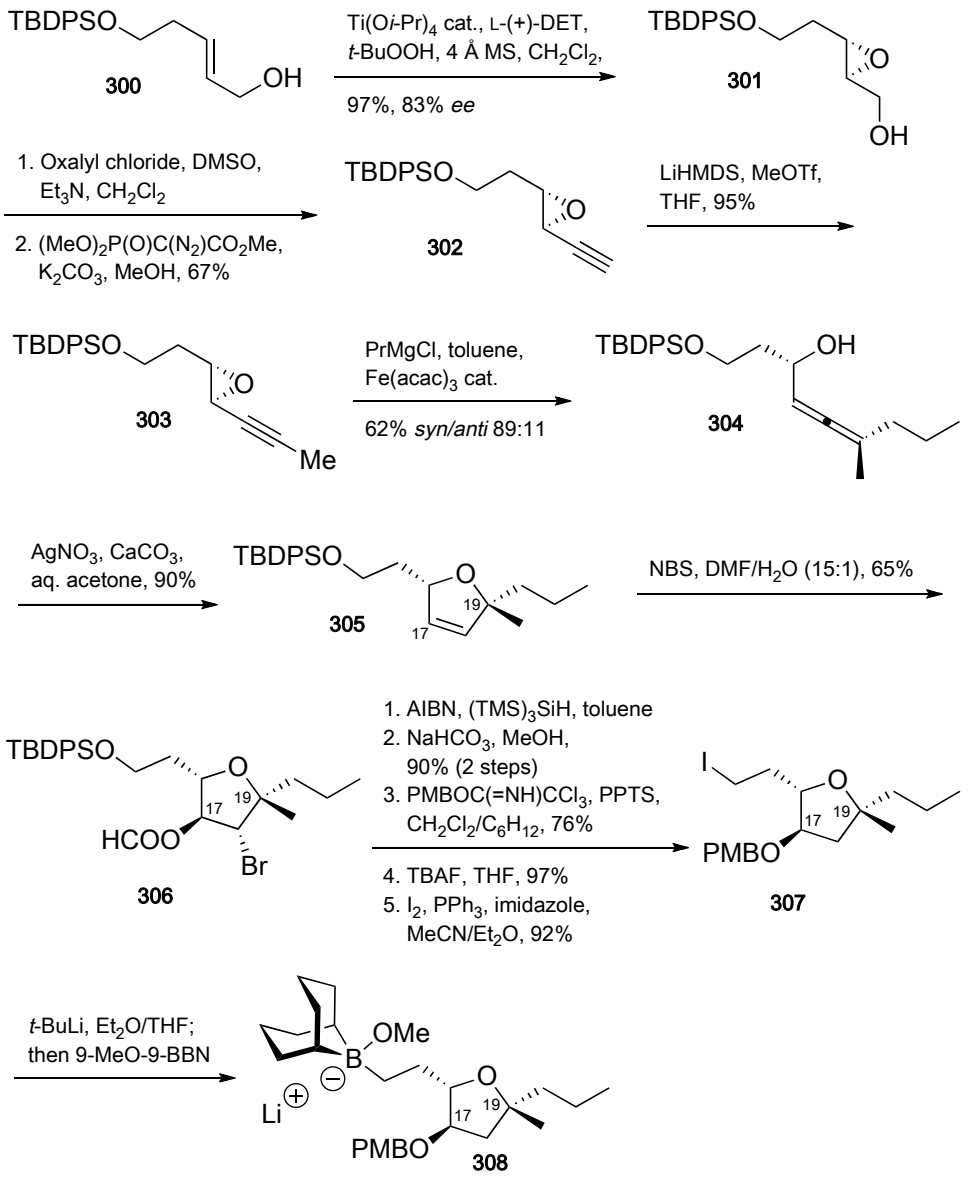

Scheme 2.3: Fürstner's Synthesis of the THF Ring Fragment

catalyst and/or reagent to the epoxide ring (**299**), which results in a directed delivery of the nucleophile as shown in Scheme 2.2.

Unfortunately, the allene isomers for **304** were not separable. As such, they moved the synthesis forward with the allene mixture to form the dihydrofuran **305**. This was achieved with strict chirality transfer, and they initially wanted to follow this

with the attachment of a hydroxy group at C(17) using a hydroboration/oxidation sequence. However, the yields from this reaction sequence were low and was thus abandoned. Eventually, they found that bromoesterification of **305** with NBS/aqueous DMF was a viable detour and were rewarded with the bromide **306** whose C(19) isomers are easily separable by flash chromatography.

To obtain **307** as the surrogate for synthon **294**, they next used $(Me_3Si)_3SiH$ with AIBN to remove the bromide group. This was then followed on uneventfully with a series of standard protecting group manipulations to give **307**.

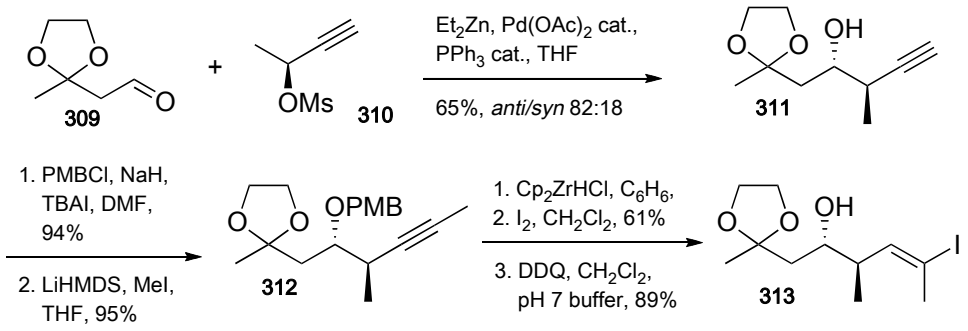

Scheme 2.4: Fürstner's Synthesis of the Second Fragment

For the second fragment represented by **295** in the retrosynthetic scheme 2.1, Fürstner intended to access it by performing a Pd-catalyzed Et_2Zn-mediated addition of the homochiral propargyl mesylate **310** to the aldehyde **309** as shown in Scheme 2.4. This was obtained as the major *anti*-isomer in 93% *ee*. After protecting the hydroxy group as a PMB-ether, the terminal alkyne was methylated and subsequently subjected to a hydrozirconation/iodination sequence. The PMB-ether was then deprotected to give the desired alkenyl iodide **313**.

As for the third and final fragment which is represented by **296** in the retrosynthetic scheme 2.1, this was accessed via the known aldehyde **314** to give the

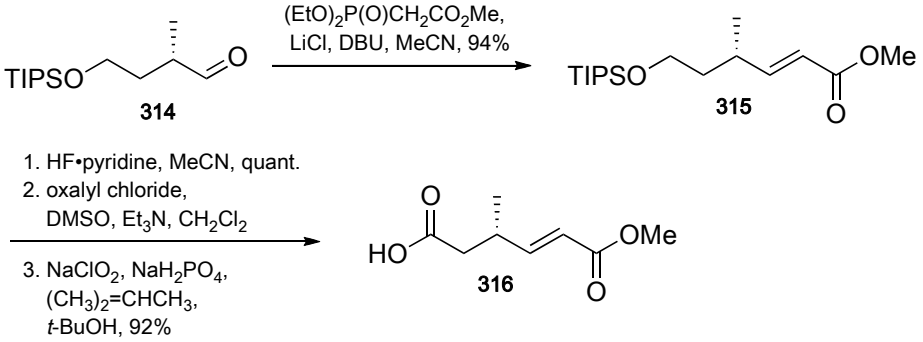

Scheme 2.5: Fürstner's Synthesis of the Third Fragment

desired acid **316** after standard manoeuvres. With all these fragments ready at hand (**307**, **313** and **316**), they can now proceed to finish off the synthesis by prudent assembly of the fragments.[36]

The various assembly options of the three appropriately protected "bifunctional" fragments considered by Fürstner are shown in Scheme 2.6. From the options

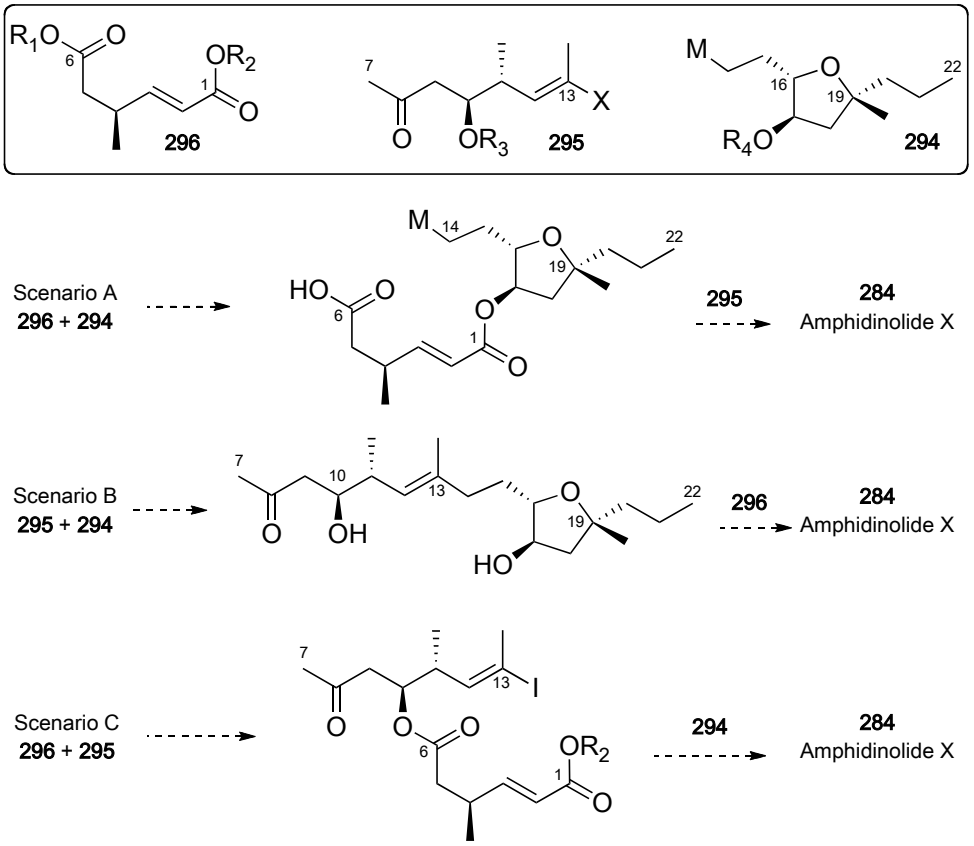

Scheme 2.6: Assembly Options Considered by Fürstner

listed, they immediately ruled out scenario A as it implies "rather severe selectivity issues during the conversion of the leaving group X at C(14)" into a nucleophile suitable for their envisaged cross-coupling.

For the remaining two options B and C, both of which looked practicable, they conducted exploratory studies and found issues with the lability of the –OH group at C(10). It turns out that this acid- and base-labile –OH group eliminates readily even under mild conditions. As such, they decided on the less risky option C where the ester linkage at C(10) is formed at an early stage. Also, another advantage with this option is the introduction of the valuable THF fragment **294** last, which hopefully would result in higher overall yields of the final product.

Hence, the acid **316** was coupled with the alcohol fragment **313** via a Yamaguchi esterification to give **317** as shown in Scheme 2.7, in preparation for the final coupling with the THF fragment and subsequent macrocyclization to complete the synthesis.

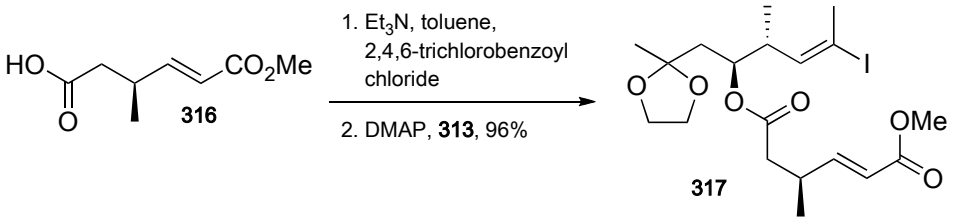

Scheme 2.7: Yamaguchi Esterification

Fürstner's endgame for the total synthesis of amphidinolide X is depicted in Scheme 2.9. Having secured two-thirds of the molecule with the assembly of **317**, they moved it forward uneventfully with their "9-MeO-9-BBN variant" of the Suzuki alkyl-alkenyl cross coupling to the THF fragment **308** and was granted

318. This was accomplished by formation of the 9-MeO-9-BBN borate complex of **307** *in situ*.

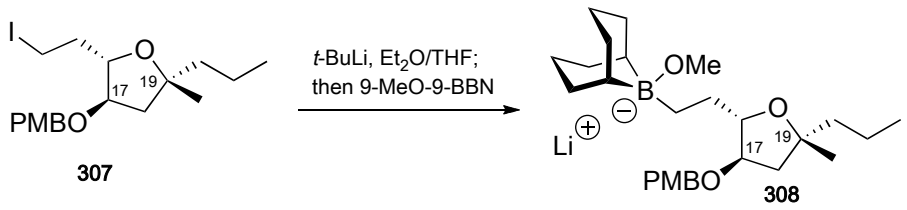

Scheme 2.8: Formation of the Borate Complex of **307**

Selective cleavage of the methyl ester in **318** was then performed with LiI in hot pyridine, followed by the deprotection of the acetal and thereafter removal of the PMB ether. With the macrocyclization partners revealed, a final reaction under Yamaguchi conditions proceeded smoothly to afford the desired product, amphidinolide X (**284**), in a yield of 62%.

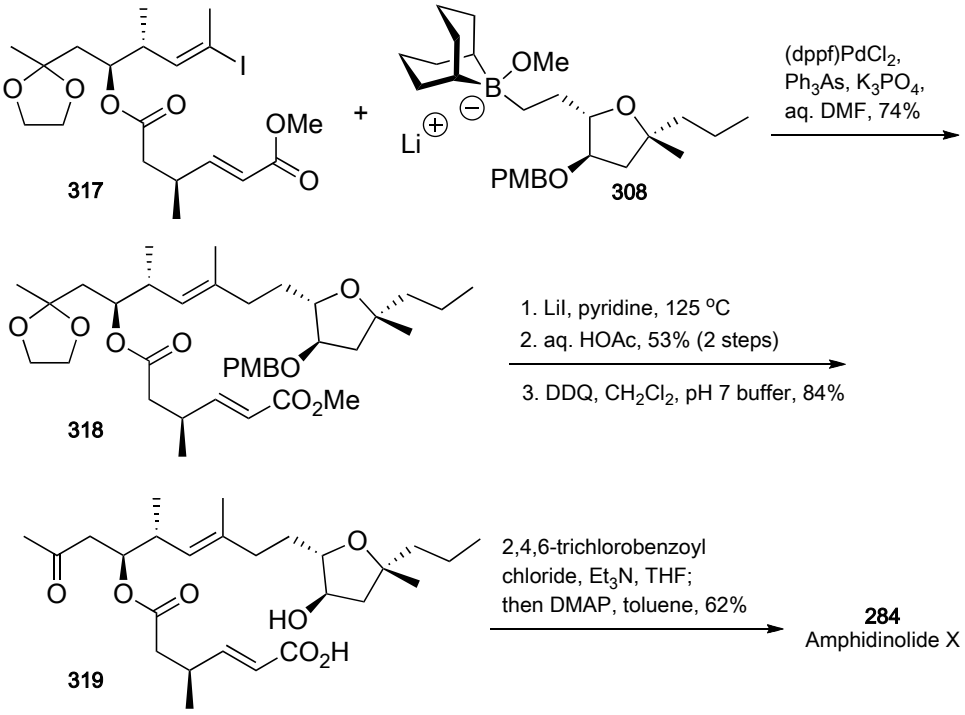

Scheme 2.9: Fürstner's Endgame for Amphidinolide X

2.2.3 Retrosynthetic Analysis by Dai *et. al.*

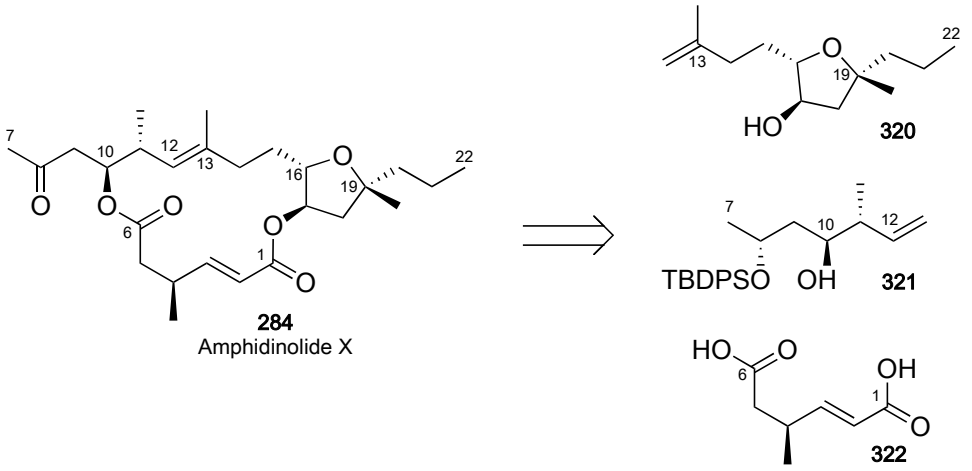

Scheme 2.10: Dai's Retrosynthetic Analysis of Amphidinolide X

The retrosynthetic analysis of amphidinolide X by Dai and his co-workers is shown in Scheme 2.10.[40,41,129] When we compare this to the retrosynthetic analysis of Fürstner *et. al.* (Scheme 2.1), we see that Dai too makes the first two obvious disconnections at the ester bonds. However, for the fragment C(7)–C(22), he intended to do a ring-closing metathesis (RCM) to form the macrocycle. Thus, the disconnection at C(12)-(13) is inevitable, giving rise to the proposed three fragments **320**, **321** and **322**. These three fragments can be further reduced to simpler precursors as depicted in Scheme 2.11. It is interesting to note their use of the methyl ester **325** where the hydroxy group functions as a masked C(8)-ketone in the amphidinolide X molecule, since this would incur additional steps in their synthesis.

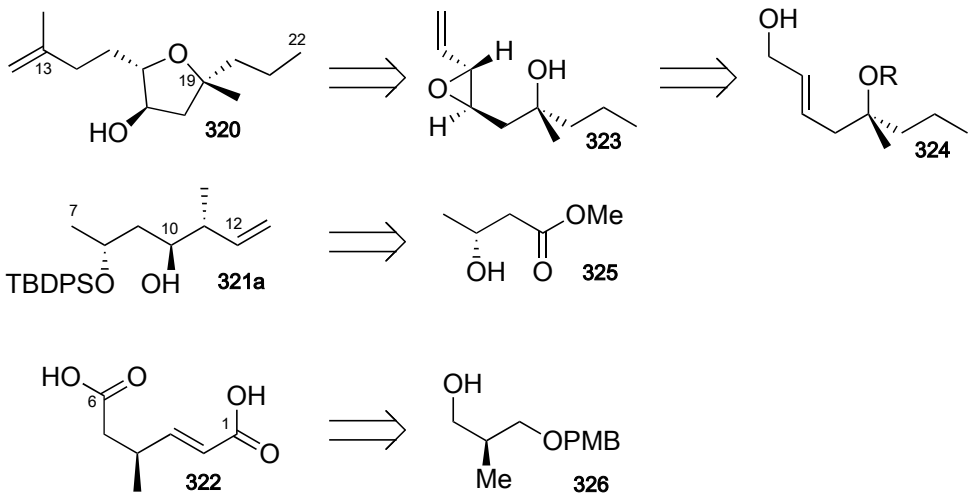

Scheme 2.11: Reduction of Fragments to Simpler Precursors

2.2.4 Synthesis by Dai *et. al.*

From the retrosynthetic analysis for the THF fragment, we see that Dai and his co-workers needed a means of generating a chiral tertiary alcohol functionality in **324**. For them, it was imperative that this was synthesized with high enantiopurity. Thus, they were glad to discover that this was possible through the use of Corey's enantioselective dihydroxylation[130] by starting from the homoallylic alcohol **327**. Their forward synthesis to generate this first fragment containing the crucial THF ring starting from the homoallylic alcohol **327** is depicted in Scheme 2.12. If this venture turns out successful, they will also have synthesized a fragment that is of use in the total synthesis of the related amphidinolide Y (**285**).

However, in terms of elegance and efficiency, these laborious 14 steps taken to just prepare the substrate **332** needed for cyclization to form the THF ring fragment pales in comparison to the outstanding strategy of Fürstner *et. al.* Yet, as Vilarrasa puts it, Dai's strategy provides for an "interesting approach to this THF ring, through an acid-catalyzed 5-*endo* cyclization".[38] In spite of that, to add insult to

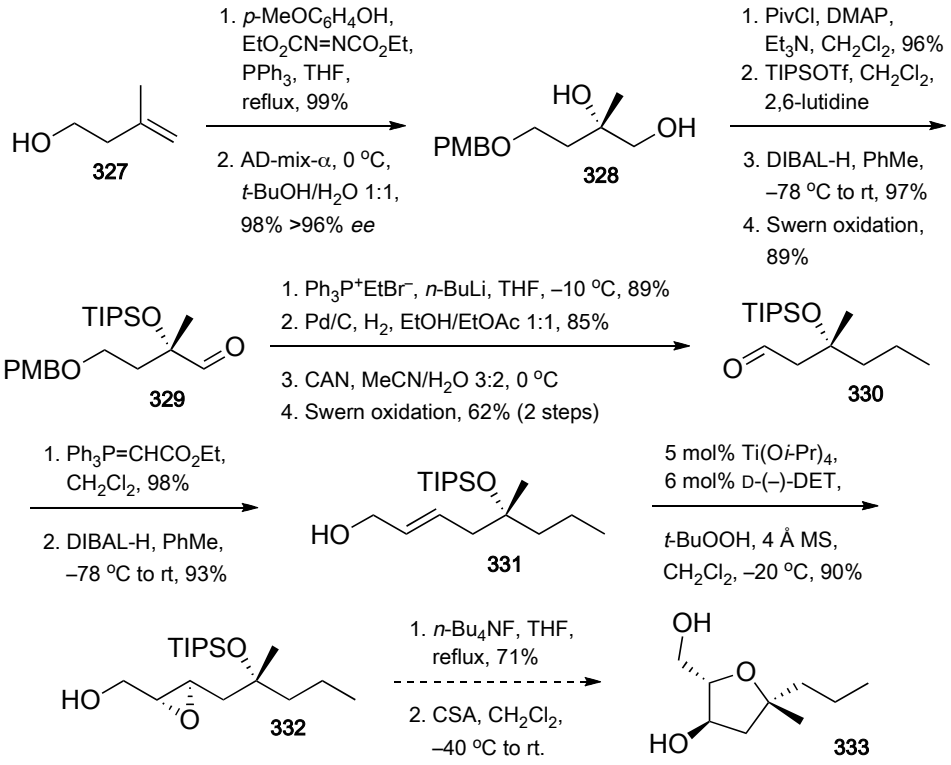

Scheme 2.12: Dai's Attempted Synthesis of the THF Ring Fragment

injury it was unfortunate for them that after performing such a grueling synthesis to finally obtain the needed epoxide **332**, acid-catalyzed formation of the THF ring from the deprotected **332** failed.

By refering to work done by the groups from Nicolaou and Borhan,[131–133] they embarked on an alternative route, converting **332** to the vinyl epoxide **334**. This eventually gave them their desired fragment **320**, via the acid-catalyzed formation of the THF ring **336**, followed by TES-protection, hydroboration with 9-BBN and coupling with 2-bromo-1-propene.[129] Thus was completed painstakingly their first of three fragments of amphidinolide X as depicted in Scheme 2.13. This THF fragment constitutes their common intermediate in the total syntheses of both amphidinolides X and Y.

For the synthesis of fragment two (**321**), Dai *et. al.* proposed to proceed via

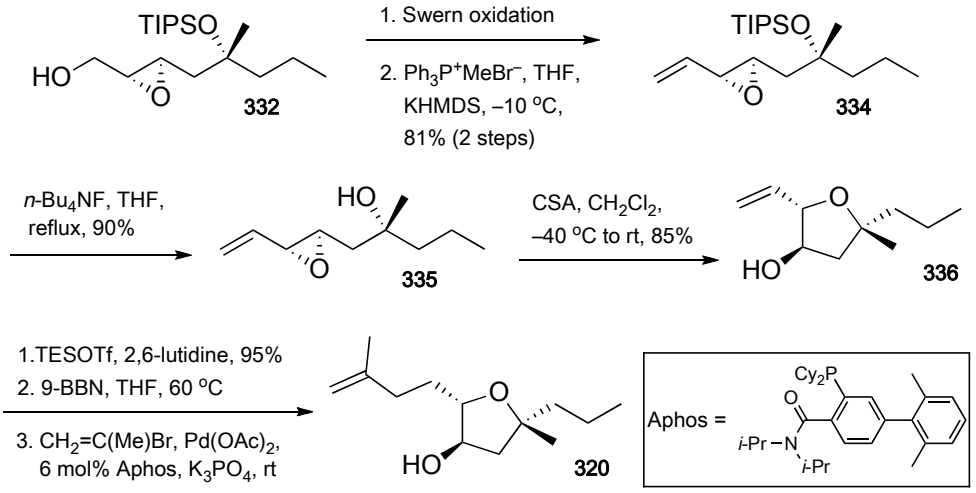

Scheme 2.13: Dai's Successful Synthesis of the THF Ring Fragment

an *anti*-selective aldehyde crotylation with either chiral boron or silicon reagents. This could be accomplished by starting from the known chiral ester **325** and converting it to the requisite aldehyde **337**,[134] before performing the crotylation. The protected hydroxy group then serves as the masked C(8) ketone moiety of amphidinolide X. As seen in Scheme 2.14, they tried both crotylating reagents from Leighton and Roush (**338a** and **338b** respectively), with the former giving excellent diasteroselectivity albeit at a lower yield.

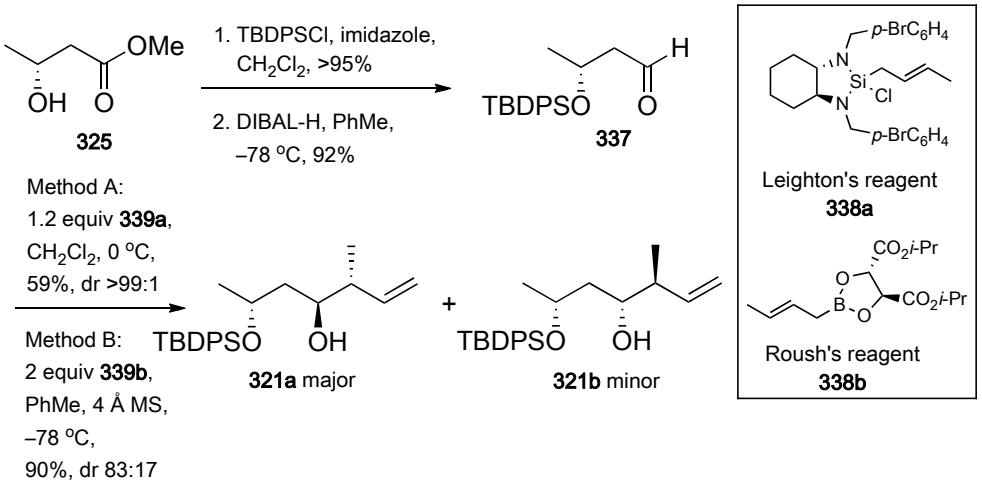

Scheme 2.14: Dai's Synthesis of the Second Fragment

Thereafter, they proceeded to the synthesis of the final fragment **339**, by beginning from another known alcohol **326**.[135,136] This proceeded uneventfully to furnish them with the acid **339**, thereby setting the stage for their first attempt at assembly of the fragments at hand.

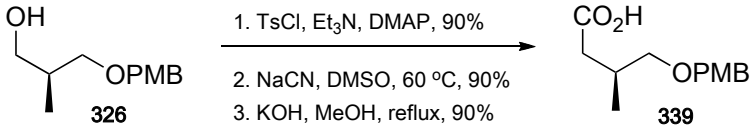

Scheme 2.15: Dai's Synthesis of the Third Fragment

As shown in Scheme 2.16, the acid **339** was condensed with the chiral homoallylic alcohol **321a** using Yamaguchi's conditions. This was then deprotected and oxidized with Dess-Martin periodinane to generate the aldehyde **341**. A subsequent Wittig olefination provided the two-carbon homologated methyl ester that was then put through a selective microwave-assisted removal of the methyl ester using LiI in pyridine to form the acid **342**.

With two-thirds of the molecule assembled, they next connected the final THF fragment **320**, again using Yamaguchi's condition, uneventfully. Thereafter, the C(8)-ketone moiety was unmasked by deprotecting the TBDPS-protected C(8)-hydroxy group, followed by a Dess-Martin periodinane oxidation. With all these manoeuvres done, they were ready for the final ring-closing metathesis (RCM) to generate the desired amphidinolide X molecule (**284**).

Based on their previous successful experience using Grubbs' second generation catalyst for their RCM as the last key step in their total synthesis of amphidinolide Y[129], they had expected to sail smoothly to the final product this time

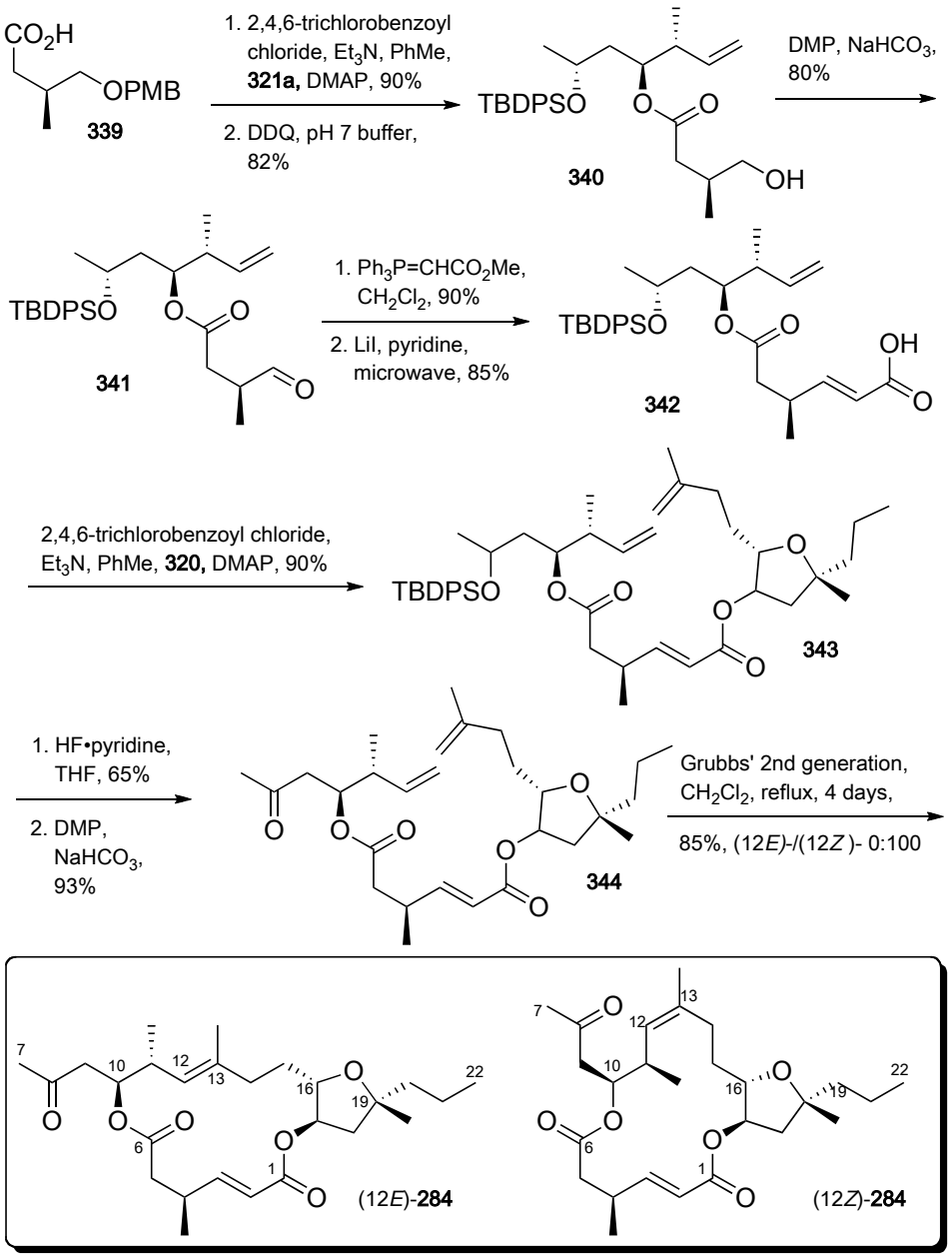

Scheme 2.16: Dai's Failed Assembly of the Fragments for Amphidinolide X

as well, with a straightforward formation of the (*E*)-isomer at the C(12)–C(13) double-bond. Unfortunately, their attempts were foiled by the production of only the (12*Z*)-isomer of amphidinolide X exclusively. With this failure at their final step in the total synthesis, they had no other options but to revert to rescreening the substrates and catalysts in order to salvage the situation. Eventually they

managed to wrest the desired (12*E*)-amphidinolide X out, only when they performed the RCM on the TBDPS-protected substrate **343** with Grubbs' second generation catalyst after refluxing for six days. Even then, the yield was less than optimal (50%), with a paltry (12*E*)-/(12*Z*)-selectivity of 29:71 that they had to settle with for the TBDPS-protected isomers of amphidinolide X (**345**) as seen in Scheme 2.17. The mixture was then deprotected with HF·pyridine, and the final

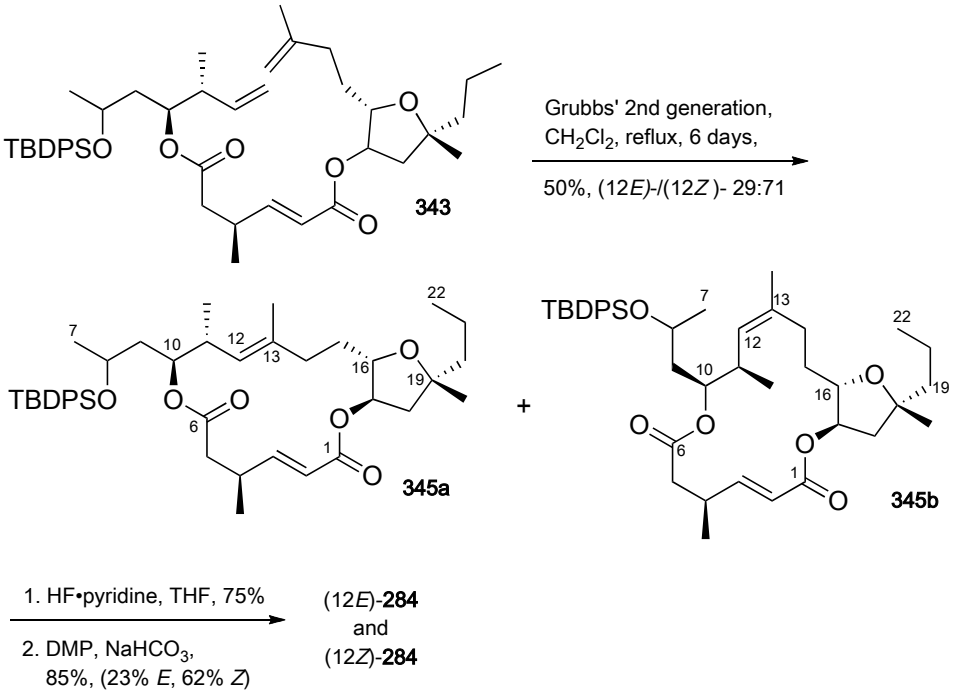

Scheme 2.17: Dai's Final Assembly of the Fragments for Amphidinolide X

C(8)-ketone unmasked after a Dess-Martin periodinane oxidation, again on the mixture. Eventually, a combined yield of 85% was obtained for the mixture, with 23% being the desired (12*E*)-isomer, thus completing their synthesis of amphidinolide X (**284**).

2.2.5 Retrosynthetic Analysis by Vatèle *et. al.*

Vatèle and co-workers only published a report on the synthesis of the common tetrahydrofuran building block of amphidinolides X and Y (**284** and **285**).[120] Their retrosynthetic analysis for this fragment is shown in Scheme 2.18. As with Dai *et. al.*, they had envisaged the formation of the THF ring via a 5-*endo-tet* cyclization, being inspired by the study of Borhan and co-workers as well.[133,137] Unfortunately for them, the paper by Dai was reported during the course of their synthesis of the THF ring.

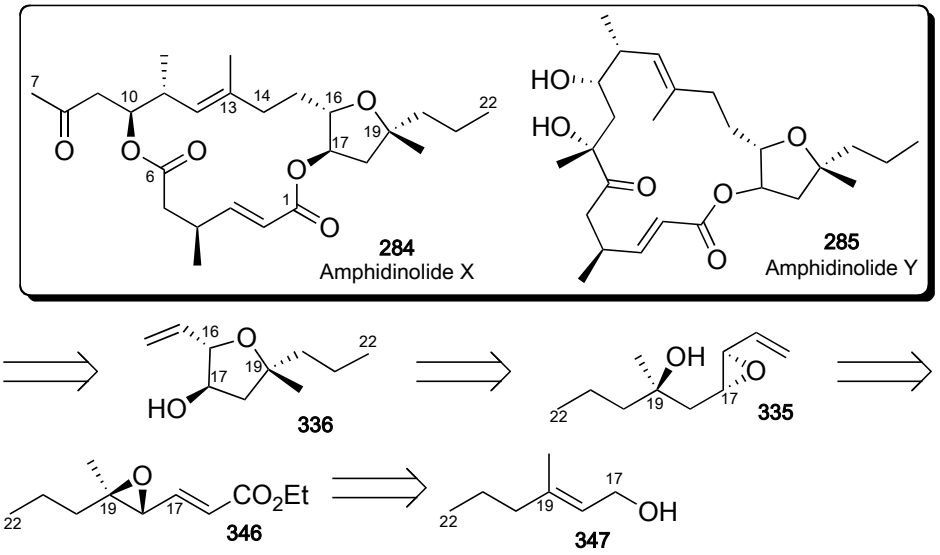

Scheme 2.18: Vatèle's Retrosynthetic Analysis for the THF Fragment of Amphidinolide X

Other features in their synthetic plans are: (i) the Tsuji Pd-catalyzed hydrogenolysis[138] of the alkenyl oxirane **346** for installing the correct oxidation state at C(17); (ii) a Sharpless asymmetric epoxidation on **347** for the installation of the tetrasubstituted chiral center at C(19). Without further ado, we proceed to the discussion of their forward synthesis of this common THF building block.

2.2.6 Synthesis by Vatèle *et. al.*

Although Vatèle had intended to obtain the same THF fragment **336** as Dai via the same mechanism, they differed in their approach to this end. As can be seen from Scheme 2.19, Vatèle went about procuring the THF fragment via the readily available and stereochemically pure alcohol **347** from geraniol (**253**). This can be made in gram quantities with an improvement to the procedure described by Mori *et. al*,[139] in an overall yield of 51% over four steps.

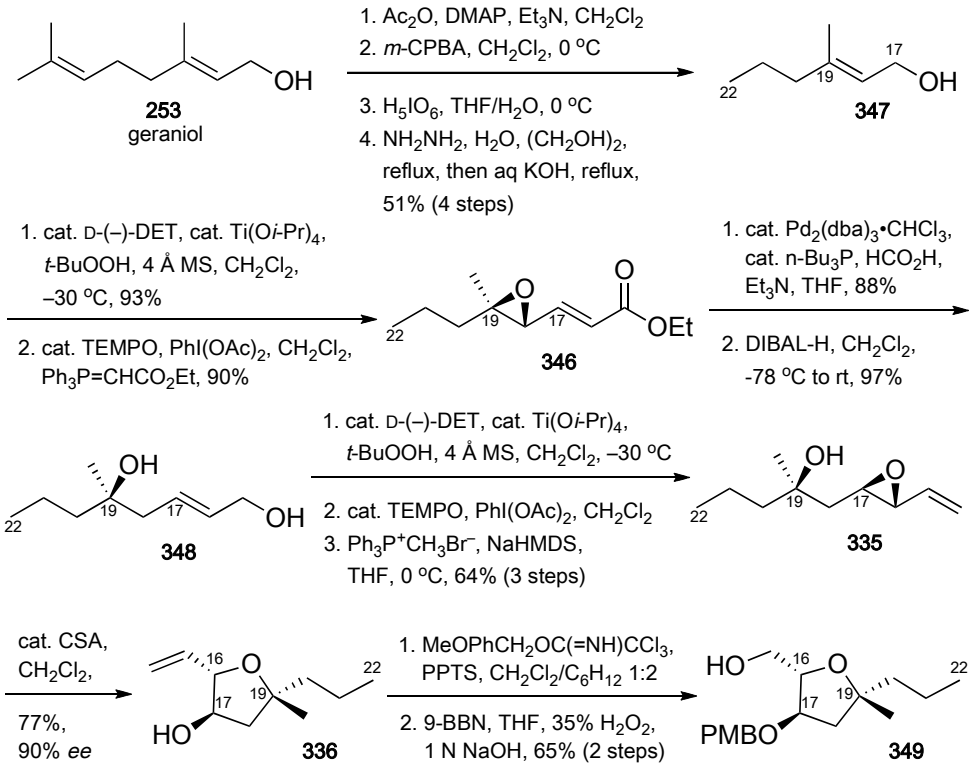

Scheme 2.19: Vatèle's Synthesis of the THF Fragment for Amphidinolide X

Asymmetric Sharpless epoxidation followed by a one-pot oxidation/Wittig olefination was performed on **347**, thereby setting in place the requisite tetrasubstituted

chiral center at C(19), which is obtained using Tsuji's regioselective reductive opening of epoxide **346** by Pd-catalyzed hydrogenolysis. This was reduced to the allylic alcohol **348** where another asymmetric Sharpless epoxidation is performed. A subsequent oxidation using Piancatelli's procedure[140] secured the aldehyde needed to generate the terminal double-bond via a Wittig one-carbon homologation for procuring the vinyl oxirane **335**.

Treatment of this epoxide with catalytic camphorsulfonic acid[131,132] yielded the desired THF fragment **336** in 77% yield and 90% *ee*. The stereochemistry was confirmed by further derivatizing it to the known alcohol **349** previously characterized by Fürstner in his synthesis.

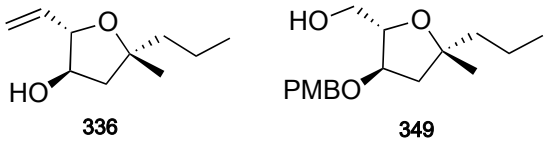

336 349

Figure 2.2: Common Vinyl THF Building Block and Fürstner's PMB-protected THF Alcohol

2.2.7 Retrosynthetic Analysis by Vilarrasa *et. al.*

The retrosynthetic analysis by Vilarrasa is depicted in Scheme 2.20, where the molecule is disconnected at the two ester bonds as routinely done.[38,39] Thereafter, Vilarrasa proposes to perform a ring-closing metathesis at C(12)–C(13) of the major fragment C(7)–C(22), hence giving the three main fragments **320**, **350** and **351** as set forth in the retrosynthetic scheme.

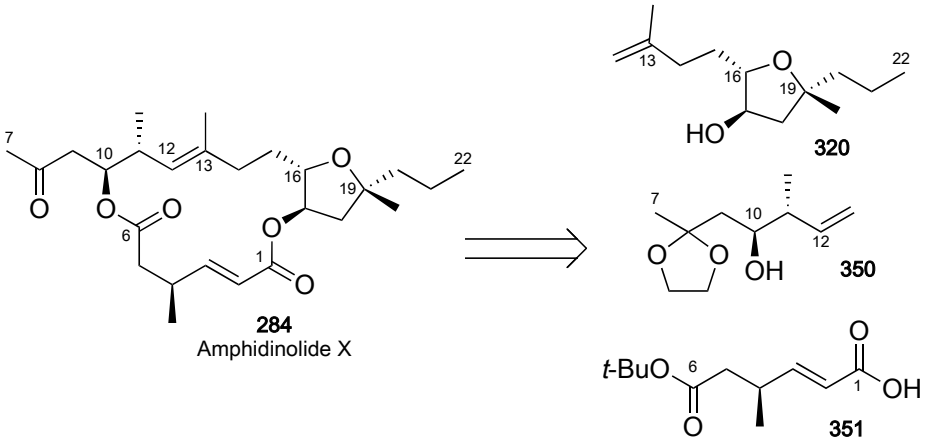

Scheme 2.20: Vilarrasa's Retrosynthetic Analysis of Amphidinolide X

In a previous report, Vilarrasa and his co-workers had already established a selenium-based formation of the THF ring via "a cyclization of an *anti* dihydroxy (allylic and homoallylic), unprecedented trisubstituted-alkene substrate" in excellent yields.[38] We delineate in Scheme 2.21 their further retrosynthesis of the THF fragment, as well as the other two main fragments of amphidinolide X.

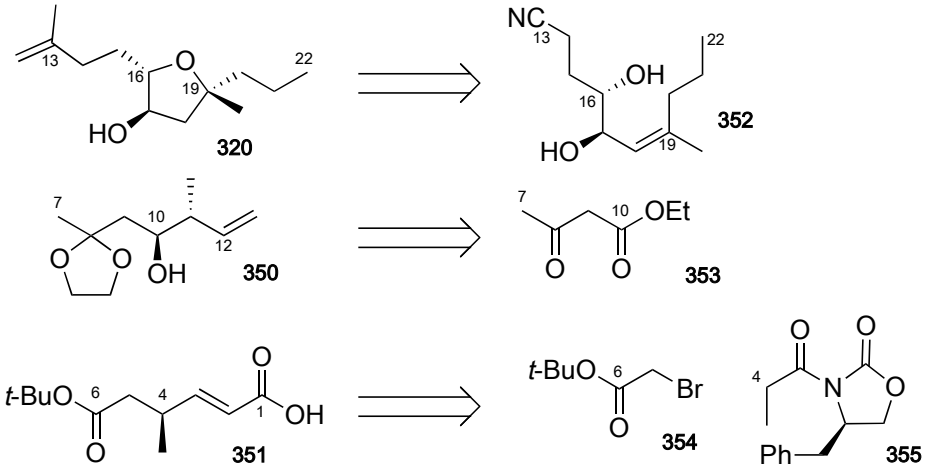

Scheme 2.21: Vilarrasa's Retrosynthetic Analysis for the Three Fragments of Amphidinolide X

Thus, the synthesis of the THF fragment will be based on the methodology developed by their group, while the C(7)–C(12) fragment (**350**) will be derived from an asymmetric crotylation on ethyl acetoacetate. For fragment **351**, they propose

an asymmetric alkylation using an Evans' chiral auxillary followed by a Wittig olefination.

2.2.8 Synthesis by Vilarrasa *et. al.*

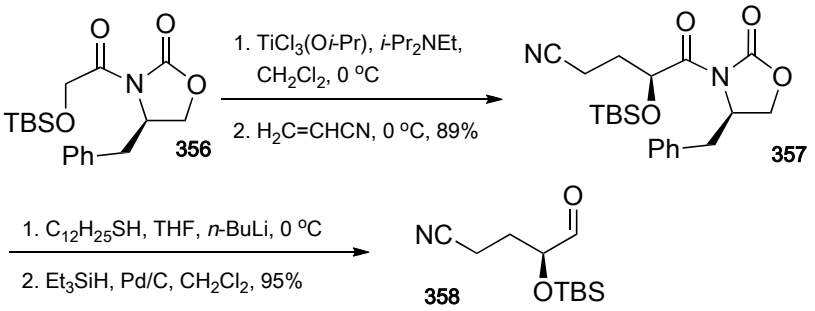

Scheme 2.22: Vilarrasa's Preparation for the Synthesis of the THF Fragment

In order to synthesize the THF fragment **320** using the selenium-based cyclization methodology developed by their group, Vilarrasa first prepared the oxonitrile **358** from the non-natural Evans' chiral auxiliary that has been TBS-protected (**356**). This was converted to the titanium enolate and subsequently treated with acrylonitrile to generate enantiopure **357** in an overall yield of 89%. Thereafter, this was reduced to the desired aldehyde **358** using Fukuyama's methodology.[141]

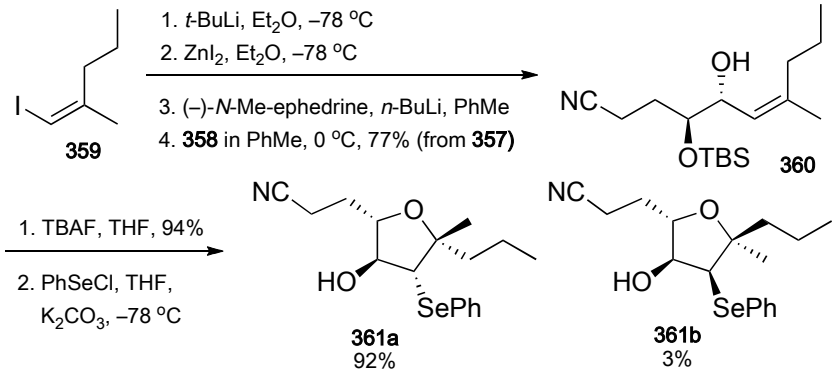

Scheme 2.23: Vilarrasa's Synthesis of the Seleno-THF Fragment

The synthesis of the THF fragment **320** was then continued by reacting the crude aldehyde **358** with an alkenyl zincate formed from the iodopentene **359**. This was then purified before removal of the TBS ether to furnish the requisite enantiopure substrate **352**, that was cyclized with PhSeCl to give **361a** in excellent yield.

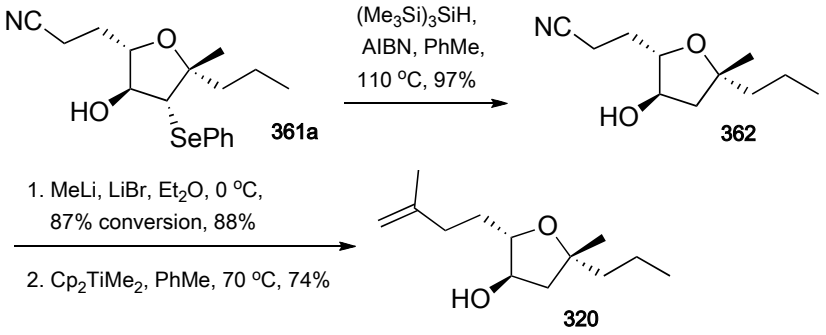

Scheme 2.24: Vilarrasa's Synthesis of the THF Fragment

As shown in Scheme 2.24, deselenylation using $(Me_3Si)_3SiH$/AIBN was followed by a sequence comprising the direct enamine formation using LiBr·MeLi that generates the methyl ketone after quenching.[142] This then underwent a Ti-mediated carbonyl olefination with dimethyltitanocene to form the methylene moiety,[143] whereupon the desired THF fragment **320** is obtained.

For the synthesis of the second fragment (**350**), Vilarrasa performed an asymmetric crotylation on the aldehyde **363** derived from ethyl acetoacetate (**353**) using the TADDOL-crotyltitanium reagent **364** reported by Hafner *et. al.*,[144] as shown in Scheme 2.25.

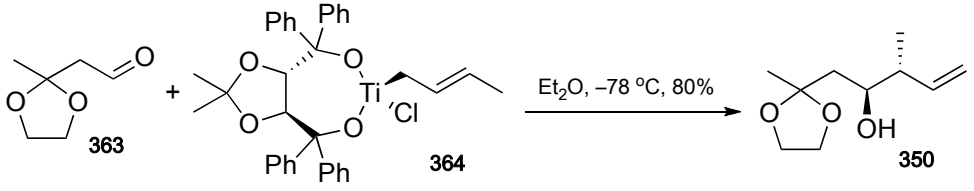

Scheme 2.25: Vilarrasa's Synthesis of the Second Fragment

The final fragment of amphidinolide X (**351**) needed by Vilarrasa was procured as shown in Scheme 2.26. Alkylation of an *N*-propanoyl derivative of the Evans' D-phenylalanine chiral auxiliary **355** using *tert*-butyl bromoacetate (**354**) generated the requisite stereocenter at C(4). After removal of the chiral auxiliary, Swern oxidation followed by a Wittig olefination yielded **366**, which upon selective hydrolysis of the methyl ester gave the carboxylic acid **351** as the desired final fragment.

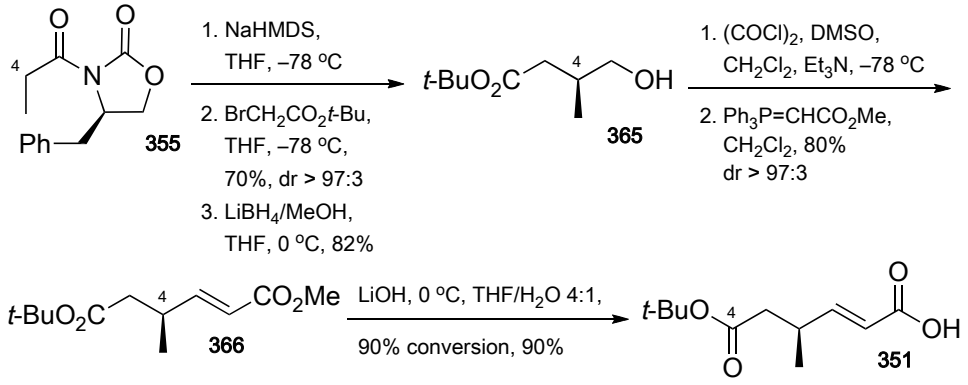

Scheme 2.26: Vilarrasa's Synthesis of the Third Fragment

With all the necessary fragments at hand, Vilarrasa *et. al.* eagerly started assembling them together to generate **368** in preparation for the final ring-closing metathesis.

However, they were disappointed by the failure of **368** or its keto-derivative (C(8)-deprotected **368**) to cyclize using varying amounts of the most promising Grubbs' second generation or Hoveyda-Grubbs' second generation catalysts. They only isolated a poor yield (30–40%) of the (12*Z*)-isomers when the RCM was performed on diastereomers of **368** with inverted configurations at C(10) and C(11).

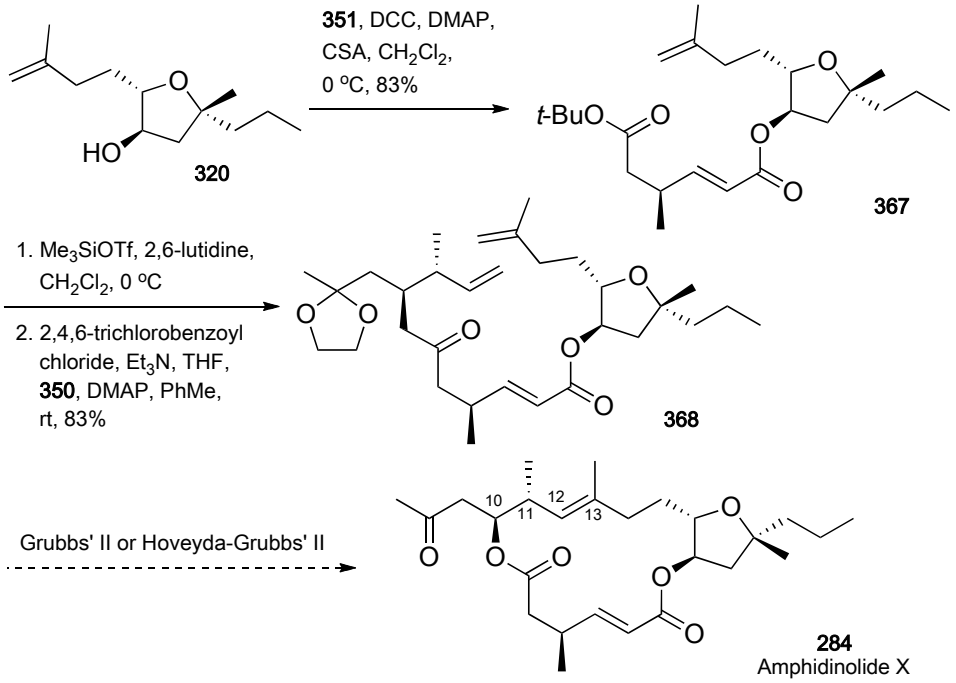

Scheme 2.27: Vilarrasa's Failed Synthesis of Amphidinolide X

Given this failure, they sought an alternative strategy to first form the challenging C(12)–C(13) double-bond by linking fragment **350** with a fragment derived from **362**. This alternative strategy is shown in Scheme 2.28.

Having protected the hydroxy moiety in **362** as the PMB ether, the nitrile functionality was transformed to the aldehyde in order to perform a Corey-Fuchs homologation to give **370**. Hydrosilylation of the terminal alkyne with Trost's catalyst gave a chlorosilane that was then coupled *in situ* to the second fragment **350** to form a silicon-tethered diene **371**. Schrock reagent catalyzed RCM gave the siloxane **372** that was converted to the hydroxyvinylsilane using MeLi, after which the hydroxy group is TBS-protected (**373**). Iododesilylation was then conducted in the fluorinated solvent $(CF3)_3CHOH$ to avoid double-bond isomerization. Subsequent to a Negishi coupling of the resultant iodoalkene with Me_2Zn, the PMB ether was removed with DDQ to provide the C(12)–C(13) double-bond

in (*E*)-conformation as **374**. A Yamaguchi esterification was then carried out on **374** and **351** to couple all three fragments together.

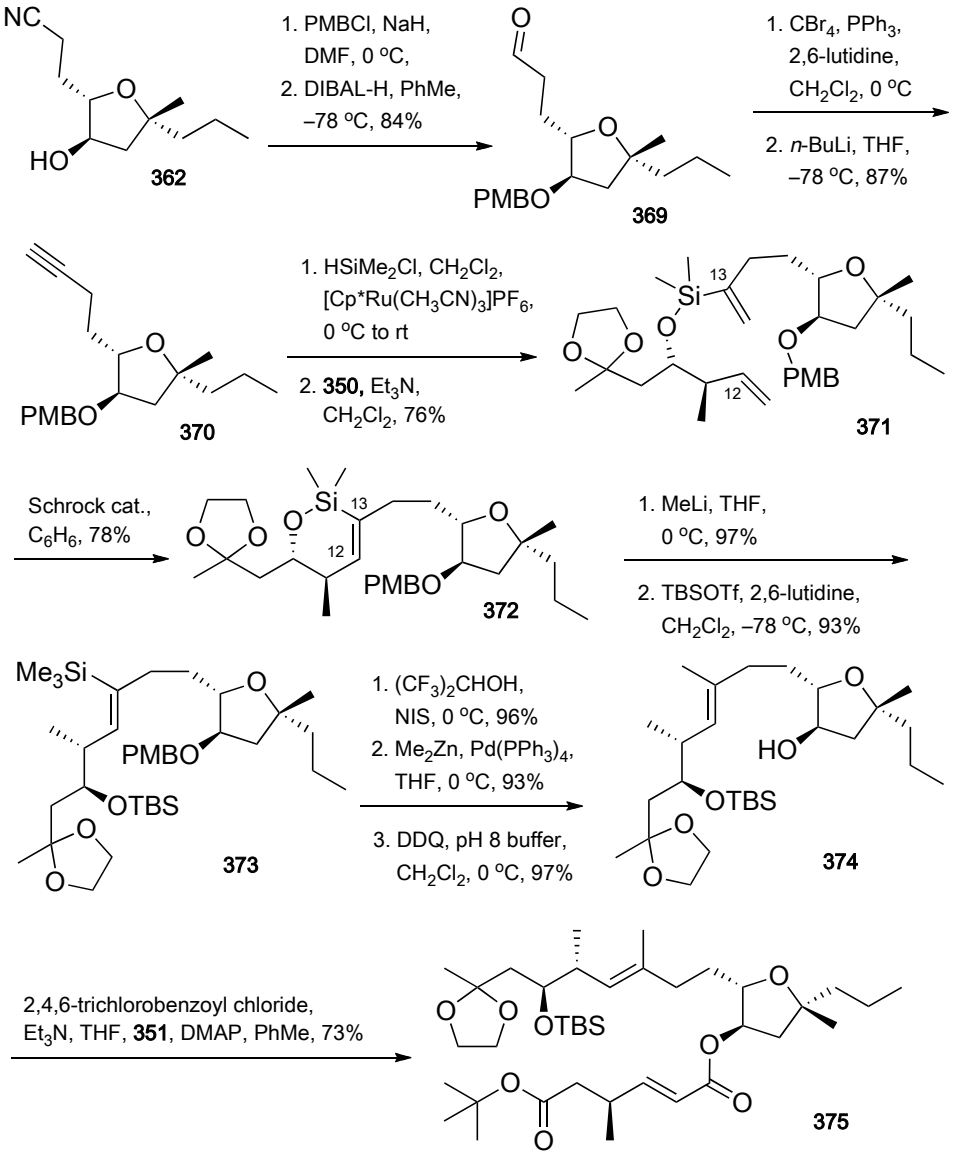

Scheme 2.28: Vilarrasa's Alternative Strategy

The *tert*-butyl ester **375** was deprotected to give the *seco*-acid **376**, in preparation for their final macrolactonization under high-dilution conditions. This was performed with the Shiina procedure as it offered a higher yield compared to that done under the Yamaguchi procedure.[145] Thus, Vilarrasa *et. al.* accomplished the

total synthesis of amphidinolide X with a new and efficient protocol, successfully overcoming a failed initial RCM.

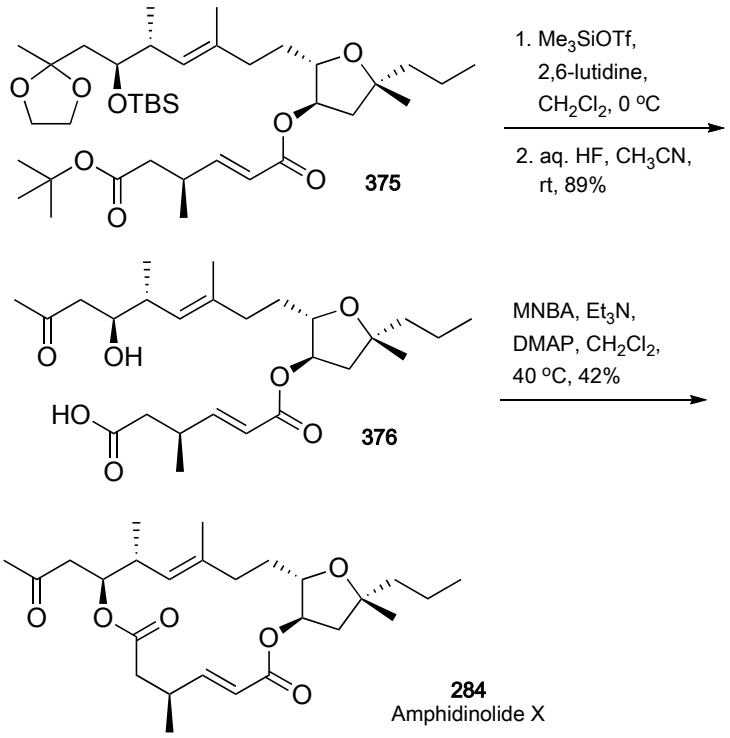

Scheme 2.29: Vilarrasa's Synthesis of Amphidinolide X via Macrolactonization

2.2.9 Retrosynthetic Analysis by Lee *et. al.*

The paper by Lee *et. al.* is an elegant total synthesis of amphidinolide X.[42] Even though the bulk of their paper is on the investigation of whether the SmI_2-mediated 5-*exo* cyclization of aldehydo β-alkoxyvinyl sulfoxides derived from tertiary alcohols proceed under sulfoxide or carbinol chirality control, their short section on its application to the total sythesis of amphidinolide X is astounding in its insightful strategy and efficiency.

What is even more surprising is their remarkable and bold synthetic plan, where not one, but two Grubbs' cross-metatheses are used, with the second metathesis being a ring-closing metathesis (RCM) to zip up the molecule. When this is put against the backdrop of multiple failures illustrated in the previous sections where RCM was used as the last key step of the total synthesis of amphidinolide X,[39,41] their successful venture indeed draws applause.

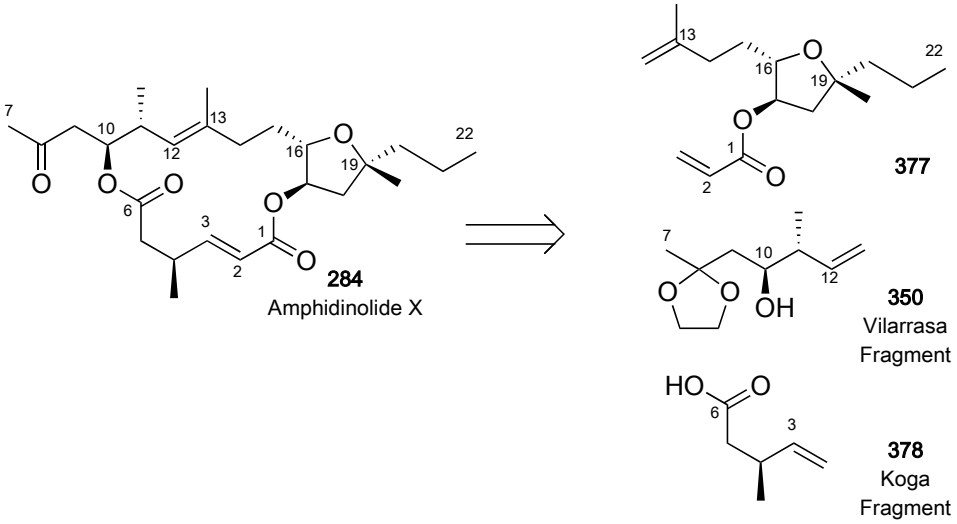

Scheme 2.30: Lee's Retrosynthetic Analysis for Amphidinolide X

Their retrosynthetic analysis for the THF fragment is shown in Scheme 2.30. Although the first obvious disconnections are at the two ester bonds, Lee *et. al.* first placed their focus on the implementation of two cross-metatheses at C(2)–C(3) and C(12)–C(13).

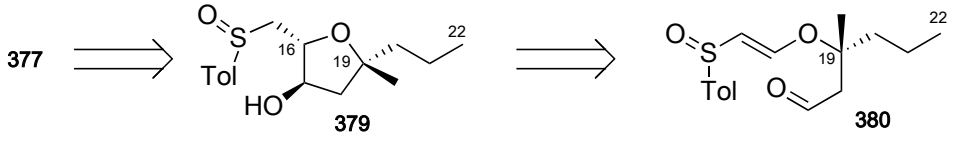

Scheme 2.31: Lee's Retrosynthetic Analysis for the THF Fragment of Amphidinolide X

Thereafter, the disconnections at the obvious ester bonds gave them two known fragments (**350**[39] and **378**[146]), and a large THF fragment that can be further broken down into the sulfoxide **380** as seen in Scheme 2.31. This sulfoxide is derived from one of the four isomers used in their methodology studies. Without further ado, we proceed to their forward synthesis proper.

2.2.10 Synthesis by Lee *et. al.*

The synthesis of the key THF fragment is depicted in Scheme 2.32. Starting from the known epoxide **381**,[147] Lee converted it to the (*E*)-β-alkoxyvinyl sulfoxide **384** by first ring-opening the epoxide with ethylmagnesium bromide in the presence of CuI to generate the tertiary alcohol **382**. This was then reacted with the chiral ethynyl *p*-tolyl sulfoxide to first generate the (*Z*)-isomer **383**, which was isomerized by I_2 to the (*E*)-isomer before PMP-deprotection using CAN.

With alcohol **384** in hand, the THF ring was formed by first oxidizing the alcohol to the aldehyde **380** using Dess-Martin periodinane, thereafter implementing their SmI_2-mediated 5-*exo* cyclization. The hydroxyoxolane **385** formed (67% yield, > 90:10 favoured product) was subsequently protected with *p*-nitrobenzoic acid, after which a Pummerer rearrangement using TFAA gave the aldehyde **386**. This was homologated to the methyl ketone **387** with an Horner-Emmons reaction and a H_2/Pd reduction.

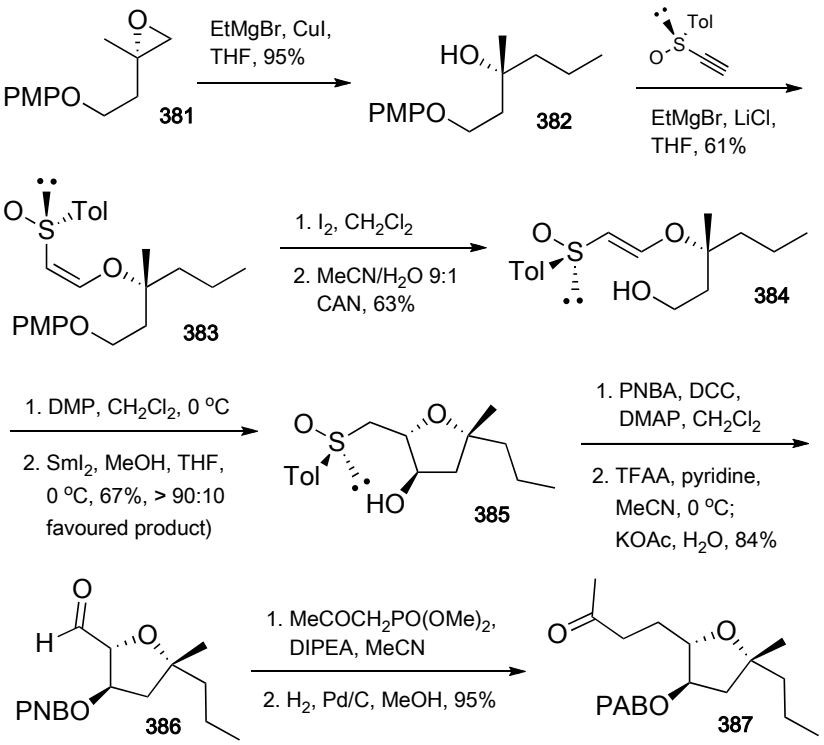

Scheme 2.32: Lee's Synthesis of the THF Fragment of Amphidinolide X

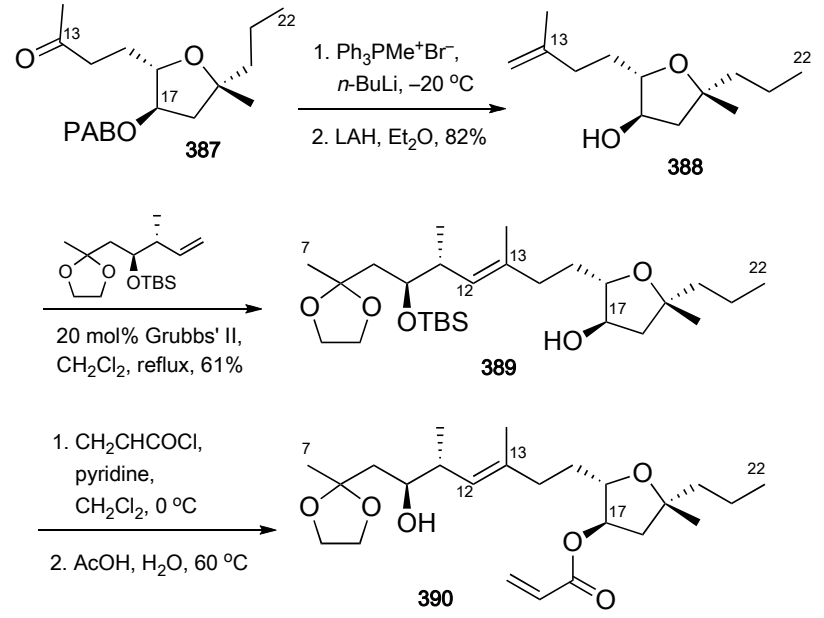

Scheme 2.33: Lee's First Cross-Metathesis

To begin their first Grubbs' cross-metathesis, the ketone group in **387** was converted to the alkene via a Wittig olefination, whilst reduction thereafter deprotected the *p*-aminobenzoyl group to reveal the hydroxy functionality on the THF ring. With the reaction sites in place, Grubbs' cross-metathesis using the second generation catalyst was performed to couple Lee's THF fragment **388** with Vilarrasa's fragment **350**. This cross-metathesis proceeded smoothly, without any (12*Z*)-isomer being detected. A reaction with acryloyl chloride at the C(17)-hydroxy to form the acrylate set in place the requisite double-bond needed for their eventual ring-closing metathesis. With that in place, the TBS-protected hydroxy group at C(10) was deprotected in preparation for the next step, yielding **390**.

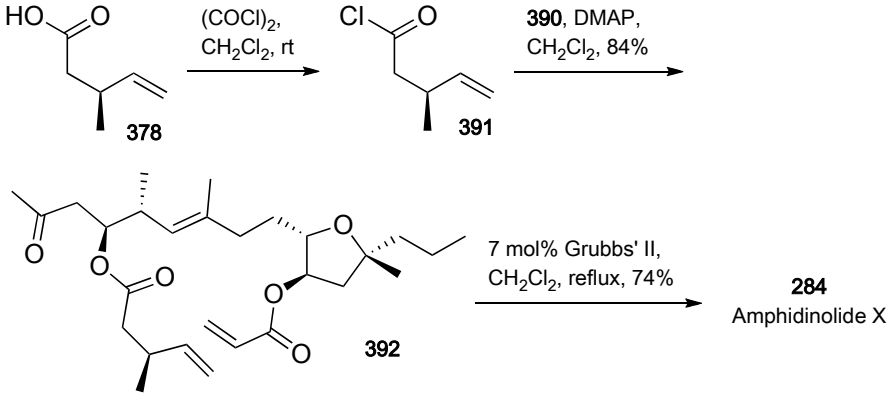

Scheme 2.34: Lee's Endgame with a Ring-Closing Metathesis

Having just a few steps to go towards the completion of the molecule, Lee converted Koga's fragment **378** into the acid chloride using oxalyl chloride, then carefully coupled this to the alcohol **390** to produce the triene **392** that is just short of the final touch — the last RCM using Grubbs' second generation catalyst. Perhaps as an anti-climax, this went on uneventfully for them to produce the desired

amphidinolide X in 74% yield. This was accompanied with just 11% of the (2*Z*)-isomer. And thus, Lee *et. al.* completed an elegant total synthesis of the molecule showcasing not only the practicality of the methodology they had developed, but also their ingenuity and excellent skills in retrosynthesis and total synthesis.

Chapter 3

Synthesis of Amphidinolide X

3.1 Introduction

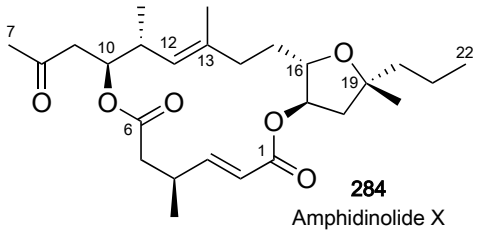

Figure 3.1: Amphidinolide X

With the review in the previous chapter of the reports covering the synthesis of amphidinolide X (**284**), we see that the primary concern for all groups engaged therein is the synthesis of the key oxolane ring with the substituents having the correct stereochemistry. Ancillary to that problem would be the final macrocyclization, which may be fraught with unanticipated complications, as encountered by the groups of Dai (pages 113 and 116) and Vilarrasa (page 124). Careful planning and trials by Fürstner's group helped them to avert two potentially catastrophic coupling strategies (page 109). Lee *et. al.* showed that RCM as the final key step is possible in excellent yield with the correct stereochemistry at the C(2)–C(3) double-bond — a report which offers insight when taken together with those from both Dai and Vilarrasa who had little or no success with the RCM at C(12)–C(13).

Having the benefit of hindsight from these excellent reports, we proceed next to our attempt at the total synthesis of amphidinolide X. In the ensuing sections, we will delve into our retrosynthetic analysis and synthesis of the molecule, implementing methodologies developed by our group.

3.2 Key Considerations on Our Retrosynthetic Strategy

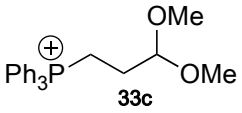

Figure 3.2: (3,3-dimethoxypropyl)triphenylphosphonium salt

In Chapters 2 and 4 of Part I (Table 2.2 and Scheme 4.8 respectively), using the homoenolate anion equivalent **33c**, we had successfully tested the practicality of the facile β,γ- to α,β-isomerization of the three-carbon homologated product after hydrolysis, both in a panel of simple substrates, and in the context of a synthesis of the acyl side chain of papulacandin D. Although we were successful in applying the methodology to that synthesis, we wanted to test the limits of the methodology with a more complex molecule such as amphidinolide X.

3.2.1 Macrolactonization Sequence

As depicted in Scheme 3.1, we took the conservative approach in our retrosynthesis, disconnecting the molecule into the three known fragments **320**, **393** and **394**. With the benefit of the reports by the groups discussed in Part II chapter 2, we wish to avoid doing a RCM as the last key step. Instead, as advised by Vilarrasa and demonstrated by Lee, we are cognizant of the importance that the coupling sequence of the fragments has in assembling the molecule.

Thus we intend to install the C(12)–C(13) double-bond early, by linking fragments **320** and **393** using Grubbs' olefin cross-metathesis. With that in place, we

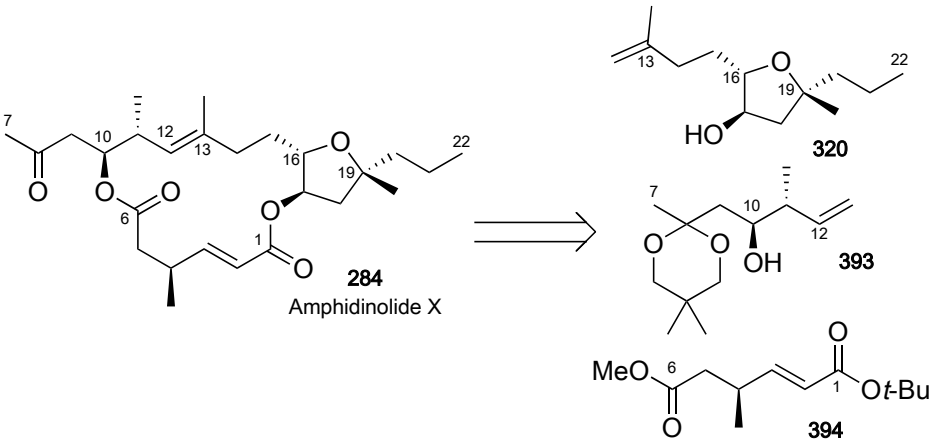

Scheme 3.1: Retrosynthetic Analysis of Amphidinolide X

will then have two available strategies for linking fragment **394** to complete the molecule: (i) coupling first at the hydroxy of C(10) followed by the hydroxy at C(17) with two Yamaguchi esterifications, reminiscent of Fürstner's strategy, or (ii) coupling first at the hydroxy of C(17) with a Yamaguchi esterification, before finishing up with a Shiina esterification on the *seco*-acid to complete the molecule, reminiscent of Vilarrasa's endgame.

3.2.2 Retrosynthesis of the Fragments of Amphidinolide X

The crux of our synthesis lies in our desire to apply three methodologies from our group to the synthesis of the fragments. As depicted in Scheme 3.2, these are: (i) the asymmetric conjugate addition using our Cu(I)/Tol-BINAP catalyst;[92,93] (ii) an asymmetric epoxidation using our azanorbornyl organocatalyst **400** (Figure 3.3) derived from (*S*)-1-phenylethylamine;[148] and (iii) the facile β,γ- to α,β-isomerization of the hydrolyzed three-carbon homologated Wittig product.

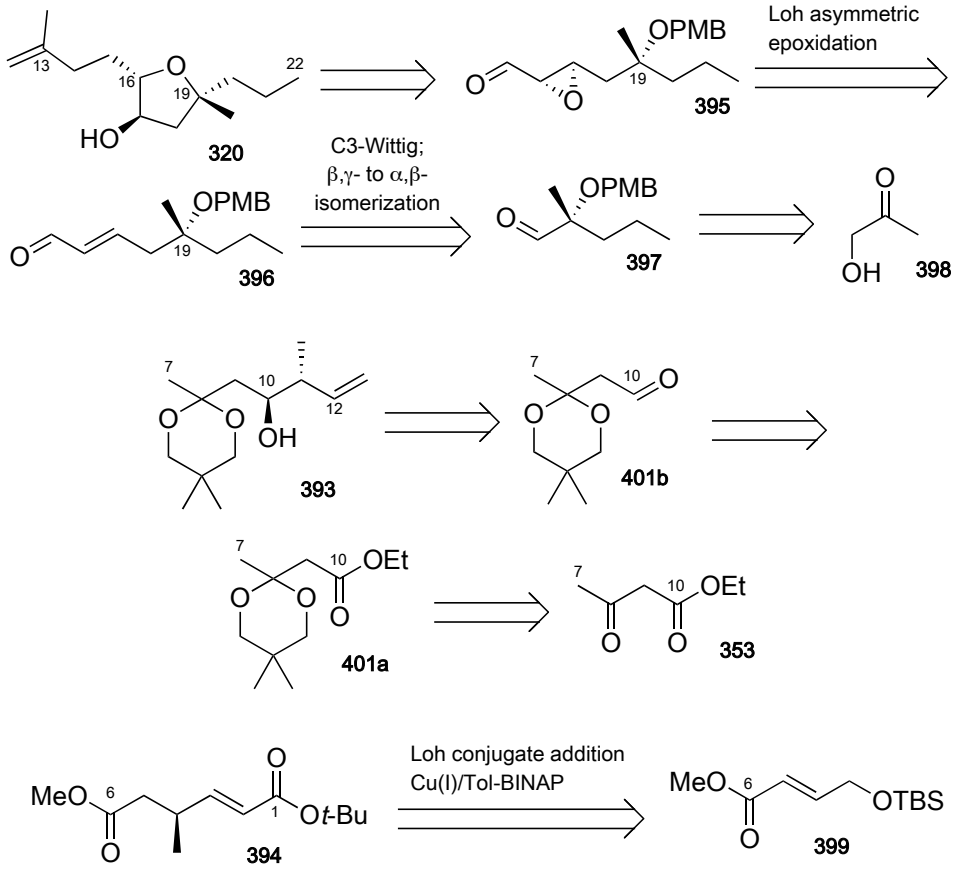

Scheme 3.2: Retrosynthetic Analysis for the Fragments of Amphidinolide X

For fragment **394**, we will be installing the chiral methyl group at C(4) using our asymmetric conjugate addition with Cu(I)/(*R*)-Tol-BINAP, by starting from **399**. This we expect to proceed without much complications as the procedure has been tried on a similar substrate by our group before.[94] Thereafter, we intend to procure the fragment **393** via an established procedure — the asymmetric Brown's crotylation on the aldehyde derived from the C(8) keto-protected ethyl acetoacetate. For this fragment, we too do not foresee any difficulties in securing it.

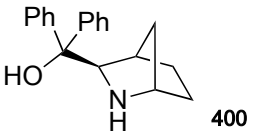

Loh's azanorbornyl organocatalyst

Figure 3.3: (1*S*,3*R*,4*R*)-2-azabicyclo[2.2.1]heptan-3-yldiphenylmethanol

3.2.3 THF Fragment of Amphidinolide X

In contrast to the previous two fragments, we expect most of our challenges in the total synthesis to arise from the generation of the THF fragment. The epoxide substrate **395** needed for conducting the 5-*endo*-*tet* cyclization to form the THF ring will be synthesized through an asymmetric epoxidation catalyzed by the azanorbornyl organocatalyst **400** developed by our group. This epoxidation in turn, is performed on the α,β-unsaturated aldehyde **396** that can be obtained by hydrolysis of a three-carbon homologated product with concomitant double-bond isomerization.

Several challenges exist in the use of these two methodologies. Firstly, the asymmetric epoxidation that we have developed had been tested only on the less reactive α,β-unsaturated ketones (Scheme 3.3) and not on the more reactive α,β-unsaturated aldehydes.[148] Also, this methodology has not been applied in the context of a natural product synthesis yet. As such, in the event that it fails, an alternative strategy would be to use similar asymmetric epoxidation catalysts developed by other groups as reviewed by Lattanzi.[149] As a last resort, we could reduce the α,β-unsaturated aldehyde into an allylic alcohol to converge with the strategies of Dai and Vatèle (Schemes 2.12 and 2.19 respectively).

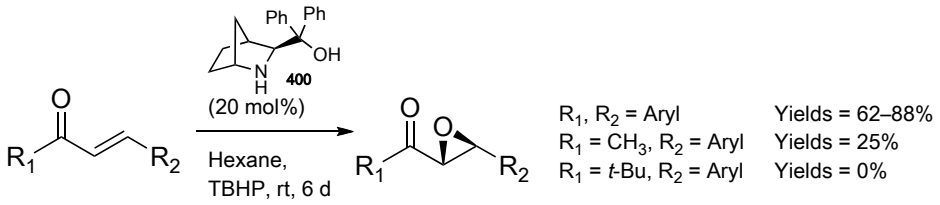

Scheme 3.3: Loh's Asymmetric Epoxidation

The second challenge we foresee is in the application of our three-carbon homologation/isomerization to form the α,β-unsaturated substrate **396** needed for epoxidation. The tertiary alcohol at C(19) has been known to eliminate readily, as the tertiary carbocation formed is relatively stable. Yet, we are willing to take this chance not only because it can help delineate the limits of our methodology, but especially because we believe that the litany of deprotection procedures for hydrolyzing dimethoxy acetals mildly without causing such eliminations would stand us in good stead.[150,151] However, in the dismal event that all these procedures fail, we can perform a C(1) + C(2) homologation instead of a direct C(3) homologation. With these considerations in mind, we proceed to our synthesis proper.

3.3 Approach Towards the Total Synthesis of Amphidinolide X

Since two of the fragments for the synthesis of amphidinolide X involve methodologies developed by our group, we started our synthesis on them first. For securing fragment three (**394**) of amphidinolide X as delineated in Scheme 3.4 with our asymmetric Cu(I)/(*R*)-Tol-BINAP catalyzed conjugate addition, the symmetrical

diol **402** was first TBS-protected as the ether **403**, after which it was cleaved via ozonolysis to form two equivalents of the aldehyde. A Wittig olefination was then executed to provide us with the methyl ester **399** that is our substrate for the asymmetric conjugate addition. This went on uneventfully to grant us the chiral methyl ester **404**.

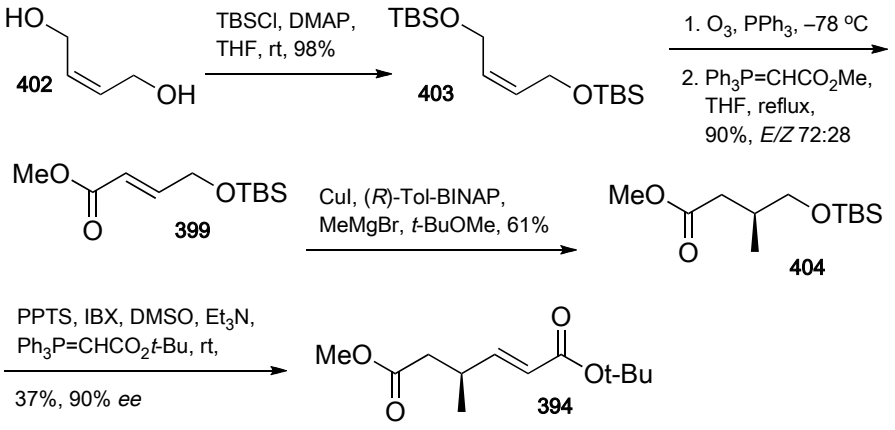

Scheme 3.4: Synthesis of the Third Fragment of Amphidinolide X

Although we tried to determine the enantiomeric excess of the product at this time, we were unable to resolve it sufficiently using the chiral HPLC columns we had at hand. The analysis was also complicated by the UV absorbance of the product being too near the UV cutoff for our solvent system. Hence, we decided to carry the synthesis forward before we determine the enantiomeric excess. A subsequent one-pot TBS-deprotection/IBX oxidation/Wittig olefination thence furnished us with the desired fragment three (**394**) of amphidinolide X we sought after. The enantiomeric excess of this product was successfully obtained as a respectable 90% *ee*. With this fragment in hand, we eagerly proceeded to the more challenging THF fragment.

Thus, as shown in Scheme 3.5 we started from the D-proline catalyzed asymmetric aldol reaction between hydroxyacetone (**398**) and cyclohexanecarboxaldehyde to obtain the *anti*-diol **405**. The diol was then protected to form the isopropylidene **406**, which is now ready for us to perform a Grignard reaction to set in place the tertiary alcohol at C(19). This went on uneventfully, giving us the requisite alcohol **407**.

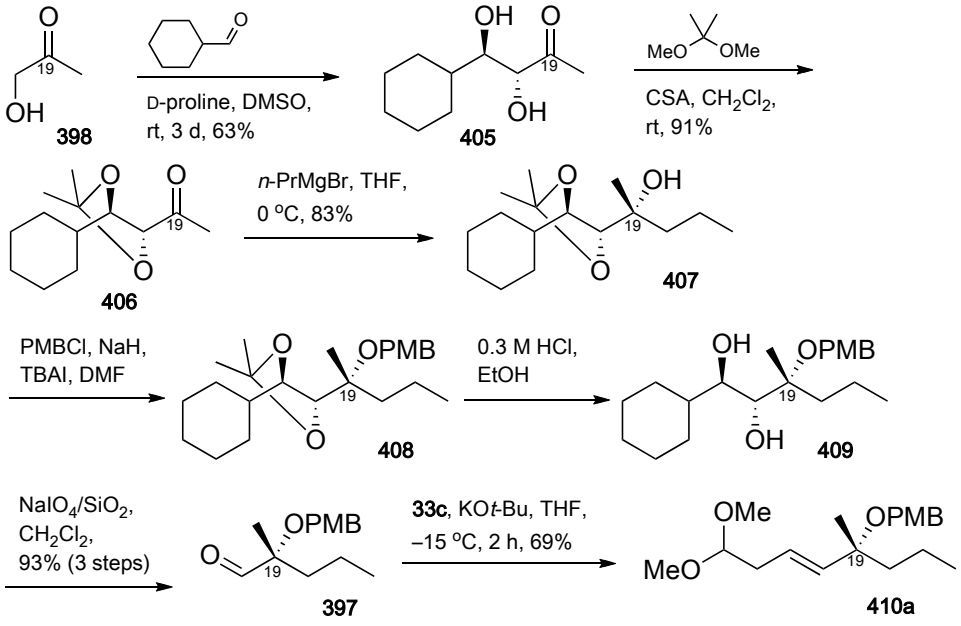

Scheme 3.5: Synthesis Towards the THF Fragment of Amphidinolide X

PMB-protection of this tertiary alcohol was done, following which the diol was deprotected. This then underwent an oxidative cleavage using sodium metaperiodate-impregnated silica gel, to generate the aldehyde **397**. The three-carbon Wittig homologation on this aldehyde with the homoenolate anion equivalent **33c** went on smoothly to grant us the dimethoxy acetal **410a** in good yield.

With the securing of this homologated acetal product **410a**, we were ready to implement the methodology developed in Part I Chapter 2. If things proceeded

well, we would be able to hydrolyze this product with concomitant isomerization to form the α,β-unsaturated aldehyde **411a**. This would then be put through our asymmetric epoxidation to supply the epoxide **395**, which can be subsequently manipulated to form the THF fragment **388** of amphidinolide X, a strategy that converges with those of Dai and Vatèle.

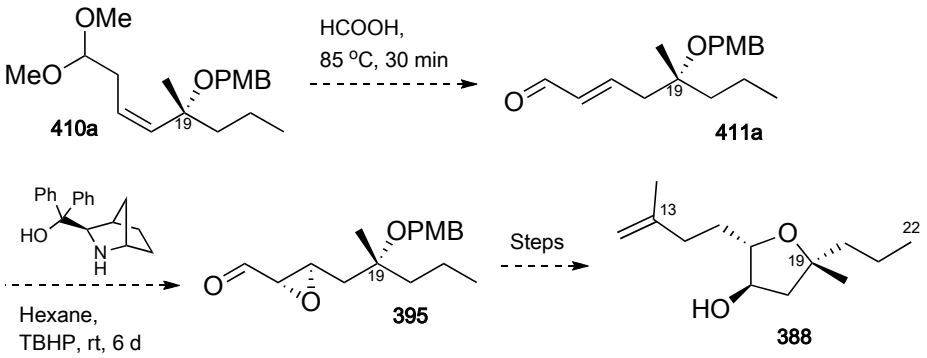

Scheme 3.6: Proposed Synthesis of the THF Fragment of Amphidinolide X

Unfortunately for us, our hydrolysis under the Barbot/Miginiac procedure[30] using hot formic acid caused decomposition of the product almost immediately. We then switched to their mild hydrolysis protocol, using the biphasic formic acid/hexane at 0 °C. This too only yielded decomposition products. As such, we tried to use other milder deprotection procedures to remove the dimethoxy acetal. We list in Table 3.1 the various conditions which we have tried.[150,151]

Regrettably, we either recovered back the starting material **410** when the conditions were too mild (Entries 3, 5, 8–10), or obtained a dehydration product (Entry 6) with loss of the protecting group. Most of the other conditions tested only caused decomposition of the starting material. A change of the protecting group from the PMB ether to a benzyl ether was to no avail, as the homologated acetal product suffered the same fate under different hydrolysis conditions.

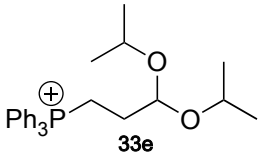

Figure 3.4: (3,3-diisopropoxypropyl)triphenylphosphonium salt

For us to apply the three-carbon homologation/hydrolysis-isomerization, probable recourse could be had from (i) the use of alternative protecting groups for the tertiary alcohol at C(19) that will enable us to deprotect the dimethoxy acetal to procure the α,β-unsaturated aldehyde **411a**; or (ii) use of the alternative homoenolate anion equivalent **33e** which can be deprotected under even milder conditions as testified to by Battersby *et. al.*[5] It was thus with much disappointment that we had to leave the synthesis at this stage.

3.4 Conclusion

Although the application of our method had ended in failure for synthesizing the THF fragment of amphidinolide X, the cause for it had been anticipated. As such, the practicality of using the facile β,γ- to α,β-isomerization from the hydrolysis of the three-carbon homologated Wittig product using homoenolate anion equivalents such as **33c** should not be written off so quickly as this synthesis has merely served to establish its scope through showing its inapplicability for substrates having a tertiary hydroxy group, especially those that can eliminate to form a conjugated system with the isomerized hydrolysis product. Indeed we propose the testing of it in the further syntheses of other natural products so as to uncover more of its strengths and inaptness. As is often the case in the

total synthesis of natural products, it is through the failures of current synthetic methodologies that serve to motivate chemists to seek alternate routes, improvise or even develop new and better methods to overcome the problems, or expand the substrate scope. With that, we look forward to future work within and without our group that can come up with better solutions to these problems and continue pushing the limits of our synthetic knowledge.

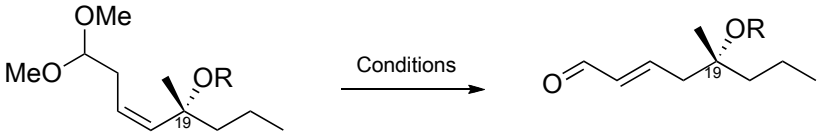

410a R = PMB
410b R = Bn

411a R = PMB
411b R = Bn

Entry	R	Hydrolysis Conditions	Results
1	PMB	HCOOH, 85 °C, <5 min	decomposition
2	PMB	HCOOH/hexane, 0 °C, 16 h	decomposition
3	PMB	AcOH, H_2O, THF, rt	SM recovered
4	PMB	AcOH, THF, 50 °C	decomposition
5	PMB	0.3 M HCl, Et_2O, rt	SM recovered
6	PMB	0.3 M HCl/THF, 50 °C	dehydration 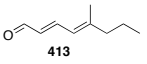 **413**
7	PMB	Amberlyst 15, acetone, H_2O, rt	decomposition
8	PMB	Amberlyst 15, THF, H_2O, rt, 4 h	SM recovered
9	PMB	SiO_2, 10% H_2O, rt	SM recovered
10	PMB	Oxalic acid, THF, H_2O, 16 h	SM recovered
11	Bn	PPTS, acetone, H_2O, rt	decomposition
12	Bn	TMSOTf, 2,6-lutidine, CH_2Cl_2, 0 °C	decomposition
13	Bn	CAN, MeCN, 60 °C, pH 8 buffer	decomposition
14	Bn	$FeCl_3/SiO_2$	decomposition
15	Bn	$FeCl_3/SiO_2$, H_2O	decomposition
16	Bn	$FeCl_3/SiO_2$, 35% acetone	decomposition
17	Bn	$LiBF_4$, MeCN, 2% H_2O, 0 °C to rt, 2 h	<10 % conversion[a]

[a] A mixture of β,γ- and α,β-unsaturated aldehydes were obtained.

Table 3.1: Alternative Procedures Tried

Chapter 4

Experimental Section

4.1 General Procedures

All experiments were conducted in oven-dried round-bottom flasks equipped with an elliptical Teflon coated magnetic stirrer bar and was stirred using a Heidolph MR3001K magnetic hotplate stirrer unless otherwise noted. Heating when required was via a water or silicone oil bath thermostated with the Heidolph EKT 3001 temperature controller.

Experiments involving air- and/or moisture-sensitive reagents were conducted in glassware dried for at least two hours in a 125 °C oven, and kept under a positive pressure with a nitrogen balloon via a rubber septum inlet. For reactions requiring more stringent conditions, a Schlenk-line was utilized under positive pressure of argon gas, together with flame-dried glassware.[108] Vacuum source was supplied using an Edwards RV3 oil pump equipped with a dry-ice/acetone cold trap.

4.2 Solvents and Reagents

All commercially available reagents and solvents were used as received without purification, unless otherwise stated. Technical grade hexane and ethyl acetate were distilled before use. Diethyl ether, dichloromethane and tetrahydrofuran were obtained from a PureSolv MD5 solvent purification system from Innovative Technologies. For more stringent requirements, tetrahydrofuran was freshly distilled over sodium sand with benzophenone as indicator to a purple colour, while

dichloromethane and *tert*-butyl methyl ether (TBME) were freshly distilled over CaH_2.[109]

Anhydrous solvents and liquid reagents were transferred using oven-dried needles and glass syringes which had been cooled to ambient temperature in a dessicator or via cannulation. Moisture from reagents were removed azeotropically with anhydrous THF prior to use where feasible.

4.3 Chromatography

Reaction progress was monitored using thin layer chromatography (TLC).

Analytical TLC was performed with Merck 60 F_{254} pre-coated silica gel plates (4 cm × 1 cm). After development, the plates were visualized with λ_{254} UV lamp and/or stained with 2,4-dinitrophenylhydrazine (2,4-DNP) or I_2. Staining with alkaline $KMnO_4$, ceric ammonium molybdate (CAM), vanillin or 50% H_2SO_4 was followed by heating using a Bosch GHG 500-2 heatgun or over a hotplate.

Preparative TLC was performed using Merck 60 F_{254} pre-coated silica gel plates (20 cm × 20 cm). The sample was applied as a narrow band (18 cm × 0.5 cm) after being dissolved in a minimal amount of solvent, 2 cm above the solvent level. After development, the plate was visualized under λ_{254} UV light, and isolated by scraping off the desired band. This was loaded into a pasteur pipette and eluted with chloroform and dried *in vacuo* to obtain the desired compound.

Flash column chromatography was carried out using SiliCycle SiliaFlash F60, 40–63 μm 60 Å silica gel powder, packed as a slurry and pre-equilibrated with the appropriate solvent system before use. Low boiling point solvents were removed *in vacuo* with a Heidolph Laborota 4000 Efficient rotary evaporator, equipped with an Eyela A-3S recirculating water aspirator and chilled with an Eyela CCA-1110. High boiling point solvents were removed with a similar setup using a Vacuubrand MZ2C or MD1C oil-free diaphram pump as vacuum source.

4.4 Physical Characterization

^{1}H NMR and ^{13}C NMR (400 MHz and 100 MHz respectively) were acquired using either JEOL ECA 400 or JEOL ECA 400SL. Unless otherwise stated, the samples were dissolved in $CDCl_3$ and chemical shifts are reported in δ units with reference to the residual proton peak from $CDCl_3$ as the internal standard (^{1}H: δ 7.26 ppm; ^{13}C: δ 77.00 ppm). Data acquisition and processing were done with the supplied JEOL Delta software. The coupling constants (J) were recorded in Hz. Abbreviations for the multiplicity of the peaks are: s (singlet), d (doublet), t (triplet), q (quartet), qn (quintet), dd(doublet of doublets), dt(doublet of triplets), br (broad), m (multiplet) and app (apparent).

FTIR spectra were acquired either neat, as Nujol mulls or KBr plates using the IRPrestige-21 spectrometer from Shimadzu, with data acquisition and processing using the supplied IRsolution software v1.21. Abbreviations for the peaks are: s

(strong), br (broad), m (medium) and w (weak) and are reported in wavenumbers (cm^{-1}).

Optical rotation data were acquired using the Jasco P-1030 polarimeter in a 1 cm × 1 cm cell with the sodium D-line at the stated ambient temperature using Spectra Manager v1.53.01 (Build 1).

Mass spectra were obtained on a Finnigan Surveyor LCQ DECA XP MAX in ESI mode with data processed using Xcalibur software v1.4SR1. High resolution mass spectra were obtained using a Waters Acquity UPLC Q-ToF Premier in ESI mode, with data processed using MassLynx v4.1 (SCN639).

GC-FID data were acquired with Agilent 6890N using helium as carrier gas, nitrogen as makeup gas and hydrogen generated from a Parker Balston H2PD-3000K hydrogen generator. HPLC data were acquired on an Agilent 1100 system equipped with a multiwavelength UV detector and fluorescence detector. Both GC and LC machines were running Chemstation software Rev.A.10.02 (1757).

Chiral GC separations were done using the Astec Chiraldex G-TA column. Chiral HPLC separations were done using Daicel OD-H, AS-H, AD-H, OJ-H or OB-H as stated. Separation parameters used were from the cited literature. For compounds where no prior literature on separation are available, method development was done in-house by the author.

4.5 Software

Chemical structures were drawn using the ChemBioOffice suite (v12.0) from CambridgeSoft. Nomenclature for compounds were obtained using MarvinSketch (Marvin v5.2.6) from ChemAxon.

Computational calculations and 3D molecular modelling were done on an 8-core Mac Pro (2 × 2.8 GHz Quad-Core Intel Xeon processors) equipped with 10 GB of 800 MHz DDR2 FB-DIMM memory. Computations were done using Gaussian for Windows (G03), with structure preparation/visualization using GaussView (GV03W). Both programs were run in Microsoft Windows XP under the virtualization software VMWare Fusion version 3.1.0 (261058) for Mac OSX (10.5.8). Computational calculations and 3D modelling were also done using Spartan '08 for Mac (v1.2.1) from Wavefunction Inc.

NMR, LC/GC/MS data were processed using the instrument specific software supplied by the vendor, or using the MNova suite v6.1.1-6384 with the NMR and MS plugins from Mestrelab Research S. L.

Document preparation was done using TeXShop v2.33 (2.33) for LaTeX from the MacTeX 2009 distribution with the *achemso* style package from the American Chemical Society. Reference management and citation were done using BibDesk v1.5.2 (1854).

4.6 Experimental Procedures

(6*Z*)-2,2,3,3,10,10,11,11-octamethyl-4,9-dioxa-3,10-disiladodec-6-ene (**403**)

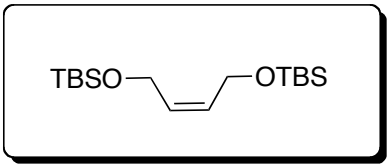

Figure 4.1: (6*Z*)-2,2,3,3,10,10,11,11-octamethyl-4,9-dioxa-3,10-disiladodec-6-ene

To a solution of commercially available *cis*-but-2-ene-1,4-diol (7.93 g, 90 mmol) in CH_2Cl_2 (150 mL) was added imidazole (20.22 g, 297 mmol) and *N,N*-dimethyl-4-aminopyridine (DMAP) (2.20 g, 18 mmol). The mixture was cooled to 0 °C with careful addition of *tert*-butyldimethylchlorosilane (33.12 g, 270 mmol). The reaction mixture was stirred at room temperature overnight and then quenched with saturated ammonium chloride solution (20 mL). Aqueous work-up was carried out and the aqueous phase was extracted thoroughly with ethyl acetate (2 × 80 mL). The combined organic layer was dried over $MgSO_4$, concentrated and purified by flash column chromatography (hexane/diethyl ether, 98:2).

Appearance: colourless oil.

Yield quantitative.

TLC: $R_f = 0.26$ (hexane/ diethyl ether, 98:2).

^{1}H NMR (400 MHz, $CDCl_3$):

δ 5.53 (t, 2H), 4.21 (d, $J = 4.1$ Hz, 4H), 0.88 (s, 18H), 0.05 (s, 12H).

^{13}C NMR (100 MHz, $CDCl_3$):

δ 130.2, 59.7, 26.0, 18.4, –5.1.

FTIR (neat): 1635, 1472, 1462, 1084.

HRMS (ESI): *m/z* $[C_{16}H_{37}O_2Si_2]^+$ 317.2332 (calculated), 317.2338 (found).

methyl (2*E*)-4-[(*tert*-butyldimethylsilyl)oxy]but-2-enoate (399)

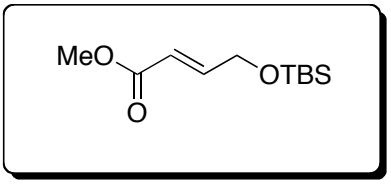

Figure 4.2: methyl (2*E*)-4-[(*tert*-butyldimethylsilyl)oxy]but-2-enoate

To a solution of TBS protected butenediol **399** (6.97 g, 30 mmol) in CH_2Cl_2 (60 mL) at –78 °C was bubbled ozone. Upon obtaining a blue solution, the reaction mixture was quenched with triphenylphosphine (7.87 g, 30 mmol), flushed with nitrogen and concentrated to obtain the crude aldehyde. A solution of the ylide, methyl (triphenylphosphoranylidene)acetate (22.67 g, 66 mmol) in THF (250 mL), was then added and the resulting mixture was allowed to reflux overnight. Aqueous workup was carried out and the aqueous layer was extracted with diethyl ether (3 × 50 mL). The combined organic extracts were dried over anhydrous Na_2SO_4 and concentrated. Purification was carried out using flash column chromatography (hexane/diethyl ether, 8:1).

Appearance: colourless oil.

Yield 6.22 g, 90% (*E/Z* 72:28).

TLC: R_f = 0.45 (*E*-isomer), 0.61 (*Z*-isomer) (hexane/ diethyl ether, 8:1).

^{1}H NMR (400 MHz, $CDCl_3$) (*E*-isomer): δ 7.00 (dt, J = 15.6, 3.6 Hz, 1H),

6.10 (dt, J = 13.7, 3.7 Hz, 1H), 4.33 (dd, J = 4.8, 1.4 Hz, 2H), 3.73 (s, 3H), 0.91 (s, 9H), 0.07 (s, 6H).

^{13}C NMR (100 MHz, $CDCl_3$) (*E*-isomer): δ 167.1, 147.7, 119.1, 62.1, 51.5, 25.8, 18.3, –5.5.

^{1}H NMR (400 MHz, $CDCl_3$) (*Z*-isomer): δ 6.37 (dt, J = 11.9, 4.6 Hz, 1H), 5.74 (dt, J = 11.0, 2.32 Hz, 1H), 4.74 (dd, J = 2.4, 2.3 Hz, 2H), 3.69 (s, 3H), 0.89 (s, 9H), 0.06 (s, 6H).

^{13}C NMR (100 MHz, $CDCl_3$) (*Z*-isomer): δ 166.5, 152.6, 117.5, 61.7, 51.2, 25.9, 18.2, –5.3.

FTIR (neat): 1724, 1647, 1471, 1437, 1402, 1098.

HRMS (ESI): *m/z* $[C_{11}H_{23}O_3Si]^+$ 231.1416 (calculated), 231.1424 (found).

methyl (3*S*)-4-[(*tert*-butyldimethylsilyl)oxy]-3-methylbutanoate (**404**)

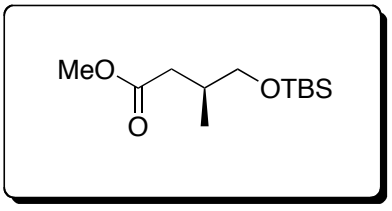

Figure 4.3: methyl (3*S*)-4-[(*tert*-butyldimethylsilyl)oxy]-3-methylbutanoate

To an oven dried 250 mL two-necked round-bottom flask was added copper (I) iodide (76.2 mg, 0.4 mmol) and (*R*)-(+)-2,2'-Bis(di-*p*-tolyl-phosphino)-1,1'-binaphthyl ((*R*)-Tol-BINAP) (0.41 g, 0.6 mmol). To these was added anhydrous CH_2Cl_2 (40 mL) and the resulting solution stirred for 15 min, after which the CH_2Cl_2 was removed under vacuum and anhydrous *tert*-butyldimethyl ether (80 mL) was introduced. The mixture was stirred for an additional 30 min until the formation of

white precipitates were observed and then cooled to –20 °C and MeMgBr (3.4 mL, 10 mmol, 3.0 M solution in Et_2O) was carefully added. Finally, a pre-cooled solution of ester **399** (4.47 g, 19.4 mmol) in anyhydrous *tert*-butyldimethyl ether (24 mL) was added via a syringe pump over 16 h. The reaction was quenched with methanol (20 mL) and saturated ammonium chloride solution at –20 °C, extracted with diethyl ether (2 × 50 mL), the combined organic extracts were concentrated and subsequently purified by flash column chromatography (hexane/diethyl ether, 8:1).

Appearance: colourless oil.

Yield 2.69 g, 61%.

TLC: R_f = 0.42 (hexane/ diethyl ether, 8:1).

^{1}H NMR (400 MHz, $CDCl_3$):

δ 3.49 (dd, J = 10.1, 5.0 Hz, 1H), 3.39 (dd, J = 10.1, 6.4 Hz, 1H), 2.48 (dd, J = 9.2, 4.6, 1H), 2,13–2.05 (m, 2H), 0.91 (d, J = 6.8 Hz, 3H), 0.88 (s, 9H), 0.02 (s, 6H).

^{13}C NMR (100 MHz, $CDCl_3$):

δ 173.7, 67.4, 51.4, 38.0, 33.0, 25.9, 18.3, 16.5, –5.5.

FTIR (neat): 1741, 1462, 1435, 1361, 1096.

HRMS (ESI): *m/z* $[C_{12}H_{25}O_3Si]^+$ 245.1573 (calculated), 245.1574 (found).

$[\alpha]_D^{21}$ = –8.9 (c = 0.468, $CHCl_3$).

1-*tert*-butyl 6-methyl (2*E*,4*S*)-4-methylhex-2-enedioate (394)

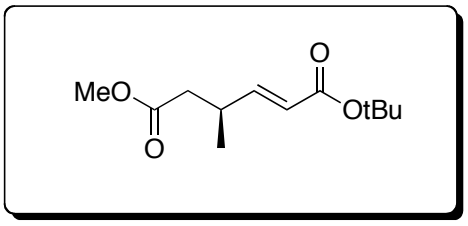

Figure 4.4: 1-*tert*-butyl 6-methyl (2*E*,4*S*)-4-methylhex-2-enedioate

To a solution of ester **404** (0.534 g, 2.16 mmol) in DMSO (5.4 mL) and water (0.2 mL) was added 2-iodoxybenzoic acid (IBX) (1.52 g, 5.41 mmol) and pyridinium *p*-toluenesulphonate (g, 0.1 mmol). The resulting mixture was stirred at room temperature for three hours, after which triethylamine (0.2 mL) was added. The ylide, *tert*-butyl (triphenylphosphoranylidene)acetate (2.45 g, 6.5 mmol), was dissolved in anhydrous THF (5.4 mL) and added to the reaction mixture and allowed to stir for 16 h.

Appearance: colourless oil.

Yield 0.18 g, 37% (purely *E*-isomer obtained).

TLC: $R_f = 0.21$ (hexane/ethyl acetate 90:10).

^{1}H NMR (400 MHz, $CDCl_3$):

δ 6.78 (dd, $J = 8.8, 6.9$ Hz, 1H), 5.74 (d, $J = 15.6$ Hz, 1H), 3.67 (s, 3H), 2.83 (m, 1H), 2.43 (dd, $J = 6.8, 15.6$ Hz, 1H), 2.30 (dd, $J = 15.1, 7.3$ Hz, 1H), 1.49 (s, 9 H), 1.10 (d, $J = 6.4$ Hz, 3H).

^{13}C NMR (100 MHz, $CDCl_3$):

δ 172.3078, 166.0110, 150.5744, 122.0673, 80.3274, 51.6771, 40.1903, 32.8250, 28.1597, 19.1152.

FTIR (neat): 2976, 1740, 1713, 1653, 1437, 1368, 1256, 1155, 976.

HRMS (ESI): m/z $[C_{12}H_{21}O_4]^+$ 229.1440 (calculated), 229.1451 (found).

cHPLC: 90% ee (Daicel Chiralpak AD-H; 0.2% *i*-PrOH/hexane; 0.5 mL/min; λ = 211, 230 nm; τ_{maj} = 15.7 min, τ_{min} = 12.8 min).

$[\alpha]_D^{21}$ = +17.0 (c = 0.294, $CHCl_3$).

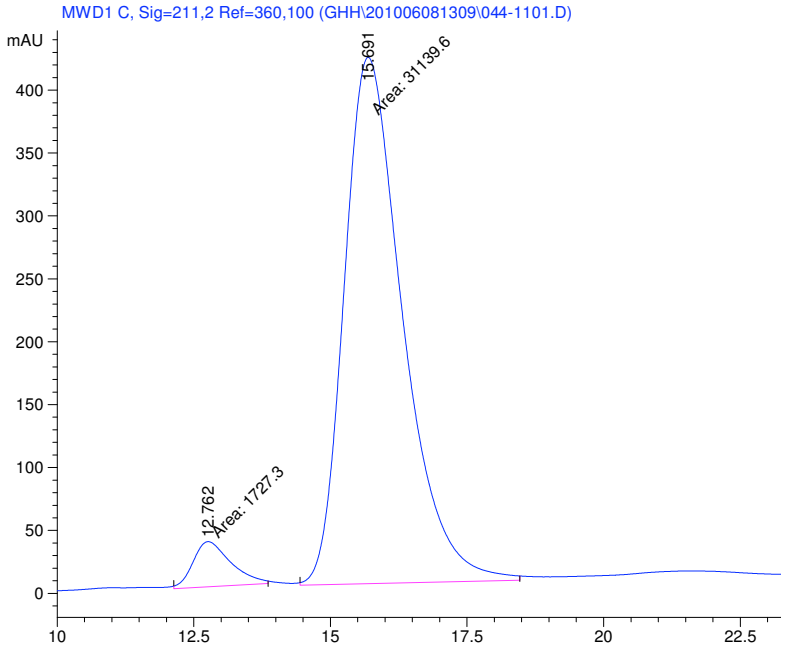

Figure 4.5: cHPLC of **394**

(3*R*,4*R*)-4-cyclohexyl-3,4-dihydroxybutan-2-one (405)

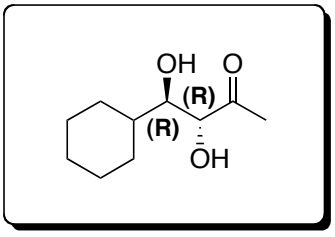

Figure 4.6: (3*R*,4*R*)-4-cyclohexyl-3,4-dihydroxybutan-2-one

To a mixture of DMSO (240 mL) and hydroxyacetone (55.5 g, 74 mmol) was added cyclohexanecarboxaldehyde (3.61g, 30 mmol), followed by D-proline (1.04 g,

9 mmol). The resulting reaction mixture was allowed to stir at room temperature for 60 h. Upon completion of reaction, half-saturated ammonium chloride solution and ethyl acetate were added with vigorous stirring. The layers were separated and the aqueous phase was extracted with ethyl acetate. The combined organic phase was then washed with water, brine, dried over anhydrous $MgSO_4$ and concentrated *in vacuo*. Purification was carried out by flash column chromatography (hexane/ethyl acetate 1:1).

Appearance: white powder.

Yield 3.5 g, 63%.

TLC: R_f = 0.50 (hexane/ethyl acetate 1:1).

^{1}H NMR (400 MHz, $CDCl_3$):

δ 4.22 (t, J = 5.5 Hz, 1H), 3.50 (d, J = 5.5 Hz, 1H), 2.30 (s, 3H), 1.75–1.59 (m, 6H), 1.24–1.11 (m, 5H).

^{13}C NMR (100 MHz, $CDCl_3$):

δ 209.8, 78.4, 39.9, 29.9, 27.8, 27.5, 26.3, 26.2, 25.9.

FTIR (Nujol mull): 3338, 2849, 1697, 1417, 1039, 874.

HRMS (ESI): m/z $[C_{10}H_{18}O_3Na]^+$ 209.1154 (calculated), 209.1160 (found).

cHPLC: 90% ee (Daicel Chiralpak AS-H, 15% *i*-PrOH/hexane, 1.0 mL/min, λ = 285 nm; t_R = 7.70 min).

$[\alpha]_D^{20}$ = –81.6 (c = 1.0, $CHCl_3$).

Lit. $[\alpha]_D$ = +83 (c = 1.0, $CHCl_3$) for (3*S*,4*S*)-4-cyclohexyl-3,4-dihydroxybutan-2-one.[152]

1-[(4*R*,5*R*)-5-cyclohexyl-2,2-dimethyl-1,3-dioxolan-4-yl]ethan-1-one (**406**)

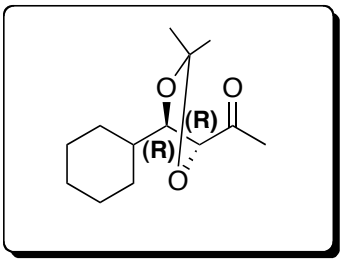

Figure 4.7: 1-[(4*R*,5*R*)-5-cyclohexyl-2,2-dimethyl-1,3-dioxolan-4-yl]ethan-1-one

To a mixture of **405** (1.86 g, 10 mmol) and 2,2-dimethoxypropane in CH_2Cl_2 (20 mL) was added camphorsulphonic acid (0.116 g, 0.5 mmol). The reaction mixture was left to stir at room temperature for 16 h, after which sodium bicarbonate solution was added to quench the reaction. The layers were separated and the aqueous phase was extracted with CH_2Cl_2 (20 mL × 2). The combined organic phase was washed with water, brine, dried over anhydrous $MgSO_4$ and concentrated *in vacuo*. Purification was carried out by flash column chromatography (hexane/ethyl acetate 90:10) to afford the desired product **406**.

Appearance: yellow oil.

Yield 2.06 g, 91%.

TLC: R_f = 0.54 (hexane/ethyl acetate 9:1).

^{1}H NMR (400 MHz, $CDCl_3$):

δ 4.26 (d, J = 7.6 Hz, 1H), 3.98 (t, J = 7.8 Hz, 1H), 2.18 (s, 3H), 1.82–1.60 (m, 5H), 1.55 (s, 3H), 1.31 (s, 3H), 1.11–0.87 (m, 6H).

^{13}C NMR (100 MHz, $CDCl_3$):

δ 209.6, 109.3, 82.7, 82.5, 37.6, 29.7, 29.2, 28.3, 26.5, 26.1, 25.3, 24.7.

FTIR (neat): 2987, 2926, 2855, 1713, 1452, 1354, 1060.

HRMS (ESI): *m/z* $[C_{13}H_{22}O_3Na]^+$ 249.1467 (calculated), 249.1470 (found).

$[\alpha]_D^{20} = +\ 0.87$ (c = 1.2, $CHCl_3$).

(2*R*)-2-[(4*R*,5*R*)-5-cyclohexyl-2,2-dimethyl-1,3-dioxolan-4-yl]pentan-2-ol (**407**)

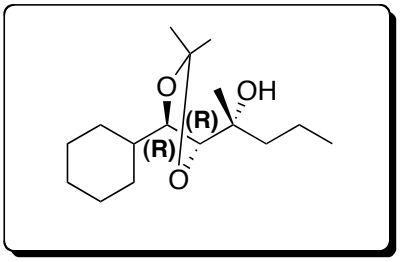

Figure 4.8: (2*R*)-2-[(4*R*,5*R*)-5-cyclohexyl-2,2-dimethyl-1,3-dioxolan-4-yl]pentan-2-ol

Preparation of *n*-propyl Magnesium Bromide: In an oven dried 2-necked round-bottomed flask was introduced magnesium turnings (0.73 g, 30 mmol), iodine (3 pearls) and anhydrous THF (30 mL). Bromopropane (3.69 g, 30.4 mmol) was added dropwise and allowed to stir at room temperature for 1 h. The resulting solution was used immediately.

Grignard Addition to Ketone 406: The freshly prepared *n*-propylmagnesium bromide solution was cooled to 0 °C. Ketone **406** (2.2 g, 10 mmol) was dissolved in anhydrous THF (50 mL) and carefully added over 17 h using a syringe pump. The reaction mixture was left to stir vigorously at 0 °C overnight. Upon completion, the reaction was quenched with ammonium chloride solution. The layers were separated and the aqueous phase was thoroughly extracted with diethyl ether. The combined organic phase was washed with brine, dried over anhydrous $MgSO_4$ and concentrated to give the desired alcohol **407** as a single isomer. The mixture was purified by flash column chromatography (hexane/ethyl acetate 9:1) and dried under vacuum to afford (*R*,*R*)-**407**.

Appearance: white solid.

Yield 2.2 g, 83%.

TLC: R_f = 0.28 (hexane/ethyl acetate 9:1).

^{1}H NMR (400 MHz, $CDCl_3$):

δ 3.84–3.81 (m, 2H), 1.90–1.87 (m, 2H), 1.68–1.45 (m, 5H), 1.44 (s, 3H), 1.35–1.15 (m, 6H), 1.28 (s, 3H), 1.15 (s, 3H), 1.1–0.89 (m, 2H), 0.88–0.84 (m, 3H).

^{13}C NMR (100 MHz, $CDCl_3$):

δ 106.3, 82.4, 81.9, 73.7, 43.0, 37.1, 32.1, 30.1, 26.6, 26.3, 25.7, 25.1, 23.3, 16.8, 14.6.

FTIR (Nujol mull): 3450, 1402, 1369, 1242, 1211, 1159, 1130, 841.

$[\alpha]_D^{21}$ = –17.9 (c = 0.268, $CHCl_3$).

(4*R*,5*R*)-4-cyclohexyl-5-[(2*R*)-2-[(4-methoxyphenyl)methoxy]pentan-2-yl]-2,2-dimethyl-1,3-dioxolane (**408**)

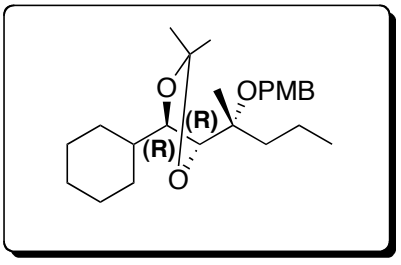

Figure 4.9: (4*R*,5*R*)-4-cyclohexyl-5-[(2*R*)-2-[(4-methoxyphenyl)methoxy]-pentan-2-yl]-2,2-dimethyl-1,3-dioxolane

Sodium hydride (2.4 g, 100 mmol, 60% dispersion in mineral oil) was weighed into an oven dried 250 mL round-bottomed flask, washed with dry hexane (20 mL × 2) and dried under vacuum. Anhydrous DMF (50 mL) was introduced and the reaction mixture was stirred at 0 °C. Alcohol **407** (2.70 g, 10 mmol) was dissolved in anhydrous DMF (50 mL) and carefully added to the reaction mixture, which was allowed to stir at 0 °C for 1 h.

Subsequently, tetrabutyl ammonium iodide (0.37 g, 1 mmol) and *p*-methoxybenzyl chloride (4.7 g, 30 mmol) were sequentially added to the reaction mixture and left to stir at room temperature for 16 h. The reaction was carefully quenched with water and extracted with ethyl acetate (2 × 80 mL). The combined organic extracts were thoroughly washed with water to remove DMF and concentrated *in vacuo* to afford a colourless oil. PMB-protected alcohol **408** was found to be acid sensitive and decomposes on purification by flash column chromatography, thus the crude product obtained was used immediately without further purification.

(1*R*,2*R*,3*R*)-1-cyclohexyl-3-[(4-methoxyphenyl)methoxy]-3-methylhexane-1,2-diol (**409**)

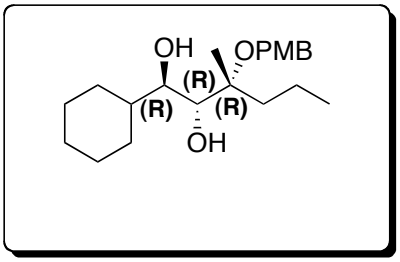

Figure 4.10: (1*R*,2*R*,3*R*)-1-cyclohexyl-3-[(4-methoxyphenyl)methoxy]-3-methylhexane-1,2-diol

To the crude product **408** was added ethanol (50 mL). Thereafter, 0.3 M HCl (50 mL) was then added to the resulting solution and the reaction mixture was allowed to stir for 1 h at 50 °C. The reaction mixture was concentrated *in vacuo*, partitioned between water (50 mL) and ethyl acetate (3 × 100 mL), dried over $MgSO_4$ and concentrated to afford crude diol **409** as an off-white solid.

The crude product, diol **409**, was employed in the subsequent oxidative cleavage reaction without further purification.

(2*R*)-2-[(4-methoxyphenyl)methoxy]-2-methylpentanal (**397**)

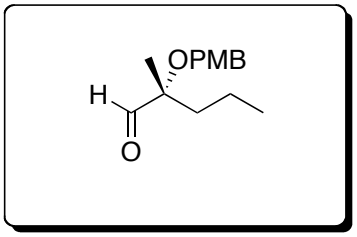

Figure 4.11: (2*R*)-2-[(4-methoxyphenyl)methoxy]-2-methylpentanal

Following reported procedures,[153] $NaIO_4$-impregnated silica gel was prepared by adding silica gel (50 g) to a vigorously stirred solution of $NaIO_4$ (12.85 g) in 25 mL water. To a solution of crude diol **409** (3.50 g,10 mmol) in CH_2Cl_2 (200 mL) was added the $NaIO_4$-impregnated silica gel (19.7 g). The resulting slurry was stirred at room temperature for 6 h, after which the solution was filtered and the solvent removed *in vacuo* to give the crude aldehyde **397**. Purification was carried out by flash column chromatography (hexane/ethyl acetate 95:5) and subsequent drying under vacuum afforded the desired aldehyde.

Appearance: colourless oil.

Yield 2.21 g, 93%.

TLC: R_f = 0.41 (hexane/ethyl acetate 9:1).

^{1}H NMR (400 MHz, $CDCl_3$):

δ 9.69 (s, 1H), 7.28 (d, J = 8.7 Hz, 2H), 6.88 (d, J = 8.7 Hz, 2H), 4.39 (q, J = 11 Hz, 2H), 3.80 (s, 3H), 1.69–1.59 (m, 2H), 1.48–1.34 (m, 2H), 1.32 (s, 3H), 0.93 (t, J = 6.9 Hz, 3H).

^{13}C NMR (100 MHz, $CDCl_3$):

δ 205.3, 159.2, 130.4, 129.1, 113.8, 82.6, 65.8, 55.3, 37.3, 18.2, 16.3, 14.5.

FTIR (neat): 1734, 1612, 1514, 1465, 1250, 1172.

HRMS (ESI): *m/z* $[C_{14}H_{20}O_3Na]^+$ 259.1310 (calculated), 259.1317 (found).

1-([(4*R*,5*E*)-8,8-dimethoxy-4-methyloct-5-en-4-yl]oxymethyl)-4-methoxybenzene (**410a**)

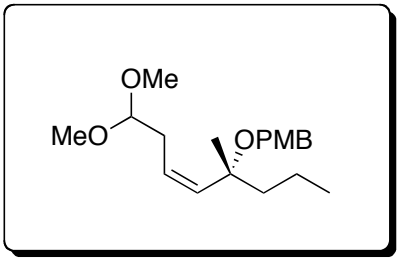

Figure 4.12: 1-([(4*R*,5*E*)-8,8-dimethoxy-4-methyloct-5-en-4-yl]oxymethyl)-4-methoxybenzene

Wittig reaction with aldehyde **410a**: The ylide from the homoenolate anion equivalent **33c** (30 mmol) was formed by adding potassium *tert*-butoxide solution (60 mL, 1.0 M in THF) to a solution of the crude phosphonium salt in anhydrous THF (25 mL). The resulting bright orange solution was allowed to stir at rt for 20 min before cooling down to –15 °C. A solution of aldehyde **397** (2.36 g,10 mmol) in anhydrous THF (10 mL) was then carefully added to the reaction mixture and stirred for 2 h at –15 °C. Upon completion of the reaction, the mixture was passed through a short plug of SiO_2 followed by purification via flash column chromatography (hexane/ethyl acetate 9:1).

Appearance: colourless oil.

Yield: 69% (purely *Z*).

TLC: R_f = 0.27 (hexane/ethyl acetate 9:1).

^{1}H NMR (400 MHz, $CDCl_3$):

δ 7.26 (d, J = 9.1 Hz, 2H), 6.85 (d, J = 9.2 Hz, 2H), 5.53–5.40 (m, 2H), 4.35–4.33 (m, 3H), 3.79 (s, 3H), 3.28 (s, 6H), 2.66–2.62 (m, 2H), 1.68–1.60 (m, 2H), 1.43–1.39 (m, 2H),

1.36 (s, 3H), 0.92 (t, J = 7.3 Hz, 3H).

^{13}C NMR (100 MHz, $CDCl_3$):

δ 135.9, 133.1, 128.8, 126.3, 113.7, 104.4, 63.8, 55.4, 53.0, 43.3, 31.8, 25.1, 17.1, 14.7.

FTIR (neat): 1614, 1514, 1465, 1247.

HRMS (ESI): m/z $[C_{18}H_{28}O_4Na]^+$ 331.1885 (calculated), 331.1889 (found).

(2*E*,4*E*)-5-methylocta-2,4-dienal (**413**)

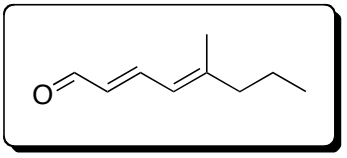

Figure 4.13: (2*E*,4*E*)-5-methylocta-2,4-dienal

Appearance: pale yellow oil.

^{1}H NMR (400 MHz, $CDCl_3$):

δ 9.57 (d, J = 8.2 Hz, 1H), 7.39 (dd, J = 15.1, 11.9 Hz, 1H), 6.16 (d, J = 11.9 Hz, 1H), 6.07 (dd, J = 15.1, 8.2 Hz, 1H), 2.31 (t, J = 7.3 Hz, 2H), 1.92 (s, 3H), 1.55–1.48 (m, 2H), 0.95 (t, J = 7.8 Hz, 3H).

ethyl 2-(2,5,5-trimethyl-1,3-dioxan-2-yl)acetate (**401a**)

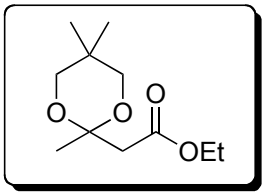

Figure 4.14: ethyl 2-(2,5,5-trimethyl-1,3-dioxan-2-yl)acetate

To a 250 mL round-bottom flask equipped with a magnetic stirrer bar was added neopentyl glycol (2.99g, 29 mmol), PTSA (0.2 g, 1 mmol), cyclohexane (40 mL) and

ethyl acetoacetate (1.2 mL 10 mmol). This was heated using a heating mantle with a Dean-Stark setup for 16 h. The reaction was cooled to rt, washed with a saturated solution of $NaHCO_3$ and water twice, before being dried over anhydrous $MgSO_4$. Solvent was removed *in vacuo* and the product was purified using flash column chromatography.

Appearance: colourless oil.

Yield: 73%.

TLC: $R_f = 0.39$ (hexane/ethyl acetate 80:20).

^{1}H NMR (400 MHz, $CDCl_3$):

δ 4.13 (q, $J = 7.3$ Hz, 2H), 3.51 (dd, $J = 14.2$, 11.4 Hz, 4H), 2.76 (s, 2H), 1.52 (s, 3H), 1.24 (t, $J = 7.3$ Hz, 3H), 0.94 (d, $J = 14.7$ Hz, 6H).

^{13}C NMR (100 MHz, $CDCl_3$):

δ 169.47, 97.27, 70.56, 60.46, 41.53, 29.82, 22.54, 22.43, 14.12.

FTIR (neat): 2980, 2957, 2870, 1736, 1242, 1098, 1080, 1040.

HRMS (ESI): *m/z* $[C_{11}H_{21}O_4]^+$ 217.1440 (calculated), 217.1437 (found).

2-(2,5,5-trimethyl-1,3-dioxan-2-yl)acetaldehyde (**401b**)

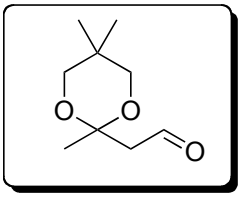

Figure 4.15: 2-(2,5,5-trimethyl-1,3-dioxan-2-yl)acetaldehyde

The protected ethyl acetoacetate **401a** (3.6883g, 17.1 mmol) was dissolved in CH_2Cl_2 (20 mL) in a 250 mL round-bottom flask. This was cooled to –78 °C and DIBAL-H (20 mL, 20 mmol, 1.2 equiv, 1.0 M solution in CH_2Cl_2) was slowly added via a syringe pump over 4 h. This was stirred for another 4 h before being quenched with

MeOH (0.5 mL). The reaction was brought to rt and stirred with saturated Rochelle salt solution (40 mL). The aqueous phase was extracted with CH_2Cl_2 (4 × 10 mL), the pooled organic phase washed with water, then brine, and dried over anhydrous $MgSO_4$. The solvent was removed *in vacuo* to yield the desired aldehyde.

Appearance: colourless oil.

Yield: 50%.

TLC: R_f = 0.53 (hexane/ethyl acetate 60:40).

^{1}H NMR (400 MHz, $CDCl_3$):

δ 9.84 (t, J = 2.8 Hz, 1H), 3.61 (d, J = 11.4 Hz, 2H), 3.43 (d, J = 11.9 Hz, 2H), 2.64 (d, J = 3.2 Hz, 2H), 1.46 (s, 3H), 1.04 (s, 3H), 0.85 (s, 3H).

^{13}C NMR (100 MHz, $CDCl_3$):

δ 200.97, 97.50, 70.49, 51.89, 29.83, 22.94, 22.34, 20.51.

FTIR (neat): 2957, 2870, 17224, 1246, 1082.

HRMS (ESI): m/z $[C_9H_{17}O_3]^+$ 173.1178 (calculated), 173.1176 (found).

APPENDIX

Appendix A

Survey of Acetal Phosphonium Salts Used in the Literature

Entry	Reactions	Ref
1	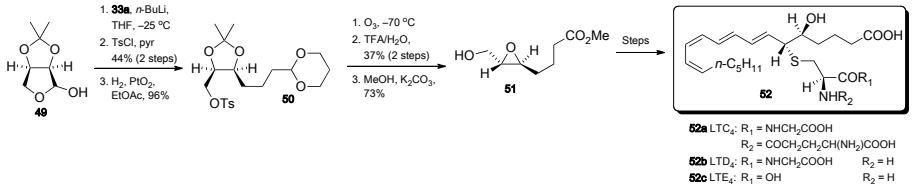	154,155
2	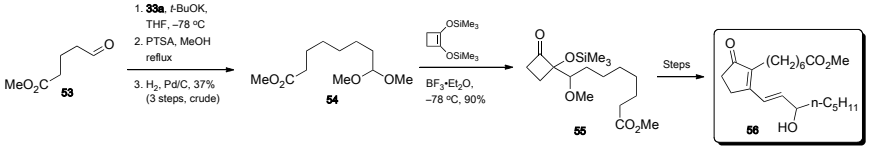	156
3	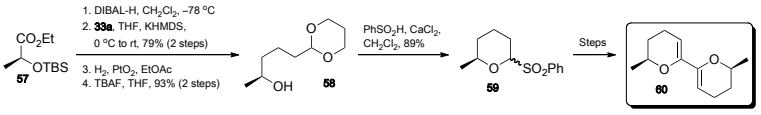	157
4	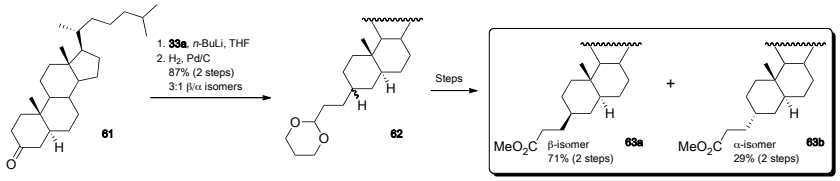	158
5	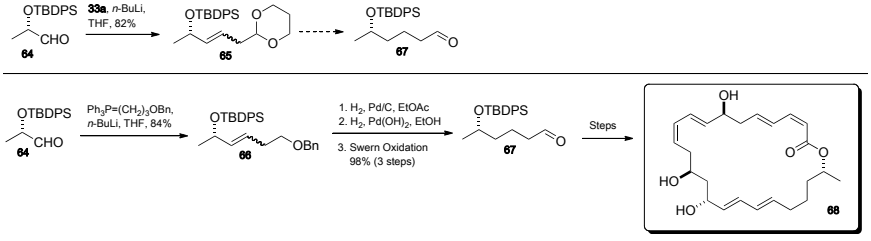	159
6	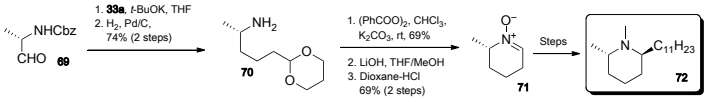	160
7	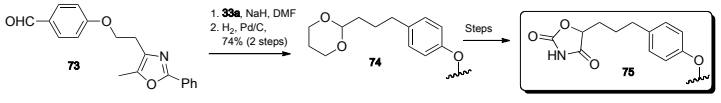	161

Table A.1: Use of Dioxanyl Phosphonium Salt **33a** in C3-Homologation

Entry	Reactions	Ref
1	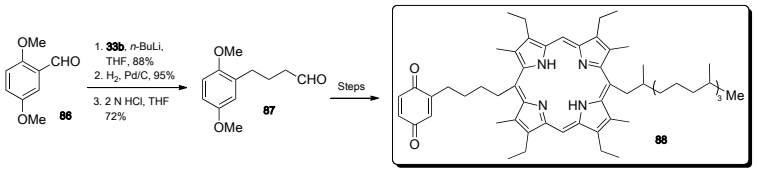	162
2	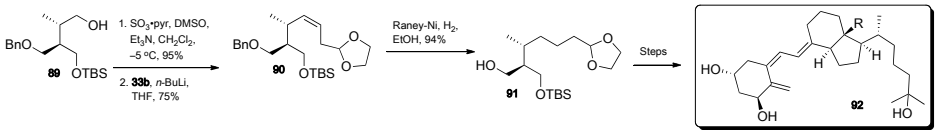	163
3	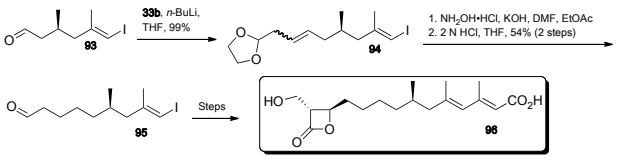	164
4	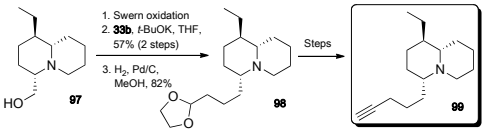	165
5	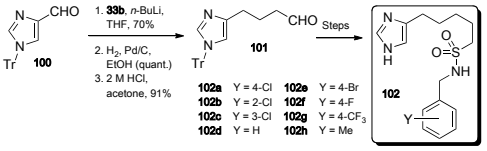	166
6	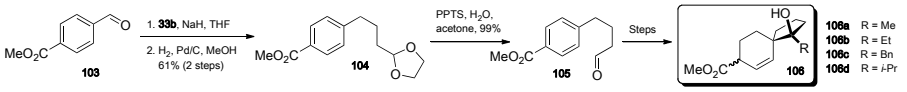	167
7	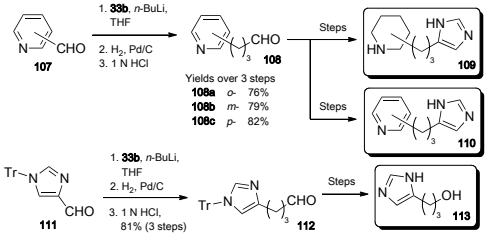	168–170
8	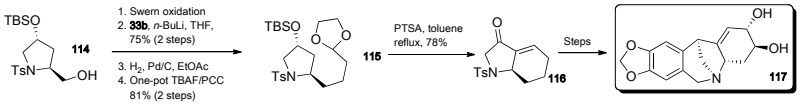	171
9	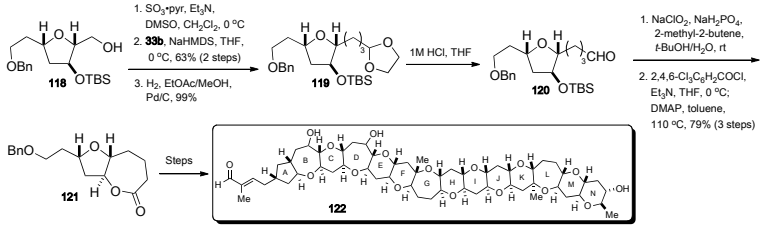	172

Table A.2: Use of Dioxolanyl Phosphonium Salt **33b** in C3-Homologation

Entry	Reactions	Ref
10	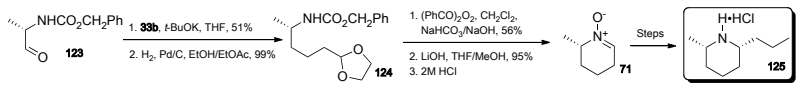	173
11	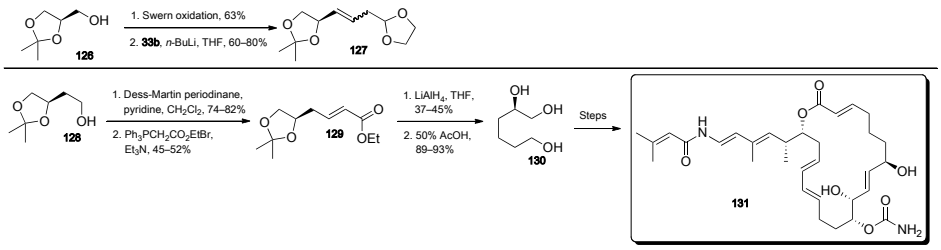	174
12	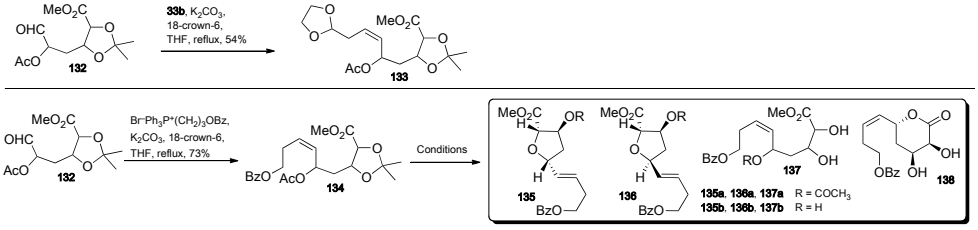	175
13	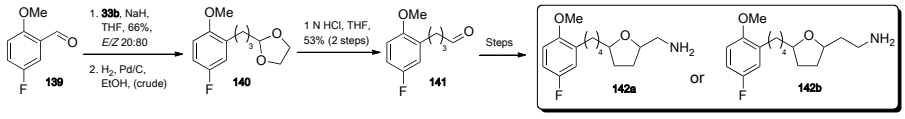	29
14	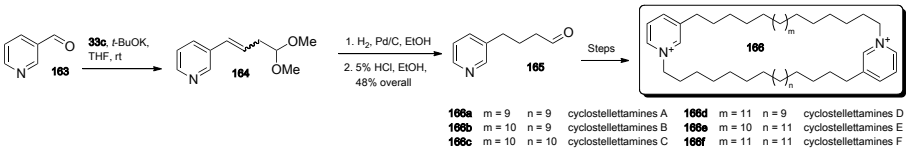	176
15		177
16	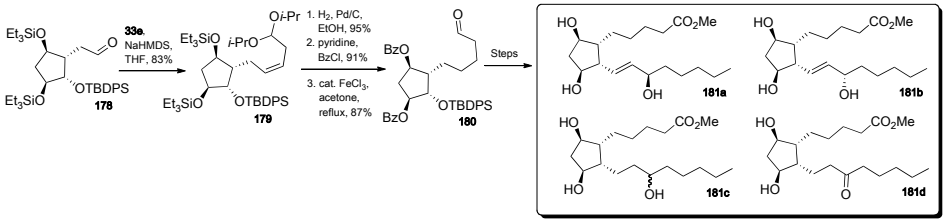	178,179

Table A.3: Use of Acetal Phosphonium Salts **33b** – **33e** in C3-Homologation

Entry	Reactions	Ref
1	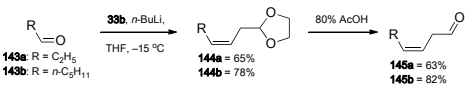	180
2	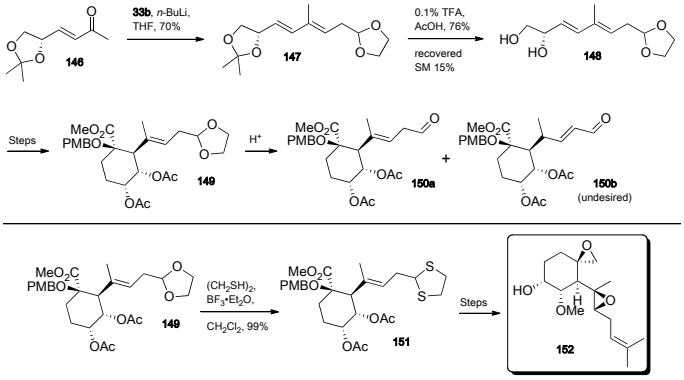	26
3	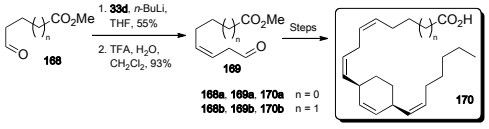	181
4	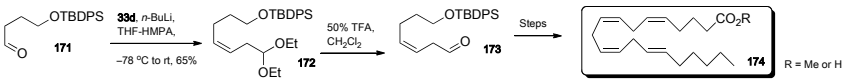	182
5	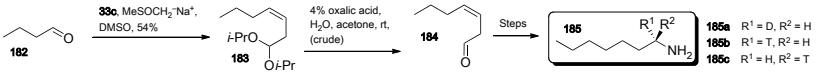	5
6	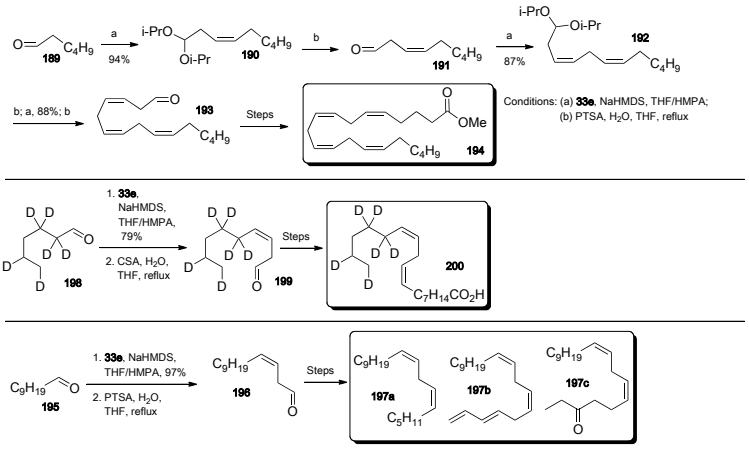	27,183–185

Table A.4: Use of Acetal Phosphonium Salts **33b** – **33e** to Generate β,γ-Aldehydes

Entry	Reactions	Ref
7	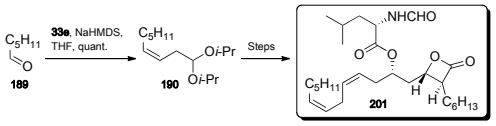	186
8	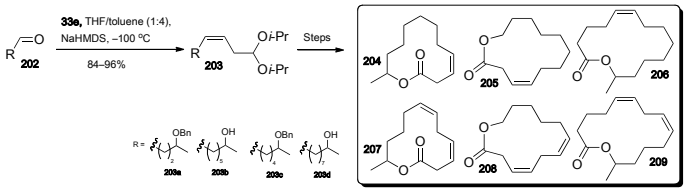	187
9	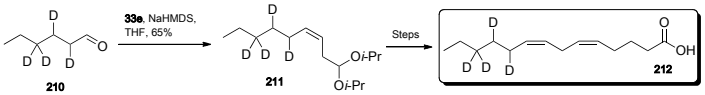	188
10		189

Table A.5: Use of Acetal Phosphonium Salts **33b** – **33e** to Generate β,γ-Aldehydes

Entry	Reactions	Ref
1	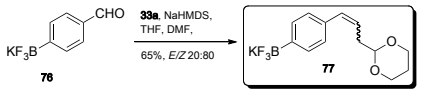	28
2	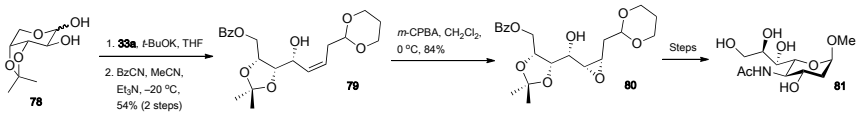	190
3	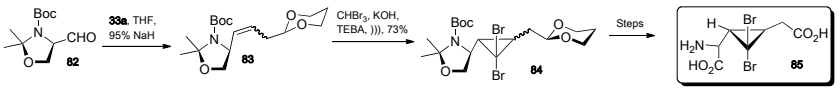	191
4	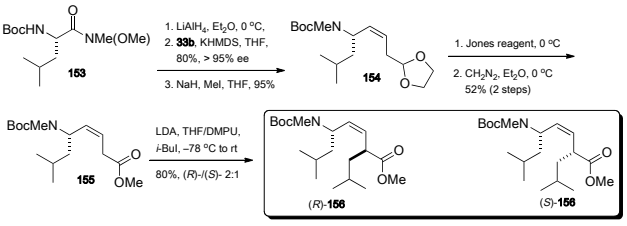	192
5	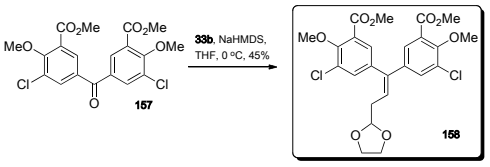	193
6	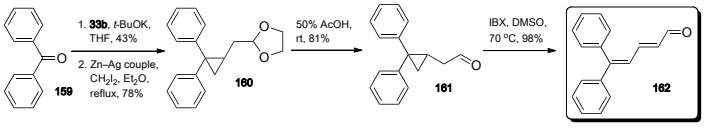	194
7	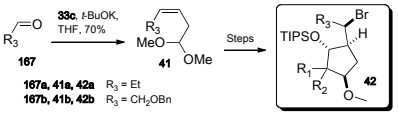	15
8	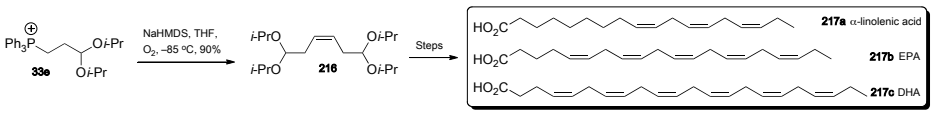	195,196
9	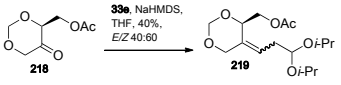	197

Table A.6: Other Uses of Phosphonium Salts **33a** – **33e**

Bibliography

[1] Stowell, J. C.; Keith, D. R. *Synthesis* **1979**, 132–133.

[2] Werstiuk, N. H. *Tetrahedron* **1983**, *39*, 205–268.

[3] Wyatt, P.; Warren, S. In *Organic Synthesis: Strategy and Control*; Wyatt, P., Warren, S., Eds., 1st ed.; John Wiley and Sons, Ltd.: Chichester, West Sussex, 2007; Chapter 13, pp 189–202.

[4] Stowell, J. C. *Chem. Rev.* **1984**, *84*, 409–435.

[5] Battersby, A. R.; Buckley, D. G.; Staunton, J.; Williams, P. J. *J. Chem. Soc., Perkin Trans. 1: Organic and Bio-Organic Chemistry (1972-1999)* **1979**, 2550–2558.

[6] Martin, S. F. *Synthesis* **1979**, 633–665.

[7] Hoppe, D. *Angew. Chem. Int. Ed.* **1984**, *23*, 932–948.

[8] Serratosa, F.; Xicart, J. In *Organic Chemistry in Action: The Design of Organic Synthesis*; Serratosa, F., Xicart, J., Eds., 2nd ed.; Elsevier Science B.V.: Amsterdam, North-Holland, 1996; Vol. 51, Chapter 5, pp 109–155.

[9] Seebach, D. *Angew. Chem. Int. Ed.* **1979**, *18*, 239–258.

[10] Caine, D.; Frobese, A. S. *Tetrahedron Lett.* **1978**, *19*, 883–886.

[11] Nakamura, E.; Kuwajima, I. *J. Am. Chem. Soc.* **1977**, *99*, 7360–7362.

[12] Nakamura, E.; Kuwajima, I. *J. Am. Chem. Soc.* **1983**, *105*, 651–652.

[13] Nakamura, E.; Kuwajima, I. *J. Am. Chem. Soc.* **1984**, *106*, 3368–3370.

[14] Sato, A.; Ito, H.; Yamaguchi, Y.; Taguchi, T. *Tetrahedron Lett.* **2000**, *41*, 10239–10243.

[15] Li, H.; Loh, T.-P. *J. Am. Chem. Soc.* **2008**, *130*, 7194–7195.

[16] Li, H. Ph.D. thesis, Nanyang Technological University, 2009.

[17] Heasley, B. *Eur. J. Org. Chem.* **2009**, 1477–1489.

[18] Schnabel, C.; Hiersemann, M. *Org. Lett.* **2009**, *11*, 2555–2558.

[19] Rowley, M.; Tsukamoto, M.; Kishi, Y. *J. Am. Chem. Soc.* **1989**, *111*, 2735–2737.

[20] Silva, L. F. *Tetrahedron* **2002**, *58*, 9137–9161.

[21] Hanson, J. R. *Nat. Prod. Rep.* **2002**, *19*, 125–132.

[22] Faulkner, D. J. *Nat. Prod. Rep.* **2002**, *19*, 1–49.

[23] Grayson, D. H. *Nat. Prod. Rep.* **2000**, *17*, 385–419.

[24] Fraga, B. M. *Nat. Prod. Rep.* **2001**, *18*, 650–673.

[25] Connolly, J. D.; Hill, R. A. *Nat. Prod. Rep.* **2001**, *18*, 560–578.

[26] Bedel, O.; Haudrechy, A.; Langlois, Y. *Eur. J. Org. Chem.* **2004**, 3813–3819.

[27] Viala, J.; Santelli, M. *Synthesis* **1988**, 395–397.

[28] Molander, G. A.; Figueroa, R. *J. Org. Chem.* **2006**, *71*, 6135–6140.

[29] Voelker, T.; Xia, H.; Fandrick, K.; Johnson, R.; Janowsky, A.; Cashman, J. R. *Bioorg. Med. Chem.* **2009**, *17*, 2047–2068.

[30] Barbot, F.; Miginiac, P. *Synthesis* **1983**, 651–654.

[31] Barrett, A. G. M.; Michael, P.; Adam, W. J. *J. Chem. Soc., Chem. Commun.* **1995**, 1147–1148.

[32] Barrett, A. G. M.; Michael, P.; Adam, W. J. *J. Chem. Soc., Chem. Commun.* **1995**, 1145–1146.

[33] Barrett, A. G. M.; Peña, M.; Willardsen, J. A. *J. Org. Chem.* **1996**, *61*, 1082–1100.

[34] Denmark, S. E.; Regens, C. S.; Kobayashi, T. *J. Am. Chem. Soc.* **2007**, *129*, 2774–2776.

[35] Lepage, O.; Kattnig, E.; Fürstner, A. *J. Am. Chem. Soc.* **2004**, *126*, 15970–15971.

[36] Fürstner, A.; Kattnig, E.; Lepage, O. *J. Am. Chem. Soc.* **2006**, *128*, 9194–9204.

[37] Fürstner, A.; Kattnig, E.; Kelter, G.; Fiebig, H.-H. *Chem. Eur. J.* **2009**, *15*, 4030–4043.

[38] Rodríguez-Escrich, C.; Olivella, A.; Urpí, F.; Vilarrasa, J. *Org. Lett.* **2007**, *9*, 989–992.

[39] Rodríguez-Escrich, C.; Urpí, F.; Vilarrasa, J. *Org. Lett.* **2008**, *10*, 5191–5194.

[40] Chen, Y.; Jin, J.; Wu, J.; Dai, W.-M. *Synlett* **2006**, 1177–1180.

[41] Dai, W.-M.; Chen, Y.; Jin, J.; Wu, J.; Lou, J.; He, Q. *Synlett* **2008**, 1737–1741.

[42] Jung, J. H.; Lee, E. *Angew. Chem. Int. Ed.* **2009**, *48*, 5698–5700.

[43] Boerma, T.; AbouZahr, C.; Ho, J. *World Health Statistics 2009*; 2009.

[44] Mathers, C.; Ma, D. F.; Boerma, T. *Global Burden of Disease 2004 Update*; 2008.

[45] Hall, H. I.; Song, R.; Rhodes, P.; Prejean, J.; An, Q.; Lee, L. M.; Karon, J.; Brookmeyer, R.; Kaplan, E. H.; McKenna, M. T.; Janssen, R. S.; for the HIV Incidence Surveillance Group, *J. Am. Med. Assoc.* **2008**, *300*, 520–529.

[46] Kurtz, M. B.; Rex, J. H. Glucan synthase inhibitors as antifungal agents. In *Drug Discovery and Design*; Scolnick, E. M., Ed.; Academic Press, 2001; Vol. 56, pp 423–475.

[47] Wood, R. L.; Miller, T. K.; Wright, A.; Mccarthy, P.; Taft, C. S.; Pomponi, S.; Selitrennikoff, C. P. *J. Antibiot.* **1998**, *51*, 665–675.

[48] Chen, H. S.; Tsai, W. P.; Leu, H. S.; Ho, H. H.; Liou, L. B. *Rheumatology* **2007**, *46*, 539–544.

[49] Letscher-Bru, V.; Herbrecht, R. *J. Antimicrob. Chemother.* **2003**, *51*, 513–521.

[50] Johnson, M. D.; MacDougall, C.; Ostrosky-Zeichner, L.; Perfect, J. R.; Rex, J. H. *Antimicrob. Agents Chemother.* **2004**, *48*, 693–715.

[51] Groll, A. H.; Walsh, T. J. *Swiss Medical Weekly* **2002**, *132*, 303–311.

[52] Leather, H. L.; Wingard, J. R. *Blood Rev.* **2006**, *20*, 267–287.

[53] Okada, H.; Kamiya, S.; Shiina, Y.; Suwa, H.; Nagashima, M.; Nakajima, S.; Shimokawa, H.; Sugiyama, E.; Kondo, H.; Kojiri, K.; Suda, H. *J. Antibiot.* **1998**, *51*, 1081–1086.

[54] Fridkin, S. K. *Clin. Infect. Dis.* **2005**, *41*, 1455–1460.

[55] Odds, F. C. *Int. J. Antimicrob. Agents* **1996**, *6*, 145–147.

[56] Balkis, M. M.; Leidich, S. D.; Mukherjee, P. K.; Ghannoum, M. A. *Drugs* **2002**, *62*, 1025–1040.

[57] Canuto, M. M.; Rodero, F. G. *Lancet Infect. Dis.* **2002**, *2*, 550–563.

[58] Sanglard, D. *Curr. Opin. Microbiol.* **2002**, *5*, 379–385.

[59] Tkacz, J. S.; DiDomenico, B. *Curr. Opin. Microbiol.* **2001**, *4*, 540–545.

[60] Traxler, P.; Gruner, J.; Auden, J. A. L. *J. Antibiot.* **1977**, *30*, 289–296.

[61] Traxler, P.; Fritz, H.; Fuhrer, H.; Richter, W. J. *J. Antibiot.* **1980**, *33*, 967–978.

[62] Baguley, B. C.; Römmele, G.; Gruner, J.; Wehrli, W. *Eur. J. Biochem.* **1979**, *97*, 345–351.

[63] Gruner, J.; Traxler, P. *Cell. Mol. Life Sci.* **1977**, *33*, 137–137.

[64] Kopecká, M. *Folia Microbiol.* **1984**, *29*, 441–449.

[65] Onishi, J. et al. *Antimicrob. Agents Chemother.* **2000**, *44*, 368–377.

[66] Römmele, G.; Traxler, P.; Wehrli, W. *J. Antibiot.* **1983**, *36*, 1539–1542.

[67] Komori, T.; Itoh, Y. *J. Antibiot.* **1985**, *38*, 544–546.

[68] Traxler, P.; Tosch, W.; Zak, O. *J. Antibiot.* **1987**, *40*, 1146–1164.

[69] Attwood, S. V.; Barrett, A. G. M.; Florent, J.-C. *J. Chem. Soc., Chem. Commun.* **1981**, 556–557.

[70] Attwood, S. V.; Barrett, A. G. M.; Carr, R. A. E.; Richardson, G. *J. Chem. Soc., Chem. Commun.* **1986**, 479–481.

[71] Barrett, A. G. M.; Carr, R. A. E.; Attwood, S. V.; Richardson, G.; Walshe, N. D. A. *J. Org. Chem.* **1986**, *51*, 4840–4856.

[72] Barrett, A. G.; Raynham, T. M. *Tetrahedron Lett.* **1987**, *28*, 5615–5618.

[73] Cane, D. E.; Liang, T. C.; Kaplan, L.; Nallin, M. K.; Schulman, M. D.; Hensens, O. D.; Douglas, A. W.; Albers-Schoenberg, G. *J. Am. Chem. Soc.* **1983**, *105*, 4110–4112.

[74] Corey, E. J.; Yu, C. M.; Kim, S. S. *J. Am. Chem. Soc.* **1989**, *111*, 5495–5496.

[75] Koppenhoefer, B.; Schurig, V. *Org. Synth.* **1988**, *66*, 151.

[76] Koppenhoefer, B.; Schurig, V. *Org. Synth.* **1993**, *Coll. Vol. 8*, 119.

[77] Katsuki, T.; Sharpless, K. B. *J. Am. Chem. Soc.* **1980**, *102*, 5974–5976.

[78] Martin, V. S.; Woodard, S. S.; Katsuki, T.; Yamada, Y.; Ikeda, M.; Sharpless, K. B. *J. Am. Chem. Soc.* **1981**, *103*, 6237–6240.

[79] Hanson, R. M.; Sharpless, K. B. *J. Org. Chem.* **1986**, *51*, 1922–1925.

[80] Gao, Y.; Klunder, J. M.; Hanson, R. M.; Masamune, H.; Ko, S. Y.; Sharpless, K. B. *J. Am. Chem. Soc.* **1987**, *109*, 5765–5780.

[81] Negishi, E.; Takahashi, T.; Baba, S.; Van Horn, D. E.; Okukado, N. *J. Am. Chem. Soc.* **1987**, *109*, 2393–2401.

[82] Denmark, S. E.; Neuville, L. *Org. Lett.* **2000**, *2*, 3221–3224.

[83] Denmark, S. E.; Baird, J. D. *Chem. Eur. J.* **2006**, *12*, 4954–4963.

[84] Denmark, S. E.; Fu, J.; Coe, D. M.; Su, X.; Pratt, N. E.; Griedel, B. D. *J. Org. Chem.* **2006**, *71*, 1513–1522.

[85] Denmark, S. E.; Fu, J.; Lawler, M. J. *J. Org. Chem.* **2006**, *71*, 1523–1536.

[86] Takaya, H.; Ohta, T.; Sayo, N.; Kumobayashi, H.; Akutagawa, S.; Inoue, S.; Kasahara, I.; Noyori, R. *J. Am. Chem. Soc.* **1987**, *109*, 1596–1597.

[87] Takaya, H.; Ohta, T.; ichi Inoue, S.; Tokunaga, M.; Kitamura, M.; Noyori., R. *Org. Synth.* **1998**, *Coll. Vol. 9*, 169–175.

[88] Teo, Y.-C.; Tan, K.-T.; Loh, T.-P. *Chem. Commun.* **2005**, 1318–1320.

[89] Teo, Y.-C.; Goh, E.-L.; Loh, T.-P. *Tetrahedron Lett.* **2005**, *46*, 6209–6211.

[90] Loh, T.-P.; Zhou, J.-R.; Yin, Z. *Org. Lett.* **1999**, *1*, 1855–1857.

[91] Lu, J.; Ji, S.-J.; Teo, Y.-C.; Loh, T.-P. *Org. Lett.* **2004**, *7*, 159–161.

[92] Lum, T.-K.; Wang, S.-Y.; Loh, T.-P. *Org. Lett.* **2008**, *10*, 761–764.

[93] Wang, S.-Y.; Ji, S.-J.; Loh, T.-P. *J. Am. Chem. Soc.* **2007**, *129*, 276–277.

[94] Chin, Y.-J.; Wang, S.-Y.; Loh, T.-P. *Org. Lett.* **2009**, *11*, 3674–3676.

[95] Wang, S.-Y.; Lum, T.-K.; Ji, S.-J.; Loh, T.-P. *Adv. Synth. Catal.* **2008**, *350*, 673–677.

[96] Wang, S.-Y.; Chin, Y.-J.; Loh, T.-P. *Synthesis* **2009**, 3557–3564.

[97] Denmark, S. E.; Fu, J. *Chem. Rev.* **2003**, *103*, 2763–2794.

[98] Denmark, S. E.; Almstead, N. G. In *Modern Carbonyl Chemistry*; Otera, J., Ed., 1st ed.; Wiley-VCH: Weinheim, Germany, 2000; Chapter 10, pp 299–401.

[99] Yamamoto, Y.; Yatagai, H.; Maruyama, K. *J. Org. Chem.* **1980**, *45*, 195–196.

[100] Koreeda, M.; Tanaka, Y. *J. Chem. Soc., Chem. Commun.* **1982**, 845–847.

[101] Seebach, D.; Prelog, V. *Angew. Chem. Int. Ed.* **1982**, *21*, 654–660.

[102] Ireland, R. E.; Norbeck, D. W. *J. Org. Chem.* **1985**, *50*, 2198–2200.

[103] Pinacho Crisostomo, F. R.; Carrillo, R.; Martin, T.; Garcia-Tellado, F.; Martin, V. S. *J. Org. Chem.* **2005**, *70*, 10099–10101.

[104] Chen, L.; Lee, S.; Renner, M.; Tian, Q.; Nayyar, N. *Org. Process Res. Dev.* **2005**, *10*, 163–164.

[105] Lee, C.-H. A.; Loh, T.-P. *Tetrahedron Lett.* **2006**, *47*, 809–812.

[106] Lee, C.-L. K.; Lee, C.-H. A.; Tan, K.-T.; Loh, T.-P. *Org. Lett.* **2004**, *6*, 1281–1283.

[107] Paul, T.; Andrade, R. B. *Tetrahedron Lett.* **2007**, *48*, 5367–5370.

[108] Shriver, D. F.; Drezdzon, M. A. *The Manipulation of Air-Sensitive Compounds*, 2nd ed.; Wiley-Interscience, 1986.

[109] Armarego, W. L. F.; Chai, C. *Purification of Laboratory Chemicals*, 6th ed.; Butterworth-Heinemann, 2009.

[110] Kobayashi, J.; Ishibashi, M. *Chem. Rev.* **1993**, *93*, 1753–1769.

[111] Norcross, R. D.; Paterson, I. *Chem. Rev.* **1995**, *95*, 2041–2114.

[112] Chakraborty, T. K.; Das, S. *Curr. Med. Chem. Anti-cancer Agents* **2001**, *1*, 131–149.

[113] Ishibashi, M.; Kobayashi, J. *Heterocycles* **1997**, *44*, 543–572.

[114] Kobayashi, J.; Tsuda, M.; Ishibashi, M. *Pure. Appl. Chem.* **1999**, *71*, 1123–1126.

[115] Kobayashi, J.; Shimbo, K.; Kubota, T.; Tsuda, M. *Pure. Appl. Chem.* **2003**, *75*, 337–342.

[116] Kobayashi, J.; Tsuda, M. *Nat. Prod. Rep.* **2004**, *21*, 77–93.

[117] Kobayashi, J.; Kubota, T. *J. Nat. Prod.* **2007**, *70*, 451–460.

[118] Kobayashi, J. *J. Antibiot.* **2008**, *61*, 271–284.

[119] Usami, Y. *Mar. Drugs* **2009**, *7*, 314–330.

[120] Doan, H. D.; Gallon, J.; Piou, A.; Vatèle, J.-M. *Synlett* **2007**, 983–985.

[121] Tsuda, M.; Izui, N.; Shimbo, K.; Sato, M.; Fukushi, E.; Kawabata, J.; Katsumata, K.; Horiguchi, T.; Kobayashi, J. *J. Org. Chem.* **2003**, *68*, 5339–5345.

[122] Napolitano, J. G.; Daranas, A. H.; Norte, M.; Fernandez, J. J. *Anti-Cancer Agents Med. Chem. (Formerly Curr, Med. Chem.)* **2009**, *9*, 122–137.

[123] He, L.; Orr, G. A.; Horwitz, S. B. *Drug Discovery Today* **2001**, *6*, 1153–1164.

[124] Yeung, K.-S.; Paterson, I. *Angew. Chem. Int. Ed.* **2002**, *41*, 4632–4653.

[125] Cameron, L. A.; Giardini, P. A.; Soo, F. S.; Theriot, J. A. *Nat. Rev. Mol. Cell Biol.* **2000**, *1*, 110–119.

[126] Gachet, Y.; Tournier, S.; Millar, J. B. A.; Hyams, J. S. *Nature* **2001**, *412*, 352–355.

[127] Usui, T.; Kazami, S.; Dohmae, N.; Mashimo, Y.; Kondo, H.; Tsuda, M.; Terasaki, A. G.; Ohashi, K.; Kobayashi, J.; Osada, H. *Chem. Biol.* **2004**, *11*, 1269–1277.

[128] Fürstner, A.; Méndez, M. *Angew. Chem. Int. Ed.* **2003**, *42*, 5355–5357.

[129] Jin, J.; Chen, Y.; Li, Y.; Wu, J.; Dai, W.-M. *Org. Lett.* **2007**, *9*, 2585–2588.

[130] Corey, E. J.; Guzman-Perez, A.; Noe, M. C. *J. Am. Chem. Soc.* **1995**, *117*, 10805–10816.

[131] Nicolaou, K. C.; Prasad, C. V. C.; Somers, P. K.; Hwang, C. K. *J. Am. Chem. Soc.* **1989**, *111*, 5330–5334.

[132] Nicolaou, K. C.; Prasad, C. V. C.; Somers, P. K.; Hwang, C. K. *J. Am. Chem. Soc.* **1989**, *111*, 5335–5340.

[133] Narayan, R. S.; Sivakumar, M.; Bouhlel, E.; Borhan, B. *Org. Lett.* **2001**, *3*, 2489–2492.

[134] Garbaccio, R. M.; Stachel, S. J.; Baeschlin, D. K.; Danishefsky, S. J. *J. Am. Chem. Soc.* **2001**, *123*, 10903–10908.

[135] Bailey, W. F.; Punzalan, E. R. *J. Org. Chem.* **1990**, *55*, 5404–5406.

[136] Heckrodt, T. J.; Mulzer, J. *Synthesis* **2002**, 1857–1866.

[137] Narayan, R. S.; Borhan, B. *J. Org. Chem.* **2006**, *71*, 1416–1429.

[138] Oshima, M.; Yamazaki, H.; Shimizu, I.; Nisar, M.; Tsuji, J. *J. Am. Chem. Soc.* **1989**, *111*, 6280–6287.

[139] Mori, K. *Tetrahedron* **1977**, *33*, 289–294.

[140] De Mico, A.; Margarita, R.; Parlanti, L.; Vescovi, A.; Piancatelli, G. *J. Org. Chem.* **1997**, *62*, 6974–6977.

[141] Miyazaki, T.; Han-ya, Y.; Tokuyama, H.; Fukuyama, T. *Synlett* **2004**, 477–480.

[142] Savarin, C. G.; Boice, G. N.; Murry, J. A.; Corley, E.; DiMichele, L.; Hughes, D. *Org. Lett.* **2006**, *8*, 3903–3906.

[143] Petasis, N. A.; Bzowej, E. I. *J. Am. Chem. Soc.* **1990**, *112*, 6392–6394.

[144] Hafner, A.; Duthaler, R. O.; Marti, R.; Rihs, G.; Rothe-Streit, P.; Schwarzenbach, F. *J. Am. Chem. Soc.* **1992**, *114*, 2321–2336.

[145] Shiina, I.; Kubota, M.; Oshiumi, H.; Hashizume, M. *J. Org. Chem.* **2004**, *69*, 1822–1830.

[146] Tomioka, K.; Suenaga, T.; Koga, K. *Tetrahedron Lett.* **1986**, *27*, 369–372.

[147] Chen, C.-L.; Sparks, S. M.; Martin, S. F. *J. Am. Chem. Soc.* **2006**, *128*, 13696–13697.

[148] Lu, J.; Xu, Y.-H.; Liu, F.; Loh, T.-P. *Tetrahedron Lett.* **2008**, *49*, 6007–6008.

[149] Lattanzi, A. *Chem. Commun.* **2009**, 1452–1463.

[150] Greene, T. W.; Wuts, P. G. M. *Protective Groups in Organic Synthesis*, 3rd ed.; John Wiley and Sons, Inc.: 605 Third Avenue, New York, 1999.

[151] Kocieński, P. J. *Protecting Groups*, 2nd ed.; Georg Thieme Verlag: Ruedigerstr. 14 70469 Stuttgart, 2000.

[152] Notz, W.; List, B. *J. Am. Chem. Soc.* **2000**, *122*, 7386–7387.

[153] Zhong, Y.-L.; Shing, T. K. M. *J. Org. Chem.* **1997**, *62*, 2622–2624.

[154] Cohen, N.; Banner, B. L.; Lopresti, R. J.; Wong, F.; Rosenberger, M.; Liu, Y. Y.; Thorn, E.; Liebman, A. A. *J. Am. Chem. Soc.* **1983**, *105*, 3661–3672.

[155] Cohen, N.; Banner, B. L.; Lopresti, R. J. *Tetrahedron Lett.* **1980**, *21*, 4163–4166.

[156] Hyuga, S.; Hara, S.; Suzuki, A. *Bull. Chem. Soc. Jpn.* **1992**, *65*, 2303–2305.

[157] Boons, G.-J.; Downham, R.; Kim, K. S.; Ley, S. V.; Woods, M. *Tetrahedron* **1994**, *50*, 7157–7176.

[158] Schaeffer, P.; Fache-Dany, F.; Trifilieff, S.; Trendel, J. M.; Albrecht, P. *Tetrahedron* **1994**, *50*, 12633–12642.

[159] Gonzalez, Á.; Aiguadé, J.; Urpí, F.; Vilarrasa, J. *Tetrahedron Lett.* **1996**, *37*, 8949–8952.

[160] Chackalamannil, S.; Wang, Y. *Tetrahedron* **1997**, *53*, 11203–11210.

[161] Momose, Y.; Maekawa, T.; Yamano, T.; Kawada, M.; Odaka, H.; Ikeda, H.; Sohda, T. *J. Med. Chem.* **2002**, *45*, 1518–1534.

[162] Sakata, Y.; Hirano, Y.; Tatemitsu, H.; Misumi, S.; Ochiai, H.; Shibata, H. *Tetrahedron* **1989**, *45*, 4717–4727.

[163] Sas, B.; De Clercq, P.; Vandewalle, M. *Synlett* **1997**, 1167–1170.

[164] Dirat, O.; Kouklovsky, C.; Langlois, Y. *J. Org. Chem.* **1998**, *63*, 6634–6642.

[165] Michel, P.; Rassat, A.; Daly, J. W.; Spande, T. F. *J. Org. Chem.* **2000**, *65*, 8908–8918.

[166] Tozer, M. J.; Buck, I. M.; Cooke, T.; Kalindjian, S. B.; Pether, M. J.; Steel, K. I. M. *Bioorg. Med. Chem.* **2002**, *10*, 425–432.

[167] Ohno, H.; Okumura, M.; Maeda, S.-i.; Iwasaki, H.; Wakayama, R.; Tanaka, T. *J. Org. Chem.* **2003**, *68*, 7722–7732.

[168] Kitbunnadaj, R.; Hoffmann, M.; Fratantoni, S. A.; Bongers, G.; Bakker, R. A.; Wieland, K.; el Jilali, A.; Esch, I. J. D.; Menge, W. M.; Timmerman, H.; Leurs, R. *Bioorg. Med. Chem.* **2005**, *13*, 6309–6323.

[169] Kitbunnadaj, R.; Zuiderveld, O. P.; Christophe, B.; Hulscher, S.; Menge, W. M. P. B.; Gelens, E.; Snip, E.; Bakker, R. A.; Celanire, S.; Gillard, M.; Talaga, P.; Timmerman, H.; Leurs, R. *J. Med. Chem.* **2004**, *47*, 2414–2417.

[170] Kitbunnadaj, R.; Zuiderveld, O. P.; De Esch, I. J. P.; Vollinga, R. C.; Bakker, R.; Lutz, M.; Spek, A. L.; Cavoy, E.; Deltent, M.-F.; Menge, W. M. P. B.; Timmerman, H.; Leurs, R. *J. Med. Chem.* **2003**, *46*, 5445–5457.

[171] Chang, M.-Y.; Chen, H.-P.; Lin, C.-Y.; ; Pai, C.-L. *Heterocycles* **2005**, *65*, 1999–2004.

[172] Tsukano, C.; Ebine, M.; Sasaki, M. *J. Am. Chem. Soc.* **2005**, *127*, 4326–4335.

[173] Eriksson, C.; Sjodin, K.; Schlyter, F.; Hogberg, H.-E. *Tetrahedron: Asymmetry* **2006**, *17*, 1074–1080.

[174] Lebar, M. D.; Baker, B. J. *Tetrahedron Lett.* **2007**, *48*, 8009–8010.

[175] Brovetto, M.; Seoane, G. *J. Org. Chem.* **2008**, *73*, 5776–5785.

[176] Wanner, M. J.; Koomen, G.-J. *Eur. J. Org. Chem.* **1998**, 889–895.

[177] Moustakis, C. A.; Viala, J.; Capdevila, J.; Falck, J. R. *J. Am. Chem. Soc.* **1985**, *107*, 5283–5285.

[178] Durand, T.; Guy, A.; Henry, O.; Vidal, J.-P.; Rossi, J.-C.; Rivalta, C.; Valagussa, A.; Chiabrando, C. *Eur. J. Org. Chem.* **2001**, 809–819.

[179] Guy, A.; Durand, T.; Roland, A.; Cormenier, E.; Rossi, J.-C. *Tetrahedron Lett.* **1998**, *39*, 6181–6184.

[180] Iwamoto, M.; Kubota, N.; Takagi, Y.; Kogami, K.; Hayashi, K. *Agric. Biol. Chem.* **1982**, *46*, 2383–2386.

[181] Stoller, A.; Mioskowski, C.; Millet, J.; Sepulchre, C.; Bellamy, F. *Tetrahedron Lett.* **1990**, *31*, 5035–5038.

[182] Berdeaux, O.; Vatèle, J.-M.; Eynard, T.; Nour, M.; Poullain, D.; Noël, J.-P.; Sébédio, J.-L. *Chem. Phys. Lipids* **1995**, *78*, 71–80.

[183] Viala, J.; Labaudiniere, R. *J. Org. Chem.* **1993**, *58*, 1280–1283.

[184] Viala, J.; Munier, P.; Santelli, M. *Tetrahedron* **1991**, *47*, 3347–3352.

[185] Viala, J.; Santelli, M. *J. Org. Chem.* **1988**, *53*, 6121–6123.

[186] Pons, J.-M.; Pommier, A.; Lerpiniere, J.; Kocienski, P. *J. Chem. Soc., Perkin Trans. 1: Organic and Bio-Organic Chemistry (1972-1999)* **1993**, 1549–1551.

[187] Boden, C. D. J.; Chambers, J.; Stevens, I. D. R. *Synthesis* **1993**, 411–420.

[188] Goese, M.; Eisenreich, W.; Kupfer, E.; Stohler, P.; Weber, W.; Leuenberger, H. G.; Bacher, A. *J. Org. Chem.* **2001**, *66*, 4673–4678.

[189] Peng, S.; McGinley, C. M.; van der Donk, W. A. *Org. Lett.* **2004**, *6*, 349–352.

[190] Maier, T.; Schmidt, R. R. *Carbohydr. Res.* **1992**, *216*, 483–494.

[191] Alcaraz, C.; Bernabé, M. *Tetrahedron: Asymmetry* **1994**, *5*, 1221–1224.

[192] Bohnstedt, A. C.; Prasad, J. V. N. V.; Rich, D. H. *Tetrahedron Lett.* **1993**, *34*, 5217–5220.

[193] Casimiro-Garcia, A.; Micklatcher, M.; Turpin, J. A.; Stup, T. L.; Watson, K.; Buckheit, R. W.; Cushman, M. *J. Med. Chem.* **1999**, *42*, 4861–4874.

[194] Nicolaou, K. C.; Montagnon, T.; Baran, P. S.; Zhong, Y. L. *J. Am. Chem. Soc.* **2002**, *124*, 2245–2258.

[195] Sandri, J.; Viala, J. *J. Org. Chem.* **1995**, *60*, 6627–6630.

[196] Sandri, J.; Viala, J. *Synthesis* **1995**, 271–275.

[197] Gras, J.-L.; Soto, T.; Viala, J. *Tetrahedron: Asymmetry* **1999**, *10*, 139–151.